Crosstalk Between Iron Homeostasis And Nitric Oxide Signalling: Impact On Cancer Cell Viability

Mimi Ariffin

A thesis submitted for the degree of

Master of Science

University of Otago, Dunedin, New Zealand

15th of March 2012

Abstract

The element iron (Fe) is essential for mammals since many enzymes require Fe as a cofactor for metabolic processes. Fe regulation is extremely important to maintain Fe homeostasis as Fe overload and Fe deprivation are cytotoxic. Fe overload can cause oxidative damage via excessive production of reactive oxygen species (ROS). On the other hand, Fe deprivation can inhibit cellular growth and lead to apoptosis. Iron regulatory proteins (IRPs) are important for maintaining cellular Fe homeostasis. Regulation of these proteins involves the redox status of the iron-sulphur (Fe-S) clusters of the enzyme aconitase. IRPs are very sensitive to oxidative stress. Excessive exposure of these regulatory proteins to ROS will disrupt cellular Fe regulation by inducing Fe trafficking in cells. The major cellular systems (e.g. mitochondrial respiratory chain) are dependent on Fe for their functionality. With a lack of Fe, these systems will be affected. The susceptibility of cells to oxidative damage will increase under Fe deprivation conditions. Therefore, potentially both Fe overload and Fe deprivation are beneficial for cancer therapy if they could be selectively induced within a tumour. In the present study, nitric oxide ($^{\bullet}$NO) released by a novel photoactive agent, tDSNO, was studied as a means of selectively impairing Fe homeostasis and exacerbating the effect of Fe deprivation. The exposure to $^{\bullet}$NO was hypothesised to cause toxicity to cancer cells by exaggerating the stress conditions, which is the characteristic of both Fe overload and Fe deprivation pathways. Results showed that the exposure of breast cancer cells (MDA-MB-231) and lung cancer cells (A549) to $^{\bullet}$NO under normal Fe homeostasis conditions was unable to promote Fe overload as the intracellular Fe content did not significantly increase relative to control ($p>0.05$). However, the efficacy of tDSNO was potentiated under conditions of Fe deprivation. A maximum cellular death of 59.1 ± 1.2% was observed after 24 h of exposure to 40 μM of tDSNO at 37^{o}C ($p<0.05$), while under these conditions, the drug tDSNO displayed a low toxicity in cells with normal Fe homeostasis. Therefore, the toxic effect of tDSNO in cancer cells was substantially

enhanced under Fe deprivation conditions. It was then concluded that this novel drug could be more effective if used in combination with Fe chelation therapy.

Acknowledgements

In the name of Allah, the Most Gracious, the Most Merciful. I would like to express my deepest appreciation to my supervisor, Dr Gregory Giles, for all his advice and guidance in all research aspects. I am sincerely grateful for having him as my supervisor, with a lot of patience when teaching and discussing my research progress. Your help and support are much indeed appreciated. I am thankful to the Universiti Teknologi MARA, for funding my study throughout these two years. I am honoured for the trust given to further my study abroad despite of thousands people demand for this opportunity. To Giles group members, thank you for keeping me company in the lab and making my days a lot more meaningful. Special thanks to Abel, Bettina, Christine, and Felix for being concern during the time I worked here. I appreciate all the time we spent together to listen to each other's problem. I would also like to thank Sebastian, who has helped me a lot in the working area. Thank you for willingly sharing some experiences and giving me some good advice, which help me a lot to become a better researcher. To Babaji and Prasanta, I am sincerely grateful for having them as always give a sincere opinion whenever I seek for explanations. To my friends, especially Fatin and Hanis, thanks for always being there to listen to me whenever I need someone to talk to. Thank you for cheering me up with the best Malay dishes ever in Dunedin when I was so stress and when I missed my mom's cooking. Last but far from least, to my lovely parents, I am eternally gratified for having you both by my side, to keep me motivated with my work. Only God knows how grateful I am to know that you are always be there, to support every single decision I made.

Table of contents

List of figures

List of abbreviations

ANOVA	Analysis of variance
ATCC	American Type Culture Collection
BSA	Bovine serum albumin
cGMP	Cyclic guanosine monophosphate
CO_2	Carbon dioxide
Cu	Copper
Cu^{2+}	Cuprous
CySNO	*S*-nitrosocysteine
DEA/$^{\bullet}$NO	Diethylamine $^{\bullet}$NO adduct
DFO	Deferoxamine
DMEM	Dulbecco's Modified Eagle Medium
DMSO	Dimethyl sulfoxide
DMT1	Divalent metal transporter 1
DNA	Deoxyribonucleic acid
Dp44mT	Di-2-pyridylketone-4,4-dimethyl-3-thiosemicarbazone
ε_{340}	Extinction coefficient at 340 nm
EDRF	Endothelium-derived relaxing factor
FAC	Ferric ammonium citrate
FBS	Foetal bovine serum
Fe	Iron
Fe^{2+}	Ferrous
Fe^{3+}	Ferric
Fe-S	Iron-sulphur
$FeSO_4$	Ferrous sulphate

$Fe_2(SO_4)_3$	Ferric sulphate
GSH	Glutathione
GSNO	*S*-nitrosoglutathione
GTN	Glyceryl trinitrite
HCl	Hydrochloric acid
HER2	Human epidermal growth factor receptor 2
H_2O_2	Hydrogen peroxide
Hpx	Haemopexin
IC_{50}	Inhibitory concentration of 50% population
IRE	Iron-responsive element
IRP	Iron regulatory protein
K_D	Dissociation constant
LIP	Labile iron pool
mADH	Mitochondrial aldehyde dehydrogenase
MAPK	Mitogen activated protein kinase
mRNA	Messenger RNA
MTT	3-(4,5-dimethylthiazol-2-yl)-2,5-diphenyltetrazolium bromide
$NaNO_2$	Sodium nitrite
NO^-	Nitroxyl anion
NO_2^-	Nitrite
NO_3^-	Nitrate
$^{\bullet}NO$	Nitric oxide
NO_2	Nitrogen dioxide
N_2O_3	Dinitrogen trioxide
NONOate	Diazeniumdiolate
NOS	Nitric oxide synthase

NSCLC	Non-small cell lung carcinomas
O_2^-	Superoxide
$^{\bullet}OH$	Hydroxyl radical
$ONOO^-$	Peroxynitrite
PBS	Phosphate buffered saline
PI	Propidium iodide
p53	Protein 53
RNA	Ribonucleic acid
ROS	Reactive oxygen species
RSH	Thiol
RSNO	*S*-nitrosothiols
RSSR	Disulphide
SCLC	Small-cell lung carcinomas
SEM	Standard error of the mean
S-N	Sulphur-nitrogen
SNAP	*S*-nitroso-*N*-acetyl-penicillamine
SNP	Sodium nitroprusside
tDSNO	*tert*-dodecane-*S*-nitrosothiol
Tf	Transferrin
TfR	Transferrin receptor
UV-Vis	Ultraviolet-visible

CHAPTER 1: INTRODUCTION

1.1 Iron (Fe)

1.1.1 Fe as an essential element

Virtually 5% of the earth's crust is composed of Fe (Richardson and Ponka, 1997). This puts Fe as the fourth most abundant element in the world and the second most abundant metal in the earth (Bothwell, 1995; Aken *et al*., 1998). In the human body, Fe is the most abundant transition metal with 3 to 4 grams per individual (~50 mg/kg) (Toyokuni, 1996; Ganz and Nemeth, 2006). The majority of this Fe is distributed in the haemoglobin of red blood cells and developing erythroid cells, followed by a significant amount of up to 600 mg scattered in macrophages, 300 mg in the myoglobin of muscles, and the excess of about 1 g is stored in the liver (the major depot of Fe) (Wang and Pantopoulos, 2011). The great abundance of Fe is coupled with the fact that all living organisms have an absolute requirement for Fe (Richardson and Ponka, 1997). Fe commonly exists in two redox states; ferrous (Fe^{2+}) and ferric (Fe^{3+}), both of which are able to donate and accept electrons, which allows Fe to participate in electron transfer reactions (Meneghini, 1997; Ponka, 1999). This flexible coordination chemistry and redox reactivity have allowed Fe to associate with proteins and regulate the functionality of biological systems.

In order to perform a broad spectrum of physiological functions, Fe must be incorporated in the haem moieties of haemoglobin, myoglobin and cytochromes (Cairo *et al*., 2002). Otherwise, Fe must be bound to enzymes in a form of non-haem moieties (Cairo *et al*., 2002). Approximately 70-75% of the haemoglobin binds Fe, making it the largest reservoir of Fe in the body (Panter, 1993). A significant drop of individual Fe levels below its normal range of 3 to 4 grams, as in the case of prolonged Fe deficiency, will result in anaemia (Goldhaber, 2003). This is frequently characterised

by the presence of small red blood cells with low haemoglobin levels (Goldhaber, 2003). For that reason, a daily Fe intake needs to be maintained at a recommended level of 8 mg/day for men and women over 51 years old and 18 mg/day for women from 19 to 50 years old (Goldhaber, 2003). It is also important not to take Fe excessively, as there have been deaths reported from accidentally ingesting large doses of Fe in a range of 40 to 1600 mg/kg (Goldhaber, 2003). This indicates that Fe can be fatal when it exceeds the limit of the body's Fe demand.

Fe catalysis is essential for cellular survival. Indeed, it has been suggested that the first step in the origin of life was catalysed by reactions that involved Fe (Richardson and Ponka, 1997). This explains the essential nature of Fe in cellular growth. Fe is an absolute requirement for cells to grow, as Fe-containing proteins catalyse key reactions that are involved in fundamental biochemical activities, such as oxygen transport, energy metabolism, respiration and DNA synthesis (Meneghini, 1997; Richardson and Ponka, 1997; Le and Richardson, 2002). Indeed, without Fe, cells are unable to proceed from the G_1 to the S phase of the cell cycle. This is the crucial checkpoint which is regulated by the Fe-containing enzyme ribonucleotide reductase (Le and Richardson, 2002). This enzyme is involved in the synthesis of DNA, where Fe serves as a cofactor to convert ribonucleotides to deoxyribonucleotides (Cooper *et al*., 1996). Therefore, if Fe is deficient in cells, both DNA synthesis and cell proliferation are inhibited, which results in a retardation of cellular growth. While Fe is indispensable for many processes in cellular systems, the ranges within which these processes occur are limited to the bioavailability of the total Fe in the body. Therefore, Fe needs to be maintained at a constant level to match the body's Fe needs.

1.1.2 Biological roles of Fe

1.1.2.1 Iron-sulphur (Fe-S) proteins

Fe-S proteins are common to most living organisms as they are among the first catalysts that cells had to work with (Beinert and Kiley, 1999). Their existence was first reported in the 1960's when researchers started to glean some information from mitochondrial studies (Beinert *et al*., 1997; Beinert, 2000, Lill, 2009). Fe-S proteins have been recognised as a sensor and catalytic centre of Fe whereby they are involved in oxidoreductive functions as an electron transfer intermediate (Gardner *et al*., 1994; Beinert *et al*., 1997; Eisenstein, 2000). Fe-S proteins contain either [2Fe-2S], [3Fe-4S] or [4Fe-4S] clusters, which are all extremely susceptible to oxidative stress (Beinert *et al*., 1997). Upon oxidation-reduction reactions, these clusters are removed or inserted into proteins, which can potentially alter protein structures by changing the preferential protein side chain ligation (Beinert *et al*., 1997).

One of the examples of Fe-S proteins is aconitase, an enzyme with a particular reactive thiol, cys^{565} (Beinert *et al*., 1996; Eisenstein, 2000). The blockage of this cysteine with a bulky residue will inactivate the enzyme. Aconitase employs a cubane [4Fe-4S] cluster for the enzyme functionality (Eisenstein, 2000). The reaction of aconitase involves a direct participation of this [4Fe-4S] cluster and therefore excludes a net oxidation and reduction of a substrate (Robbins and Stout, 1989). Aconitase catalyses a stereospecific dehydration/rehydration reaction for the conversion of citrate to isocitrate in the second and third steps of the Krebs cycle (Robbins and Stout, 1989). These steps are crucial for the cellular energy metabolism.

Early research on tissue extract has demonstrated that there are two isoforms of aconitase, namely mitochondrial and cytosolic aconitase (Beinert and Kennedy, 1993). The mitochondrial and

cytosolic aconitase have a structural similarity, although they are two distinctly different enzymes that are coded on different chromosomes (Beinert and Kennedy, 1993). The crystal structure of aconitase indicates that it has two regions that contain four domains (Eisenstein, 2000). These domains are separated by a cleft in between domains 1-3 and domain 4 (Figure 1). The first three domains are tightly associated to each other and located near the [4Fe-4S] cluster. The fourth domain is more loosely associated with the first three domains. The extent of the opening and closing of the cleft is dependent on the availability of [4Fe-4S] cluster (Eisenstein, 2000). This cleft provides an accessible region for the solvent to disrupt the [4Fe-4S] cluster and regulate the aconitase function. The regulation of aconitase function is one important mechanism by which Fe is regulated in cellular Fe homeostasis where Fe is sequestered in a form of [4Fe-4S] cluster.

Figure 1 Crystal structure of aconitase enzyme. Domains are coloured as: domain 1 is blue, domain 2 is yellow, domain 3 is green and domain 4 is orange, whereas [4Fe-4S] is coloured pink. The fourth domain is loosely associated with the first three domains, where they are separated into two regions. The cleft in between the two regions is important for the solvent accessibility to [4Fe-4S] as it can regulate the activity of the enzyme.

1.1.2.2 Haem proteins

Biological systems depend on haem proteins to perform a wide variety of cellular functions. The haem or Fe-porphyrin complex is a prosthetic group that serves as an active centre of haem proteins (Paoli *et al.*, 2002). In the company of haem proteins, haems are able to carry out a number of diverse activities ranging from electron transfer, oxygen transport and storage, signal transduction, control of gene expression and metal ions storage (Reedy and Gibney, 2004; Mayfield *et al*., 2011). Research on the protein structure determination has shown that nature uses various different scaffolds and architectures to bind haem. By exploring this area, researchers started to discover numerous haem proteins in biological systems. Haem proteins were first recognised from the structural characterisation of haemoglobin and myoglobin (Paoli *et al.*, 2002) and their involvement in biological functions was first reported from oxygen transport properties of haemoglobin (Reedy and Gibney, 2004). The involvement in oxygen transport and storage is the reason that haemoglobin and myoglobin account for the ubiquitous presence of haems in vertebrates and invertebrates (Paoli *et al.*, 2002). Haem proteins were further discovered to be involved in electron transfer as respiratory pigments and named as cytochromes (Reedy and Gibney, 2004).

As a vital cofactor in living organisms, haem serves as a key player in Fe homeostasis. Fe is incorporated and sequestered in the active centre of haem structure and specifically referred to as the ferrous complex of protoporphyrin IX (Reedy and Gibney, 2004). In the cellular system, haem is synthesised in the mitochondria or is imported from the extracellular space through the plasma membrane for insertion into haem proteins (Chen *et al*., 2011). Free haem, which is not incorporated into haem proteins, is highly cytotoxic due to its capability to catalyse oxidation (Kumar and Bandyopadhyay, 2005). The lipophilicity of haem exaggerates its cytotoxic effect as this will allow haem to intercalate into membranes and impair lipid bilayers by catalysing cytotoxic lipid peroxide production via lipid peroxidation (Kumar and Bandyopadhyay, 2005). This may

damage other organelles and DNA through the formation of oxidative stress. Furthermore, an accumulation of free haem from the release of haem proteins has been implicated in some pathological diseases (Kumar and Bandyopadhyay, 2005). In sickle cell disease, a severe hemolysis has been found to breach the haem detoxification system, causing an excessive accumulation of free haems, which allows them to exert damaging effects. Therefore, free haem in the cellular system needs to be bound and sequestered.

In mammals, the protein haemopexin (Hpx) is one of the haem proteins that are involved in Fe homeostasis (Paoli *et al.*, 1999). Hpx is an acute phase protein that is used to protect against oxidative damage of free haem (Paoli *et al.*, 1999). It is one of the four most abundant proteins in blood serum that has the highest affinity to bind haem with K_d less than 1 pM (Paoli *et al.*, 2002). Despite the high affinity binding, the bound haem is released via a specific receptor on liver cells when the haem-Hpx complex is internalised into the cells by receptor-mediated endocytosis (Paoli *et al.*, 1999). The crystal structure of haem-Hpx complex indicates that haem is bound between two β-propeller domains in a bis-histidyl ligation (Figure 2). Both the domain interface and the flexible loop region that are involved in haem binding are likely to play a role in the mechanism of ligand association and dissociation (Paoli *et al.*, 1999). The high affinity binding is obtained through electrostatic interaction inside the complex by anchoring the propionate groups into the domain-domain interface (Paoli *et al.*, 2002). Haem is released from haem protein through a mechanism that involves the labile property of one of the histidines in the Fe's bis-histidyl coordination. This labile property allows the dissociation of haem from the haem protein. Overall, the haem-Hpx complex demonstrates the importance of both haem and haem proteins in regulating Fe homeostasis where Fe is sequestered in a form of porphyrin ring.

Figure 2 Crystal structure of haem-Hpx complex. β-propeller domains are coloured red, haem group is green and disulphide bonds are yellow. Haem is bound between two β-propeller domains, where both the domain interface and the flexible loop region that are involved in haem binding are likely to play a role in the mechanism of ligand association/dissociation.

1.1.2.3 The labile iron pool (LIP)

The LIP is defined as a pool of chelatable and metabolically active forms of intracellular Fe. It consists of both Fe^{2+} and Fe^{3+} that are loosely coupled with molecular complexes such as organic anions (phosphates and carboxylates), polypeptides and surface components of membranes (e.g. phospholipid head groups) (Konijn *et al*., 1999; Kakhlon and Cabantchik, 2002). Under normal physiological conditions, the LIP of a mammalian cell consists of less than 5 μM of Fe. This is a minor fraction of the total cellular Fe concentrations which can range from 20 to 100 μM (Esposito *et al*., 2002). At any particular time, approximately 0.1% (~3 mg) of the total Fe in the body will circulate in this exchangeable transit pool with only a small fraction of Fe entering and leaving the body on a daily basis (Huang, 2003). Naturally, the LIP has the capacity to promote the formation of reactive oxygen species (ROS). It consists of chemical components that are potentially involved in redox cycling. Operationally, the balance between the LIP components and the ROS levels are dependent on the rise and fall pattern of Fe as the changes are based on Fe transportation and sequestration (Kakhlon and Cabantchik, 2002). In order to keep the ratio of the two compartments constant, the cellular Fe levels are maintained homeostatically within a relatively narrow

concentration range (Esposito *et al*., 2002). This is to meet the cellular metabolic demand for Fe while minimising the potential for ROS formation. Although the LIP is associated with a diverse population of ligands and proteins, any changes following the biochemical stimuli are normally transitory and homeostatic in nature. Therefore, it serves as a crossroad for cellular Fe metabolism.

1.1.3 Fe metabolism

1.1.3.1 Proteins of Fe metabolism

Cellular Fe levels in mammalian cells are steadily maintained through the modulation of Fe uptake and storage (Konijn *et al*., 1999). For that purpose, intracellular Fe levels are tightly regulated by transferrin receptor (TfR) and ferritin proteins (Beinert *et al*., 1997; Kennedy *et al*., 1997; Gehring *et al*., 1999). TfR is responsible for mediating the uptake of Fe into the cells whereas ferritin is responsible for the intracellular Fe storage. The expressions of both proteins are important for maintaining a balanced Fe homeostasis (Konijn *et al*., 1999). It is agreed that an increase in intracellular Fe levels will initially appear in the LIP, but the excess Fe will eventually be sequestered in the ferritin protein. The ferritin molecule is assembled from 24 polypeptide subunits of two ferritin types, namely H- and L-ferritin (Ganz and Nemeth, 2006). One molecule of ferritin is capable of binding up to 4500 Fe atoms per polymer molecule with the association constant approximately 10^{36} M (Konijn *et al*., 1999; Huang, 2003; Ganz and Nemeth, 2006). Fe is transported in and out of ferritin by pores, through which Fe^{2+} can enter to interact with ferroxidase at the centre of the molecule. Fe^{2+} is then transformed into the less toxic Fe^{3+} for storage in the ferritin cavity (Harrison and Arosio, 1996; Geissler and Singh, 2011). For Fe to exit the ferritin, it has to be reduced but may also be released during ferritin's lysosomal degradation (Ganz and Nemeth, 2006). Besides TfR and ferritin, transferrin (Tf) is also involved in the process of Fe metabolism. Tf is a serum glycoprotein that binds two atoms of Fe (Bali *et al*., 1991). Tf is a major

Fe transport protein in mammals and functions to deliver Fe from the sites of storage and absorption, to the sites of utilisation (Iacopetta and Morgan, 1983). So far, Tf is the only known source of Fe for haemoglobin synthesis (Aisen *et al*., 1999; Eisenstein, 2000). One third of Tf binding sites are saturated with Fe to avoid the aggregation of non-protein-bound Fe.

1.1.3.2 Cellular Fe transportation

Cellular Fe uptake occurs through several mechanisms. A very important one is regulated by TfR that allows a fine control of Fe homeostasis in mammalian cells (Meneghini, 1997; Aisen *et al*., 1999). Serum Tf is the primary means of Fe transportation which provides most of the Fe required for physiological needs. High affinity uptake of Tf is mediated by endocytosis of the Tf-TfR complex (Bali *et al*., 1991). This is the main pathway for Fe uptake in many cells such as reticulocytes (Levy *et al*., 2005) and hepatocytes (Uchiyama *et al*., 2008). Once the Tf-TfR complex is internalised into the cells, Fe is released from Tf via a process of endosomal acidification. A proton pump promotes acidification of the endosome to pH 5.5 and triggers the release of Fe^{3+} from Tf that remains bound to TfR (Bali *et al*., 1991; Aisen *et al*., 1999; Wang and Pantopoulos, 2011). The ferrireductase Steap3 reduces Fe^{3+} to Fe^{2+}, which is then transported into the cytoplasm through the action of divalent metal transporter 1 (DMT1) (Bali *et al*., 1991). Once transported into the cytosol, Fe becomes part of the LIP and will subsequently be transported into mitochondria and other organelles for cellular usage, or into ferritin for storage (Oria *et al*., 1995; Napier *et al*., 2005). The apo-Tf-TfR complex is then returned to the cell surface with the affinity of Tf to TfR dropping approximately 500-fold (Wang and Pantopoulos, 2011). At an extracellular pH of 7.4, the complex dissociates so that Tf is available to bind other Fe ions (Bali *et al*., 1991) (Figure 3).

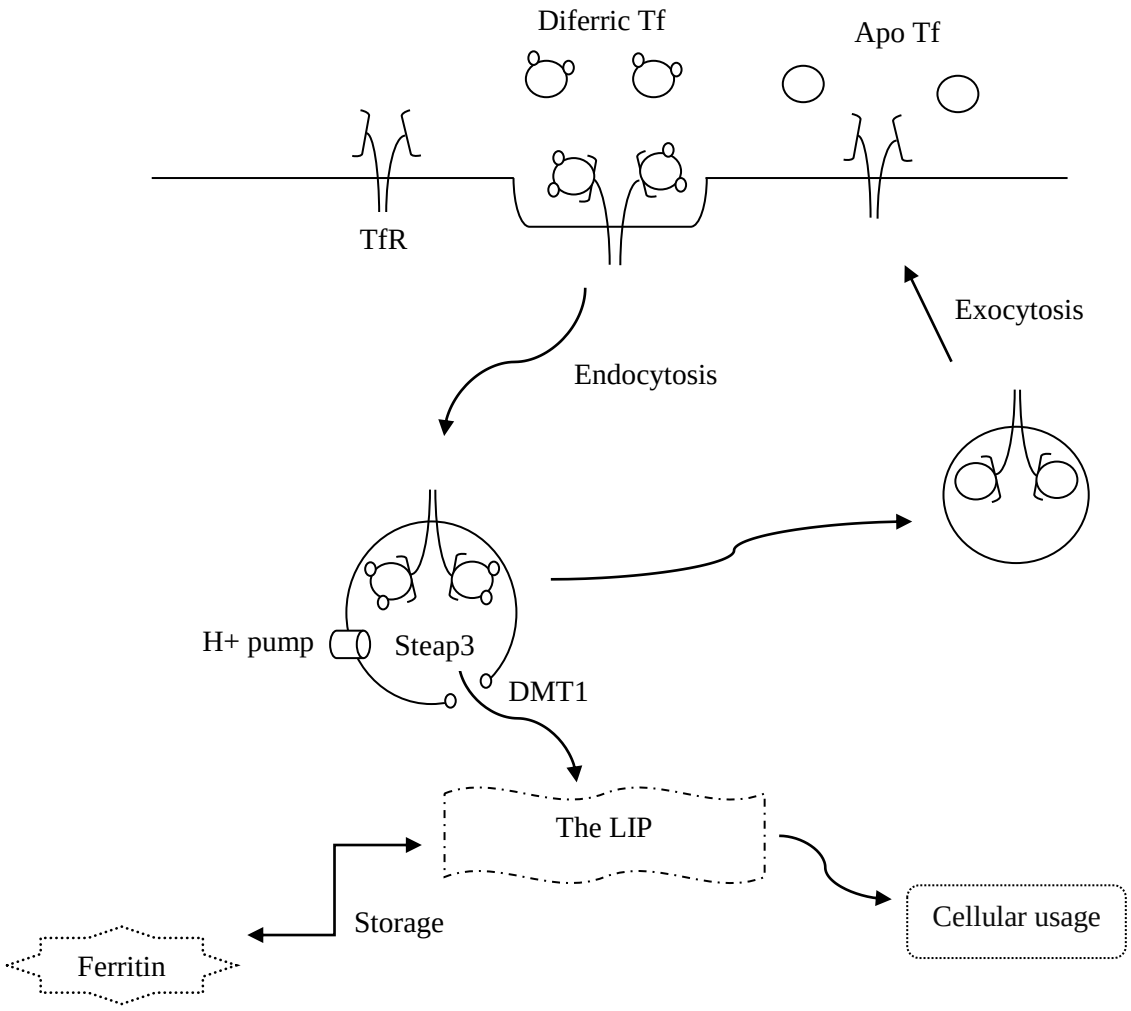

Figure 3 Mechanism of Fe transportation. Primary Fe uptake occurs via Tf-TfR-mediated endocytosis. A proton pump acidifies the endosome, causing Fe to be released from the Tf-TfR complex. Fe is reduced by Steap3 and transported across the endosomal membrane to the cytosol via DMT1. Fe in the LIP is directed to the cellular constituents for metabolic utilisation, or transported into ferritin for storage. The apo-Tf-TfR complex is exported to the cell surface by exocytosis and Tf is released from TfR to bind other Fe ions.

1.1.3.3 Post-transcriptional control of Fe metabolism

The cellular Fe uptake by TfR and the intracellular Fe storage by ferritin are controlled by the IRE/IRP regulatory system (Hentze and Kuhn, 1996). Iron regulatory proteins (IRPs) are cytosolic RNA-binding proteins that bind a specific binding protein, known as iron-responsive element (IRE) (Richardson *et al*., 1995). The messenger RNAs (mRNAs) of TfR and ferritin contain IREs in their untranslated regions, which constitute the binding sites for IRPs (Gehring *et al*., 1999). Ferritin

mRNA contains a single IRE in its 5' untranslated region whereas TfR mRNA contains five IREs in its 3' untranslated region (Beinert *et al*., 1997; Gehring *et al*., 1999). When IRP binds IRE in the 5' untranslated region of ferritin mRNA, the translation of the ferritin protein is blocked and the expression of ferritin protein is repressed. On the other hand, when IRPs bind at least three of five IREs in the 3' untranslated region of TfR mRNA, the TfR mRNA will be protected from nucleolytic degradation and the expression of TfR protein will be up-regulated (Beinert *et al*., 1997). These processes demonstrate the mechanism by which the expressions of TfR and ferritin proteins are post-transcriptionally controlled by IRPs in an opposing sense in order to regulate the mammalian Fe metabolism.

1.1.3.4 Sensing Fe: IRPs as an aconitase and a binding protein

Cellular Fe homeostasis in mammalian cells is regulated by IRPs. These IRPs are sub-divided into two groups, namely IRP1 and IRP2, both of which are 62% homologous in amino acid sequence (Samaniego *et al*., 1994; Guo *et al*., 1995; Aisen *et al*., 1999; Eisenstein, 2000). IRP1 is an important bifunctional protein as it can function as a binding protein and as an aconitase enzyme (Gehring *et al*., 1999; Eisenstein, 2000). In response to increased cellular Fe levels, Fe will accumulate inside IRP1 and assemble a cubane [4Fe-4S] cluster. The cluster assembly renders the IRP1 to be a cytosolic aconitase, which prevents the binding on IRE binding sites of TfR mRNA (Beinert *et al*., 1997; Aisen *et al*., 1999; Gehring *et al*., 1999; Richardson *et al*., 2010). This will down-regulate the expression of TfR protein due to destabilisation of TfR mRNA. Concomitantly, this increases the ferritin Fe storage in cells as a result of increased ferritin translation. On the other hand, when cells are deprived of Fe, IRP1 will have a high affinity for IRE binding sites of TfR mRNA. The uptake of Fe into the cells will be increased by up-regulating the transcription of TfR protein (Richardson *et al*., 1995). The switch between RNA binding activity and aconitase activity is mutually exclusive as it does not involve any change of IRP1 level (Aisen *et al*., 1999).

Although IRP1 and IRP2 respond in a similar way to cellular Fe changes, the mechanism that regulates their RNA binding activities are different (Guo *et al*., 1995). For example, the binding of IRP1 and IRP2 on IRE are decreased in a Fe repletion condition. However, a decrease in IRP1 binding activity occurs due to a switch into an aconitase form and it occurs without changing the IRP1 levels (Guo *et al*., 1995). On the other hand, a decrease in IRP2 binding activity occurs due to a reduction of IRP2 levels. One possible explanation is that IRP2 is highly sensitive to oxidative stress due to the presence of a conserved cysteine- and proline-rich stretch of 73-amino-acid region (Guo *et al*., 1995). This sequence is encoded by a separate exon and appears to be unstructured. Therefore, it is thought responsible for IRP2 degradation. Although the mechanism of degradation is unclear, IRP2 is oxidised and subjected to the ubiquitination and proteosomal degradation upon the binding of Fe to these amino acid residues (Guo *et al*., 1995; Eisenstein, 2000). In order to maintain a constant level of IRP2, the rapid degradation requires a regulation of *de novo* protein synthesis (Bouton *et al*., 1996).

In contrast to IRP1, IRP2 has a lack of aconitase activity (Bouton *et al*., 1996; Aisen *et al*., 1999). Although IRP2 contains three cysteine residues that are cluster ligands in aconitase enzymes, it has never been observed to assemble a [4Fe-4S] cluster (Beinert *et al*., 1996). Investigations of the IRP2 amino acid sequence indicate that the substitution of Arg^{474} and Ser^{669} to Lys^{611} and Asn^{853}, two amino acids which are essential for the enzyme activity, is the reason why IRP2 does not exhibit aconitase activity (Guo *et al*., 1995). Moreover, IRP2 lacks Ser^{642} which acts as the base in proton abstraction in the aconitase reaction (Beinert *et al*., 1996). Hence, IRP2 is not expected to be converted to an active aconitase. Taking all the limitations of IRP2 and the fact that IRP1 is more abundant, IRP1 is more important than IRP2, although the significance of two IRPs in Fe homeostasis is still unclear (Gehring *et al*., 1999).

1.1.4 Fe-induced cytotoxicity

1.1.4.1 The Fenton reaction

In the Fenton reaction, free Fe^{2+} reacts with hydrogen peroxide (H_2O_2) with the resultant formation of hydroxyl radicals ($^{\bullet}OH$) (Zepp *et al*., 1992; Meneghini, 1997; Tian *et al*., 2010) (Figure 4). This is a paradox in the role of Fe for living organisms. On the one hand, Fe is essential for life, as it serves as a biological catalyst and is an essential component of most enzymes involved in cellular growth (Eisenstein, 2000). On the other hand, the chemical properties of Fe have created problems for living organisms. The redox activity of the Fenton chemistry may become hazardous for the organisms, as the $^{\bullet}OH$ produced can promote cellular stress (Meneghini, 1997; Ponka, 1999). Moreover, the abundance of Fe in biological systems relative to other metals exaggerates its deleterious effects, and this may be attributed to a larger source of $^{\bullet}OH$ (Meneghini, 1997). In the human body, the ratio of Fe to copper (Cu) is 80 to 1 (w/w), which is extremely high, suggesting that Fe is a major element contributing to ROS-induced cellular toxicity (Mordechai, 1988).

$$Fe^{2+} + H_2O_2 \rightarrow Fe^{3+} + {}^{\bullet}OH + OH^{-}$$

Figure 4 The Fenton reaction. Ferrous iron reacts with hydrogen peroxide to form hydroxyl radical together with the formation of ferric iron and the hydroxyl anion.

1.1.4.2 Fe overload

The augmentation of Fe uptake has recently been reported to cause Fe overload in the body (Huang, 2003). This occurs when the total Fe in the body exceeds 5 grams (Huang, 2003). Some evidence has shown that Fe overload is harmful to humans. Those who suffer from hereditary hyperferritinemia cataract syndrome, who have high levels of Fe stored in ferritin, have been discovered to have high oxidative damage in the eyes (Meneghini, 1997). Non-anaemic adults who

have been supplemented with Fe have been shown to have Fe overload and overproduction of pro-oxidants in their bodies (Huang, 2003). This accumulation of free Fe initiates lipid peroxidation in cellular organelles (Myers *et al*., 1991). For example, lipid peroxidation in the mitochondria modifies the permeability state of the membrane and alters solutes and ion transportation, leading to swelling and lysis of the mitochondria (Masini *et al*., 2000). This leads to the damage of microsomes that reduces cytochrome activity (Poderoso *et al*., 1999). Mitochondrial oxidative metabolism in the Fe overload condition indicates a decrease in mitochondrial respiratory control ratio, suggesting Fe-induced mitochondrial lipid peroxidation has occurred (Masini *et al*., 2000). An excessive amount of Fe also initiates lysosomal membrane lipid peroxidation. It increases the lysosomal fragility that interferes with normal fusion of lysosomes with the canalicular membranes (Myers *et al*., 1991). Such alterations inhibit the lysosomal membrane proton pump and increase the intralysosomal pH levels, leading to lysosomal disruption and ultimately in cell death (Myers *et al*., 1991). The participation of Fe in lipid peroxidation indicates that Fe needs to always be chaperoned in order to limit oxidative damage.

1.1.4.3 Fe deprivation

The body's Fe stores are affected by dietary Fe intake and by the cellular Fe usage (Punnonen *et al*., 1997). Consequently, Fe deprivation may occur in a person with a low Fe-containing diet and Fe malabsoption. In adults, serum ferritin concentrations normally range from 15 to 300 µg L^{-1} with 1 µg L^{-1} being equivalent to approximately 8 mg of stored Fe (Geissler and Singh, 2011). When this concentration drops to approximately 60 µg L^{-1}, the intestinal Fe uptake and transportation will respond to Fe deprivation (Hallberg *et al*., 1997; Geissler and Singh, 2011). However, if Fe absorption is insufficient, Fe will be absorbed from the body's tissues. This is reflected in a decrease of circulating Tf saturation. In consequence, Fe delivery to the required sites will be decreased and cause impairment to the cellular Fe-dependent functions especially erythropoiesis

(Geissler and Singh, 2011). This may lead to a decrease of haemoglobin levels and development of anaemia.

Fe deficiency and Fe deficiency anaemia are the most common Fe-related diseases that are major health problems worldwide (Lynch, 2011). They affect hundreds of millions of people and cause a wide range of negative consequences. This includes maternal and child mortality, impaired cognitive and physical development of children, and reduced physical performance and work capacity in adults (Lynch, 2011; Geissler and Singh, 2011). The cellular response to Fe deprivation is a complex process as it involves multiple molecules and signalling pathways (Saletta *et al*., 2011; Yu and Richardson, 2011). One of the most affected molecules is the classical target ribonucleotide reductase, an enzyme that is involved in the reduction of ribonucleotides to deoxyribonucleotides in the synthesis of DNA (Darnell and Richardson, 1999).

Several other molecules have been recognised as possibly being involved in the cellular response to Fe deprivation. This includes proteins that are involved in mitogen activated protein kinase (MAPK) pathway (Yu and Richardson, 2011). Treating several lines of cancer cells including lung cancer, neuroepithelioma and melanoma cells with Fe chelators has markedly increased phosphorylation of stress-activated protein kinases such as JNK and p38 (Yu and Richardson, 2011). This subsequently phosphorylates the downstream protein p53 and leads to apoptosis. Therefore, the effect of Fe deprivation is far broader than just the effect on the classical ribonucleotide reductase. It is likely to involve interactions between several molecular players, in which their possible roles in cell signalling remain to be elucidated. Of a particular concern in Fe deprivation is the problem faced by the industrialised and developing countries as Fe deficiency has become a serious health problem among the citizens.

1.1.5 Carcinogenesis and metabolic role of Fe

1.1.5.1 Cancer cell propagation

In mammals, cell proliferation is required for embryogenesis and cellular growth, as well as for proper function of adult tissues (DeBerardinis *et al*., 2008). The process of cancer formation begins when cells in a part of the body start to grow out of control. Cancer is believed to arise from a series of sequential mutations that occur as a result of genetic instability and/or environmental factors (Golub, 2001). The transition of a normal somatic cell to a cancer cell involves activation of oncogenes and inactivation of tumour suppressor genes. These allow cancer cells to escape the normal control of cellular proliferation, differentiation, migration and death (Lala and Chakraborty, 2001). The frequency of somatic mutations can lead to carcinogenesis in human beings (Lala and Chakraborty, 2001). Molecular changes in the DNA of a founder cell will make the cell unable to control its proliferation and results in the formation of cancer. These changes can vary from a single to multiple mutations in the genome of the original cancer cell. These mutations will affect the control of cell proliferation through impaired cell differentiation (Soto and Sonnenschein, 2011).

Cell division is essential for the complex process of human carcinogenesis. Cell division per se increases the risk of genetic errors required for the formation of single stranded DNA mutations (Pike *et al*., 1993). Epidemiological evidence indicates that increased cell division is a common denominator in the pathogenesis of many human cancers (Preston-Martin *et al*., 1990). In the face of DNA damage, more than one genetic mistake must occur in order for cancer to develop (Cohen and Ellwein, 1991). An increase in the amount of irreparable DNA is attributed to cellular division as division must occur in order for DNA error to be propagated before it can be repaired. Although it is unclear what specific genetic errors occur, or how they occur, a multiple event is required for cancer to develop. This event, which involves multiple steps, is later referred to as initiation,

promotion and progression (Abel *et al*., 2009). Some cancers require a stimulation of cell division for the primary carcinogenic action to occur, thus emphasising the need for cell division in cancer formation.

1.1.5.2 Fe and the risk of cancer

Fe has been positively associated with carcinogenesis. Several lines of evidence support the role of Fe as a cancer initiator or cancer promoter (Stevens *et al*., 1994; Huang, 2003; Chua *et al*., 2010). High dietary intake of Fe has been reported in some epidemiological studies to be associated with elevated cancer risk (Toyokuni, 1996; Huang, 2003). This is the reason why Fe overload is more of a problem than Fe deficiency in meat-eating populations. Given that Fe is essential for cellular growth, it may increase the risk of cancer by enhancing the chances for cancer cells to survive and proliferate (Le and Richardson, 2002). Additionally, Fe may increase the risk of cancer due to its redox reactivity.

Fe-binding sites on macromolecules have been suggested to serve as centres for the repeated production of $^{\bullet}OH$ (Mordechai, 1988). An overproduction of $^{\bullet}OH$ leads to multi-hit effects at the binding site, and causes site-specific damage that initiates neoplastic transformation (Mordechai, 1988). This has been shown in previous studies where Fe^{3+} that is bound to the biological components such as DNA and proteins has undergone cyclic reduction and reoxidation and caused damage to the molecules it is bound to (Mordechai, 1988; Toyokuni, 1996). Furthermore, it has been shown that a Fe^{3+} complex injected into rats caused a 2.5-fold increase in the formation of oxidised DNA (Umemura *et al*., 1990). This may initiate carcinogenesis if it promotes DNA modification. Moreover, based on the capability of Fe to induce lipid peroxidation and cause protein damage (as discussed in section 1.1.4.2), this will further increase the chances for Fe to drive carcinogenesis. A failure in cellular redox regulation, particularly in the antioxidant defence system

to compensate for the overproduction of ROS, may exaggerate the oxidative effect and result in an eventual formation of cancer.

1.1.5.3 Correlation between Fe and cancer

1.1.5.3.1 The role of ferritin in cancer

The body's Fe storage, ferritin, protects cells against oxidative damage by decreasing the cytosolic LIP. However, overexpression of ferritin may lead to the opposite effect, suggesting that Fe sequestered in the ferritin may eventually become pro-oxidant (Wang and Pantopoulos, 2011). Compared to their non-malignant cells-of-origin, cancer cells have an enhanced Fe storage system. In colon cancer for example, the expression of ferritin protein is higher than normal colonic epithelial cells, suggesting that Fe is stored securely in cancer cells to avoid unwanted oxidation with cellular proteins (Toyokuni, 1996). This explains why the body's Fe storage is associated with the prognosis of some cancer types in humans. In neuroblastoma patients, serum ferritin has been reported to increase up to 37-54% at stage III and IV of the disease, which is rarely seen in stage I and II patients (Hann *et al*., 1985). The analysis of free survival progressions has indicated that the increase of ferritin levels was parallel to the poor prognosis of the disease progression (Hann *et al*., 1985). This suggests that cancer cells use ferritin as an additional mechanism to survive over oxidative stress. Besides, this also suggests that serum ferritin is a useful marker for cancer diagnosis and prognosis, which may be of value in characterising and defining patients who are less likely to respond to cancer treatment.

1.1.5.3.2 The role of TfR in cancer

It has been reported that cancer cells have a high requirement for Fe (Richardson and Baker, 1990; Richardson and Baker, 1994; Richardson *et al*., 1994). This is reflected by an increase in the expression of TfR protein in cancer cells when compared to their normal counterparts (Walker and Day, 1986; Soyer *et al*., 1987; Kondo *et al*., 1990). This is not surprising as it allows cancer cells to import more Fe for a rapid proliferation rate. Moreover, Fe is required for the metabolic processes, including mitogenic signalling pathways as well as for DNA synthesis of the rapidly dividing cells (Richardson and Baker, 1990; Richardson *et al*., 1994; Daniels *et al*., 2006; Habashy *et al*., 2010). It has been reported that the expression of TfR protein in neoplasms is associated with tumour stage and progression (Cavanaugh *et al*., 1999). In addition, there has been a correlation between the dependency of some tumour cells on TfR for proliferation, and the metastatic behaviour at a secondary tumour site (Cavanaugh *et al*., 1999). The indicated connection between metastatic capability, TfR responsiveness and TfR expression in certain tumours has inspired our interest in investigating the role of TfR in lung and breast cancers, as an increased expression of TfR protein compared to their normal counterparts has been reported in both cancers (Faulk *et al*., 1980; Walker and Day, 1986; Kondo *et al*., 1990; Cavanaugh *et al*., 1999). Moreover, it has long been reported that the lungs are the most frequent site of breast cancer metastasis (Minn *et al*., 2005), which may be attributed to the presence of high TfR protein expression.

1.1.5.3.2.1 Breast cancer

Breast cancer is the most common malignancy among women (Al-Hajj *et al*., 2003). Statistics in New Zealand show that the incidence of breast cancer has markedly doubled within a period of 40 years with 10,424 women were identified with breast cancer from 1996 to 2000 (Curtis *et al*., 2005; Sarfati *et al*., 2006). Breast cancer is a heterogeneous disease that comprises a variety of

pathological entities (Simpson *et al*., 2005). The risk of having breast cancer is associated with ovarian hormones which correlate to age (Pike *et al*., 1993). Increased breast cancer incidence is thought to be hugely due to increasing lifetime exposure to oestrogen (Sarfati *et al*., 2006). However, other factors need to be considered as the impact of various factors on breast cancer incidence is varied (Pike *et al*., 1993). From an oncologist's point of view, breast cancer patients can be categorised into three main groups. First are those with positive hormone receptor, where the oestrogen receptor may be a potential target for therapeutic options. Second are those with human epidermal growth factor receptor HER2, who will receive HER2 directed therapy. Third are those who have none of the oestrogen, progesterone and HER2 receptors. This group is known as having a triple negative breast cancer, for whom chemotherapy is the only systemic therapy available (Reis-Filho and Tutt, 2008).

Triple negative breast cancers are more aggressive than other breast cancer types and account for 10 to 15% of all breast carcinomas (Bauer *et al*., 2007; Reis-Filho and Tutt, 2008). Those who suffer from this cancer are normally characterised by a poor prognosis and a lack of responsiveness to the usual endocrine therapies (Bauer *et al*., 2007). Indeed, they have a poorer survival rate than those with other breast cancer types, regardless of the disease stage (Bauer *et al*., 2007). Of interest, breast cancer cells have been shown to express high levels of TfR protein compared to normal breast cells (Faulk *et al*., 1980). A study conducted by Walker and Day (1986) examined a variety of breast carcinomas for the expression of TfR protein. They reported that 70% of the breast carcinomas investigated was positive for TfR protein expression compared to normal breast cells that have no evidence or a relatively low expression of TfR protein. In addition, the overexpression of TfR has also been correlated to the metastatic capability of breast cancer cells (Cavanaugh *et al*., 1999). This suggests that breast cancer cells have a high requirement for Fe for rapid proliferation. Therefore, investigating the cellular Fe regulation in breast cancer may reveal the molecular mechanism by which Fe is regulated by cancer cells for their survival and proliferation.

1.1.5.3.2.2 Lung cancer

Lung cancer is one of the most common malignant tumours with an increasing trend of incidence over the past decade. It is currently the first or second most frequent cancer among men and the third or fourth most frequent cancer among women (Janssen-Heijnen and Coebergh, 2001). At the beginning of the 20th century, the incidence of lung cancer was very low in New Zealand. However, it has increased dramatically to become a major cause of cancer death, and accounts for 19% of all cancer deaths with approximately 1500 deaths per year (Stevens *et al*., 2007). The prevalence of lung cancer mortality in New Zealand has also been reported to increase among Maori compared to non-Maori, mainly due to their heavy smoking behaviour (Stevens *et al*., 2008).

Lung cancer is classified based on clinicopathological features as small-cell lung carcinomas (SCLC) and non-small cell lung carcinomas (NSCLC) (Bhattacharjee *et al*., 2001). SCLC is a highly malignant carcinoma and is characterised based on neuroendocrine features (Bhattacharjee *et al*., 2001). On the other hand, NSCLC, which is subcategorised into adenocarcinomas, squamous cell carcinoma and large-cell carcinomas, is histopathologically and clinically different from SCLC. Adenocarcinomas are the most common malignancy of NSCLC (Bhattacharjee *et al*., 2001). Currently, both SCLC and NSCLC are cured with chemoradiotherapy, but patients normally cannot easily endure the side effects of the treatment. Therefore, a new method is needed for lung cancer therapy.

A study conducted on adenocarcinomas of lung reported that lung cancer cells were positive for TfR protein expression relative to their normal counterpart (Kondo *et al*., 1990). This was evidenced from an immunohistological staining, whereby normal bronchoalveolar epithelial cells were found to be negative for TfR but strongly positive in alveolar macrophages (Kondo *et al*., 1990). The immunoreactivity has been reported to be proportionally related to the stage of lung

cancer (Kondo *et al*., 1990). This strongly suggests that lung cancer cells have a high requirement for Fe in order to progress to an advanced stage. Therefore, the presence of high TfR protein expression in lung cancer cells suggests a new molecular target for the treatment of lung carcinomas, all of which may provide a better treatment with fewer side effects to the patients.

1.1.6 Therapeutic use of Fe

Cancer cells frequently develop multidrug resistance to chemotherapy agents (Liang *et al*., 2009; To *et al*., 2010). Considering this, new methods of inhibiting cancer cell growth are urgently required. Fe is one of the biological targets that has been extensively studied and has a promising outcome so far. Several lines of evidence suggest that cancer cells proliferation can be inhibited using Fe-chelating agents (Richardson *et al*., 1995; Darnell and Richardson, 1999). Their ability to inhibit cellular growth reflects the essentiality of Fe in a number of metabolic pathways, including DNA synthesis. Currently, deferoxamine (DFO) is the most widely used Fe chelator, which has a high affinity and specificity for Fe^{3+} (Darnell and Richardson, 1999). DFO is clinically used for acute Fe poisoning, as well as for the treatment of Fe overload in thalassemia patients (Richardson *et al*., 1994; Lederman *et al*., 1984).

Interestingly, DFO has been shown to be extremely cytotoxic to neoplastic cells while having a marginal effect on normal cells (Becton and Bryles, 1988; Richardson *et al*., 1994). DFO possesses an anti-proliferative activity, whereby it is implicated in cell cycle arrest and inhibition of cellular growth (Richardson *et al*., 1994; Lederman *et al*., 1984; Richardson, 2002). Retardation of cellular growth has been shown in one *in vitro* study of human lymphocytes, whereby a depletion of Fe by micromolar concentrations of DFO inhibits 50% of ribonucleotide reductase activity and prevents the cells from completing the S phase of the cell cycle progression (Lederman *et al*., 1984). The inhibition of cellular growth by DFO has also been shown to increase p53-transactivated genes,

WAF1 and GADD45, which leads to cell cycle arrest and apoptosis (Darnell and Richardson, 1999). Despite its efficacy as an anti-proliferative agent, the effect of DFO is limited by its short half-life and its low lipophilicity and membrane permeability (Le and Richardson, 2004; Yu and Richardson, 2011). Moreover, DFO has a poor absorption from the gut and requires a long subcutaneous administration of about 12 to 24 h a day for 5 to 6 times a week (Gao and Richardson, 2001). Therefore, this has prompted researchers to investigate the anti-proliferative activity of other Fe chelators.

A recent development in studies of Fe chelators has generated other Fe chelators, which have an improved lipophilicity and a more potent anti-proliferative activity at preventing cancer cell growth (Whitnall *et al*., 2006). One such chelator that exerts its efficacy both *in vitro* and *in vivo* is di-2-pyridylketone-4,4-dimethyl-3-thiosemicarbazone (Dp44mT) (Whitnall *et al*., 2006). Dp44mT has a better lipophilicity, cytotoxicity and selectivity against human tumours (Rao *et al*., 2009). Dp44mT has been shown to decrease tumour weight in mice by 47% in 5 days of treatment, indicating a potent and rapid cytotoxicity (Yuan *et al*., 2004). This cytotoxicity has been shown to be mediated by the mitochondrial apoptotic pathway, which accounts for a prominent 29-fold increase of caspase-3 activity (Yuan *et al*., 2004). In a later study, the cytotoxic mechanism of Dp44mT has been shown to involve the inhibition of DNA topoisomerase 2α (Rao *et al*., 2009). This finding has been then proposed as the primary mechanism by which Dp44mT inhibits cancer cell growth. Indeed, this finding indicates that Dp44mT has a very selective effect in mediating its cytotoxicity. All of these studies suggest that novel Fe chelators have a more potent and a broader anti-tumour activity due to their unique mechanism of action. This is promising as they can be used to overcome the resistance of cancer cells against the current available treatments. In addition, these studies also proved that Fe is indispensable for the cell cycle progression, through which it can be used as a major molecular target to inhibit the growth of cancer cells.

1.2 Nitric oxide ($^{\bullet}$NO)

1.2.1 $^{\bullet}$NO overview

In the past few years there has been an explosion of interest in $^{\bullet}$NO, a molecule that occupies a central role in the physiological system. $^{\bullet}$NO is a short-lived molecule, produced from L-arginine by nitric oxide synthase (NOS) (Colasanti and Suzuki, 2000; Lala and Chakraborty, 2001). There are three isoforms of NOS, two of which are calcium dependent: NOS1 (neuronal NOS) and NOS3 (endothelial NOS), and the other is NOS2 (inducible NOS), which is calcium independent. $^{\bullet}$NO which is produced by NOS1 and NOS3 at a sustained, low level in a range of pico to nanomolar concentrations, is involved in physiological events (Hofseth *et al*., 2003). On the other hand, $^{\bullet}$NO which is produced by NOS2 in a range of micromolar concentrations upon cellular induction, is potentially involved in pathological processes (Colasanti and Suzuki, 2000; Hofseth *et al*., 2003). This represents a dual personality of $^{\bullet}$NO as either cytotoxic or cytoprotective depending on its concentrations.

$^{\bullet}$NO was first discovered as an endothelium-derived relaxing factor (EDRF) (Furchgott and Zawadzki, 1980). It is the key mediator for a wide variety of physiological processes including vasodilation, neurotransmission, platelet aggregation and Fe metabolism (Hofseth *et al*., 2003). $^{\bullet}$NO has a high lipophilicity in nature that allows the molecule to easily diffuse through cell membranes (Hirst and Robson, 2007). The capability of $^{\bullet}$NO to diffuse several hundred microns through tissues makes it a perfect signalling molecule. This accounts for the role of $^{\bullet}$NO in physiological and pathophysiological processes (Hirst and Robson, 2007). Indeed, this property of $^{\bullet}$NO suggests that it is rapidly synthesised on demand in response to stimuli (Miller and Megson, 2007). However, the molecular arrangement of $^{\bullet}$NO leaves an unpaired electron, thus making the molecule a free radical.

Therefore, •NO can react with other molecules and cause damaging effects (Lala and Chakraborty, 2001; Hirst and Robson, 2007). This attributes to the involvement of •NO in a wide variety of pathological disorders, including cancer, in which overwhelming evidence suggest the role of •NO in the early initiation of cancer formation (Oshima and Bartsch, 1994; Tamir and Tannenbaum, 1996; Patel *et al*., 1999).

1.2.2 The role of •NO in carcinogenesis

•NO is a small diatomic free radical that can generate the production of many reactive intermediates (Lala and Chakraborty, 2001). This accounts for its bioactivity as a mutagenic molecule. Continuous exposure to •NO in moderate to high concentrations may have an active role in carcinogenesis (Fukumura *et al*., 2006). However, the net effect of •NO also depends on other factors including target cell types as well as its interactions with other reactive radical species, metal ions and proteins (Thomsen *et al*., 1995; Hofseth *et al*., 2003). In the course of defence against pathogenic particles, NOS2 is induced to produce •NO up to micromolar concentrations. This concentration is high enough to promote neoplastic transformation, which is presumed to be the initial step in cancer formation. Moreover, the •NO produced may remain for a long period in the cellular system and can possibly act on healthy neighbouring epithelial cells and drive carcinogenesis (Hofseth *et al*., 2003; Fukumura *et al*., 2006).

•NO-induced carcinogenesis can occur via several mechanisms. First, •NO has the capability to cause DNA damage through a process of nitrosation (Tamir *et al*., 1996). It is known that autooxidation of •NO will form dinitrogen trioxide (N_2O_3), which is an electrophilic nitrosating agent that is commonly involved as an intermediate in nitrosation (deRojas-Walker *et al*., 1995). Nitrosation of primary amines produces alkylating intermediates that can react with DNA at several

nucleophilic sites and cause deamination of the nucleobases (Tamir and Tannenbaum, 1996; Tamir *et al*., 1996). Given that many purines and pyrimidines are primary aromatic amines, N_2O_3 can directly damage the DNA by deaminating DNA nucleobases and causing DNA strand breaks (Tamir and Tannenbaum, 1996; Xu *et al*., 2002). On the other hand, nitrosation of secondary and tertiary amines will form *N*-nitrosamines (deRojas-Walker *et al*., 1995). *N*-nitrosamines are known to be carcinogenic due to the formation of methylating agents that can be a source of DNA strand breaks from the addition of methyl groups to a number of nucleophilic sites on the DNA bases (Wyatt and Pittman, 2006). Therefore, these methylating agents will eventually cause DNA damage. Additionally, DNA damage can also be initiated by $^{\bullet}NO$ through oxidative damage (Tamir and Tannenbaum, 1996). The reaction of $^{\bullet}NO$ and superoxide (O_2^-) will produce peroxynitrite ($ONOO^-$), which is a stronger and a more active reactive radical species compared to $^{\bullet}NO$ (Radi *et al*., 1991). $ONOO^-$ can rapidly destroy DNA by attacking both deoxyriboses and causing mutations and DNA strand breaks (Patel *et al*., 1999; Lala and Chakraborty, 2001).

The second mechanism suggesting a role for $^{\bullet}NO$ in carcinogenesis is the induction of mutations in the p53 tumour suppressor gene (Murata *et al*., 1997). The inactivation of p53 has been shown to be due to single base substitutions, preferentially C:G to T:A at CpG sites in the p53 coding region (Cho *et al*., 1994; Murata *et al*., 1997). Besides containing sequence specific for DNA binding activity of p53 protein (residue 102-292), this region is also preferential due to the encoded amino acids that are important for maintaining the tertiary structure of the protein by coordination of zinc (Murata *et al*., 1997). As well as inducing mutations, $^{\bullet}NO$ exposure also results in the up-regulation of p53 gene transcription (Forrester *et al*., 1996). Therefore, the possibility for mutations to occur is higher as single stranded DNA exposed during transcription is more vulnerable to mutagenesis (Murata *et al*., 1997). Mutation will cause structural changes in the p53 DNA binding domain, which will result in loss of DNA binding and inactivate p53 as a transcription factor.

1.2.3 Interaction of •NO and Fe

The activity of •NO in the physiological system is pervasive. It is not restricted to DNA but also involves other cellular constituents. Of our interest, the switch of IRPs' functions between the IRE binding activity and the aconitase activity can be operated by •NO (Pantopoulos and Hentze, 1995; Oliveira and Drapier, 2000). •NO has been shown to increase the stability of TfR mRNA against targeted degradation, which in return inactivates aconitase activity (Weiss *et al*., 1994; Gardner *et al*., 1997). The stabilisation of TfR mRNA causes an increase in TfR protein expression while repressing ferritin mRNA translation (Richardson and Baker, 1992; Gardner *et al*., 1997). These effects mimic the consequence of Fe starvation. The molecular mechanism involves the interaction of •NO with metal Fe in the centre of aconitase and causes a removal of labile Fe atom in the [4Fe-4S] cluster (Pantapoulos *et al*., 1994). This results in the release of free Fe in a form of Fe-nitroxyl complex (Pantopoulos and Hentze, 1995; Ford *et al*., 1998). For example, the binding of •NO to haem proteins will form Fe-nitroxyl haem that potentially causes haem poisoning. Therefore, this interaction mediates •NO-induced cytotoxicity as loss of Fe results in a termination of essential metabolic functions such as mitochondrial respiration, DNA synthesis and Krebs cycle (Pantapoulos *et al*., 1994). Taking into account the significant involvement of •NO in biological processes, especially in regulating cellular Fe metabolism, there has been a remarkable increase in research being conducted to generate synthetic compounds that can release •NO *in vivo*.

1.2.4 •NO-donating drugs

Despite its structural simplicity, •NO has a complex chemistry, granting the molecule a variety of biological actions (discussed in section 1.2.1). The characteristics and functions of •NO make the molecule useful for therapeutic use. However, •NO is a difficult molecule to handle with a very limited half-life of ~6 s (Beckman and Koppenol, 1996). Moreover, •NO easily reacts with oxygen to form nitrogen dioxide (NO_2), making it an even more difficult molecule to handle. Considering this, a carrier for •NO, termed •NO donor, is needed to stabilise the short-lived molecule so that it can at least be delivered to the required site. Current research has made an advance to the development of •NO donors, two of which have been used clinically and the rest are still under investigation.

1.2.4.1 Clinically used •NO donors

1.2.4.1.1 Glyceryl trinitrite (GTN)

Organic nitrates are the most frequently used •NO donor and the most common one is GTN, also known as nitroglycerine (Miller and Megson, 2007). GTN is used for acute relief of pain associated with angina: its ointments are normally used for the treatment of anal fissure (Fenton *et al*., 2006) and its transdermal patches are used in heart failure and chronic angina (Yurtseven *et al*., 2003). The chemical structure of GTN indicates that it contains three nitro-oxy ester groups, but it only releases one molar of •NO upon bioactivation (Bennett *et al*., 1989). The *in vivo* release of •NO from GTN requires catalysis from a specific enzyme, namely mitochondrial aldehyde dehydrogenase (mADH) (Chen *et al*., 2002). In the presence of as low as nanomolar concentrations of GTN, mADH can catalyse the formation of •NO together with the formation of 1,2-glyceryl-

dinitrate (Chen *et al*., 2002). This formation has been shown to increase cyclic guanosine monophosphate (cGMP) and cause relaxation of vascular smooth muscle, leading to vasodilation and increased blood flow (Chen *et al*., 2002).

1.2.4.1.2 Sodium nitroprusside (SNP)

Another clinically used •NO donor is SNP. It is a drug of choice in clinical studies, which is used extensively in the case of hypertensive crises to rapidly lower blood pressure (Butler and Glidewell, 1987; Miller and Megson, 2007). SNP is relatively stable in the physiology and therefore requires either light or tissue-specific mode of release for •NO production (Grossi and D'Angelo, 2005). In spite of its efficacy, the clinical use of SNP has a marked limitation as it has a potential to form cyanides, compounds which are highly cytotoxic (Butler and Glidewell, 1987; Bates *et al*., 1991). One mole of SNP is capable of releasing four to five moles of cyanide, which may cause cyanidosis in patients (Butler and Glidewell, 1987).

1.2.4.2 Current developments in •NO donors

1.2.4.2.1 Diazeniumdiolate (NONOate)

NONOate is a class of •NO donors that consists of a diolate group that is bound to a nucleophile adduct via a nitrogen atom (Miller and Megson, 2007). In the cellular system, NONOate decomposes spontaneously at physiological pH and temperature, resulting in a formation of approximately 2 molar equivalents of •NO (Miller and Megson, 2007). The rate of NONOate decomposition is dependent on the structure of nucleophile adduct it is bound to, of either primary or secondary amine or polyamine (Miller and Megson, 2007). The release of •NO by NONOate follows first-order kinetics, and thus the rate of its decomposition is easily predicted (Mooradian *et*

al., 1995). This quantitative release of •NO has made NONOate a potentially useful tool for research. One of the NONOates that has been extensively studied is diethylamine •NO adduct (DEA/•NO), which is used frequently for the study of cardiovascular disease (Vanderford *et al*., 1994). DEA/•NO is a potent vasodilator as it causes a decrease in pulmonary and systemic arterial pressure (Vanderford *et al*., 1994). It has been shown that DEA/•NO reverses vasospasm and prevents the occurrence of cerebral vasospasm in a primate model (Pluta *et al*., 1997). This suggests the potential use of NONOate as a targeted therapy for the treatment of delayed cerebral vasospasm. However, NONOate is still under investigation to confirm its efficacy and safety without any systemic toxicity.

1.2.4.2.2 *S*-nitrosothiols (RSNO)

RSNO are biological metabolites of •NO detected in extracellular and intracellular spaces (Hogg, 2000). They were first discovered to be involved in biological processes through investigations of guanylyl cyclase activation, where RSNO are implicated as intermediates in •NO-dependent and guanylyl cyclase-independent signalling processes (Hogg, 2000; Batchelor *et al*., 2010). Reactive protein thiols (RSH) are regarded as a major intracellular target of •NO, in which a direct reaction will form thiol disulphide (RSSR) and nitroxyl anion (NO^-) (Kharitonov *et al*., 1995; Hogg, 2002). The reaction of •NO with RSH at a neutral pH will produce *S*-nitrosocysteine (CySNO) and *S*-nitrosoglutathione (GSNO), two of the RSNO that exist *in vivo* (Al-Sa'doni and Ferro, 2000) (Figure 5).

$$N_2O_3 + RSH \rightarrow RSNO + NO_2^- + H^+$$

Figure 5 General formations of *S*-nitrosothiols. Nitric oxide via dinitrogen trioxide reacts with thiol to form *S*-nitrosothiol together with nitrite and hydrogen ion.

RSNO are biologically stable molecules with the bond between sulphur and nitrogen a stable covalent bond (Hogg, 2002). The bond is slightly polar, as sulphur is more negative than nitrogen (Hogg, 2002). RSNO are not particularly susceptible to homolysis to break the bond to form $^{\bullet}NO$, but under certain circumstances, RSNO may decompose and be metabolised to form $^{\bullet}NO$ (Hogg, 2002). Several factors have been recognised to affect the stability of RSNO. First, the presence of cuprous ion (Cu^{2+}) at concentrations as low as 10^{-5} M has been shown to increase the susceptibility of RSNO to catalytic decomposition (Butler *et al*., 1998). $^{\bullet}NO$ will be released from RSNO upon the interaction of Cu^{+}, which reacts as an intermediate to bind nitrogen atom of $^{\bullet}NO$. This will produce RS^{-} and Cu^{2+}, both of which will undergo recirculation to regenerate Cu^{+} and RSSR upon dimerization of RS^{-} (Butler *et al*., 1998) (Figure 6).

$RSNO + Cu^{+} \leftrightarrow X$

$X \rightarrow RS^{-} + {}^{\bullet}NO + Cu^{2+}$

$RS^{-} + Cu^{2+} \rightarrow \frac{1}{2} RSSR + Cu^{+}$

Where X is the complex by which RSNO react as a metal ligand

Figure 6 Copper-mediated RSNO decomposition. Copper ion reacts as an intermediate to interact with *S*-nitrosothiol and releases nitric oxide together with the formation of thiol disulphide. The presence of copper ion enhances nitric oxide release from RSNO.

Second, the enzymatic activity of γ-glutamyl transpeptidase also enhances the decomposition of RSNO (Askew *et al*., 1995). In this reaction, γ-glutamyl transpeptidase catalyses the cleavage of one of the peptide bonds in glutathione (GSH) and releases glycylcysteine. Concomitantly, the glutamyl moiety will be transferred to another amine. The fission of the cysteine-glutamic acid peptide bond will form *S*-nitrosoglycylcysteine that will decompose to $^{\bullet}NO$ with the expected formation of glycylcysteine disulphide (Askew *et al*., 1995).

Third, the exposure of RSNO to strong, direct light also accelerates its decomposition (Sexton *et al*., 1994; Zhelyaskov *et al*., 1998). The excitation of RSNO upon absorption of light has been shown to peak at 340 and 545 nm, and this has been found to cleave the S-N bond and release •NO (Sexton *et al*., 1994). The decomposition of GSNO via this mechanism has been investigated *in vitro* using HL-60 leukaemia cells (Sexton *et al*., 1994). Photoactivated GSNO has caused ~60% of cell death compared to ~40% cell death without photoactivation. This result suggests the potential cytotoxic effect of •NO released by GSNO, which brings us to the design of our group's synthesised •NO donating drug.

1.2.4.2.3 Novel •NO donor: *tert*-dodecane-*S*-nitrosothiol (tDSNO)

tDSNO is a new drug based on the *S*-nitrosothiol functionality, which has been designed by the Giles Group as a •NO releasing drug (Giles *et al*., 2008). tDSNO is a light sensitive drug, which absorbs light at 340 nm with the extinction coefficient (ε_{340}) equal to 675 $M^{-1}cm^{-1}$. In buffer systems, sustained photoactivation of 20 µM tDSNO has been shown to release •NO at the rate of 0.46 ± 0.10 $\mu M^{-1}min^{-1}$ with a half-life of approximately 4 h upon photoactivation and 50 h in the absence of light (Gang and Kumari, unpublished data). The sensitivity of tDSNO to the light is used as the main switch to its activation mechanism. Considering several factors including metal ions and enzymatic activities, and for the most part, the light, the stability of tDSNO is dependent on the factors available. The biochemical activity and the cytotoxicity of tDSNO upon exposure to light are currently under investigation.

Category	•NO donors	Half-life	Chemical structure
Clinical use	GTN	3 min	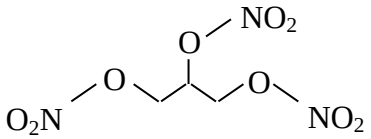
	SNP	2 min	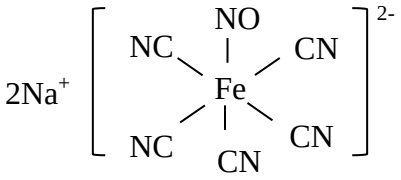
Under investigation	DEA/•NO	4 min	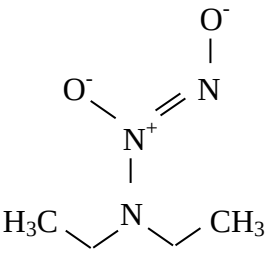
	GSNO	≥ 90 min	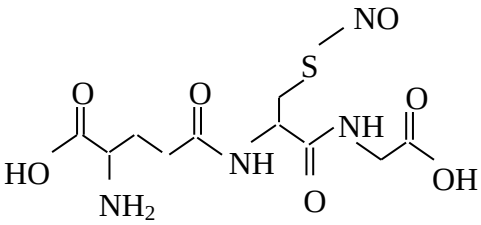
	tDSNO	4 h - light 50 h - dark	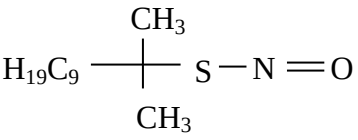

Figure 7 Chemical structures of •NO donors. GTN and SNP are currently used in clinical area whereas DEA/•NO, GSNO and tDSNO are some of •NO donors that are still under investigation.

1.3 Hypotheses

As a substantial crosstalk exists between Fe and •NO homeostatic mechanisms, we hypothesised that modulating Fe levels in cancer cells would change their resistance to •NO, thus increasing the effectiveness of tDSNO drug treatment. This was explored through the following experimental questions:

1. **Does a low level of •NO release cause cells to import Fe to cytotoxic levels?**

   Firstly, we hypothesised that •NO released from tDSNO would promote cancer cells into continuously importing Fe. This would lead to Fe overload, which was predicted to cause Fe toxicity in cancer cells. Additionally, as excessive free Fe is highly susceptible to Fenton chemistry, an accumulation of Fe above normal cellular levels was predicted to catalyse the toxic effects of background ROS production in cancer cells.

2. **Does Fe deprivation increase the susceptibility of cells to •NO-induced cytotoxicity?**

   Secondly, we hypothesised that •NO released by tDSNO would be more cytotoxic to Fe-deprived cancer cells compared to cells with normal Fe homeostasis. Fe deprivation was predicted to cause cellular growth inhibition and lead to apoptosis. This effect was predicted would be exaggerated upon the exposure of •NO.

By answering these questions, we aimed to evaluate if modulating cellular Fe levels would increase the therapeutic activity of the drug tDSNO, eventually leading to a novel anti-cancer treatment.

1.4 Objectives

The experiments were designed to evaluate the effect of •NO from tDSNO exposure using the following approaches.

1. For the evaluation of Fe overload in cancer cells, we aimed to:

- *Determine the extent to which •NO caused an increase in Fe uptake in cancer cells.*

  Human triple negative breast cancer cells, MDA-MB-231, and human epithelial-like lung carcinoma cells, A549, were used to study the effect of •NO on cellular Fe uptake. Cells were exposed to 5, 25 and 40 μM of tDSNO for 24 h under the conditions of photoactivation and non-photoactivation. Intracellular Fe content was then measured using an Fe uptake assay. In order to enhance Tf-bound Fe uptake, ferric ammonium citrate (FAC) was used as an external Fe supply. It was predicted that upon exposure to •NO, intracellular Fe uptake would increase.

- *Measure the cytotoxic effect of increased in Fe levels on cancer cell viability.*

  For this purpose, MDA-MB-231 and A549 cells were exposed to a range of tDSNO concentrations (from 2 to 350 μM). The exposure was performed for 24 h under photoactivation and non-photoactivation conditions. Then, cancer cell viability was measured using the MTT assay, which is commonly used in high throughput screening. It was predicted that high levels of intracellular Fe would exaggerate the effects of •NO-induced stress, resulting in an increase in the apparent cytotoxicity of the drug tDSNO.

2. For the evaluation of cytotoxicity of tDSNO in Fe deprivation, we aimed to:

- *Determine the cytotoxic effect of tDSNO in Fe-deprived cancer cells.*

  DFO was used in order to deprive cancer cells (MDA-MB-231) of Fe. DFO was chosen as it has been used in the clinic as a potent Fe chelator and can effectively chelate Fe from a range of cell types including human melanoma, leukaemia, neuroblastoma and neuroepithelioma cells (Richardson and Baker, 1992; Richardson, 2002). Following 24 h of exposure to DFO from 10 to 300 μM, cells were exposed to tDSNO from 40 to 80 μM for 24 to 48 h. The cytotoxicity was then measured after completing both treatments by measuring cell viability using the MTT assay. As a result of Fe deprivation, the cells were predicted to have a lack of essential survival mechanisms and be more susceptible to apoptosis, and hence be more sensitive to $^{\bullet}$NO-induced cytotoxicity.

CHAPTER 2: MATERIALS AND METHODS

2.1 The synthesis of tDSNO

tDSNO was synthesised in our laboratory under an argon atmosphere using *tert*-dodecanethiol and *tert*-butyl nitrite, both of which were purchased from Sigma-Aldrich. Argon gas was passed through a flask to purge oxygen from the flask and 3.7 mM of *tert*-dodecanethiol was added followed by 4.1 mM of *tert*-butyl nitrite. The argon gas was stopped right after the addition of both chemicals, but the reaction mixture was continuously stirred for 15 min on ice. The product was obtained by evaporating the solution using a rotary vacuum evaporator at a pressure of 250 to 300 mbar for 15 min, and tDSNO was characterised by ultraviolet-visible (UV-Vis) spectroscopy using a wavelength scan ranging from 300 to 800 nm. The formation of tDSNO was confirmed by the absorbance at 340 nm and 550 nm, as these are characteristics of RSNO. The tDSNO obtained was stored at -20^{o}C in a dark container, as it is a light sensitive drug. To allow for decomposition upon storage, drug levels were re-established prior to each experiment using ε_{340} equal to 675 $M^{-1}cm^{-1}$.

2.2 Cell culture techniques

2.2.1 Cell maintenance

This study was entirely conducted *in vitro* using MDA-MB-231 and A549 cells. Both cell lines were purchased from the American Type Culture Collection (ATCC). All reagents were purchased from Invitrogen unless otherwise stated. Cells were grown in advanced Dulbecco's Modified Eagle Medium (DMEM) containing 2% foetal bovine serum (FBS), 1% stabilised antibiotic antimycotic solution and 1% GlutaMAX-I. Cells were cultured in 75 cm^2 flasks and incubated at 37^{o}C, humidified with 5% CO_2. Cells were passaged when they reached 80% confluency using 0.25%

Hyclone ® Trypsin to detach the cells from the flasks. Cells were centrifuged for 3 min at 2000 rpm, 20^{o}C to obtain cell pellet to be used for cell seeding.

2.2.2 Cell seeding

For any particular experiment unless otherwise stated, MDA-MB-231 cells were seeded at 100,000 cells per mL and A549 cells at 80,000 cells per mL. Both cell lines were seeded in a volume of 100 µL per well for 96-well plates and 2 mL per well for 6-well plates. Cell counting was performed using Hausser Scientific Bright-Line Hemocytometer under Olympus CK40 microscope. Cells were considered ready for an experiment when 80% confluency was achieved.

2.3 Lysate preparation

All steps were conducted on ice. Media in plates were removed and cells were washed with 1 mL of PBS. After removing PBS, cells were incubated for 10 min with 150 µL of Tris-HCl lysis buffer (1% Triton X-100, 10 mM Tris, pH 8.5) that contained protease inhibitor (1x) purchased from Roche Diagnostics. The monolayer cells were scraped thoroughly into the lysis buffer and centrifuged for 15 min at 12,500 rpm, 4^{o}C. The cell lysates obtained were transferred into new microfuge tubes for further experiments.

2.4 Bradford assay

A calibration curve of bovine serum albumin (BSA) was first obtained for a measurement of protein content. 10 mg of BSA dissolved in 1 mL of Tris-HCl lysis buffer (0.1% Triton X-100, 10 mM Tris, pH 8.5) was diluted from 0.1 to 1.0 mg mL^{-1}. 10 µL of each solution was pipetted into microfuge tubes and 1 mL of Bradford reagent diluted in distilled water (1:4 v/v) was pipetted into

the microfuge tubes and incubated for 5 min. Then, the solution was transferred into a 12-well plate. The absorbance of blue colour formed was measured at 595 nm, blanked with 10 µL of Tris-HCl lysis buffer (0.1% Triton X-100, 10 mM Tris, pH 8.5) mixed with 1 mL of diluted Bradford reagent. The same procedure was repeated to measure protein content in cell lysates.

2.5 Treatment administrations

2.5.1 tDSNO

tDSNO stock solution was prepared in an absolute dimethyl sulfoxide (DMSO) solution. Prior to any particular experiment, the absorbance of stock tDSNO was measured using UV-Vis spectroscopy and ε_{340} equal to 675 $M^{-1}cm^{-1}$. This stock solution was then diluted into the required concentration using 0.1% (v/v) DMSO as the vehicle for tDSNO delivery. This concentration was kept constant for all experimental treatments and controls. MDA-MB-231 and A549 cells were exposed tDSNO to either as a single treatment or with a combination of other drugs, at concentrations stated in figure legends.

2.5.2 FAC

1 mM of FAC (Sigma-Aldrich) stock solution was prepared with 5 mM of ascorbate in distilled water at least 2 h in advance and stored at 37^{o}C to ensure that more than 90% of Fe was in Fe^{2+} form (Tulpule *et al.*, 2010). This stock solution was diluted to a particular concentration in advanced DMEM and used for cellular treatments. FAC was administered to MDA-MB-231 and A549 cells either as a single treatment or combined with tDSNO at concentrations stated in figure legends.

2.5.3 DFO

DFO (Sigma-Aldrich) is the Fe chelator that was used to bring Fe to low levels. 1 mM of stock DFO was prepared in PBS and diluted to a particular concentration in advanced DMEM to be used for cellular treatments.

2.6 Photoactivation technique

Following a treatment with tDSNO, MDA-MB-231 and A549 cells were photoactivated for 1 h under a 100 W light bulb, which was positioned 55 cm above the centre of the transparent plate. After 1 h photoactivation, the photoactivated cells were transferred to the incubator for the duration of the assay. Unless otherwise stated, a set of non-photoactivated cells were used as a control, in which case control cells were incubated with tDSNO at 37^{o}C in the incubator without exposure to light.

2.7 MTT assay

All cytotoxicity assessments in both MDA-MB-231 and A549 cells were performed using 3-(4,5-dimethylthiazol-2-yl)-2,5-diphenyltetrazolium bromide (MTT) assay. It is a colourmetric assay that is well established to assess the viability and the proliferation of cells in cell culture environment (Fotakis and Timbrell, 2006). The assay only detects living cells, which is based on the cleavage of tetrazolium ring by the mitochondrial enzyme, succinate dehydrogenase, to produce a visible dark blue formazan crystal (Denizot and Lang, 1986; Fotakis and Timbrell, 2006; Almazan *et al*., 2000). The formazan crystal formed is impermeable to the cell membrane and thus remains in the healthy cells (Fotakis and Timbrell, 2006). The amount of MTT cleaved is equal to the amount of blue formazan generated (Gerlier and Thomasset, 1986).

Following any particular treatment, MDA-MB-231 and A549 cells were washed with 100 µL of PBS to remove any remaining drug residue. Then, 100 µL of 0.4 mg mL^{-1} of MTT solution prepared in advanced DMEM was added to the 96-well plate to replace the existing media. Cells were then incubated for 3 h at 37^{o}C. After 3 h, media was removed and 200 µL of DMSO solution was added to the wells to dissolve the formazan crystal formed. The absorbance was read at 550 nm using a microplate reader (Bio-Rad Benchmark Plus). Cell viability was calculated as a percentage of control using the following formula:

$$\text{Cell viability (\%)} = \frac{\text{Average (absorbance in each treatment - absorbance of the blank)}}{\text{Average (absorbance of control - absorbance of the blank)}} \times 100$$

The inhibitory concentration (IC_{50}) value was defined as the concentration of a drug that reduced the absorbance to 50% of that found for the control.

2.8 The ferrozine assay

2.8.1 Fe calibration curve

A ferrozine based colourmetric assay was used to quantify the formation of ferrous iron-ferrozine complex as a measurement of Fe content inside the cells. The ferrozine Fe detection reagent was prepared by dissolving 6.5 mM ferrozine, 6.5 mM neocuproine, 2.5 M ammonium acetate and 1 M ascorbate in distilled water. Then, a standard curve for the measurement of solution Fe concentration was established using 0 to 200 µM of ferrous sulphate ($FeSO_4$). 100 µL of $FeSO_4$ dissolved in 10 mM HCl was mixed with 100 µL of Tris-HCl lysis buffer (1% Triton X-100, 100 mM Tris, pH 8.5) and 100 µL of 1.4 M HCl. The mixture was then incubated for 2 h at 60^{o}C. After 2 h, the solution was cooled down and 30 µL of the ferrozine Fe detection reagent was added,

followed by 30 min incubation at room temperature. After 30 min, the solution was pipetted into a 96-well plate and the absorbance was read at 550 nm.

Upon optimisation, this assay was capable of detecting Fe^{2+} by forming a purple coloured solution when the ferrozine Fe detection reagent was added. The absorbance of the complex formed was maintained for at least 60 min. In a solution, Fe is present in both Fe^{2+} and Fe^{3+} forms. Therefore, to determine whether this assay measures Fe^{2+} or Fe^{3+}, ferric sulphate ($Fe_2(SO_4)_3$) was used to replace $FeSO_4$. Similar to $FeSO_4$, a purple coloured solution was formed upon the addition of the ferrozine Fe detection reagent. This indicated that the assay could detect both Fe^{2+} and Fe^{3+}. However, since the ferrozine Fe detection reagent contained ascorbate, Fe^{3+} might be reduced to Fe^{2+}, thus suggesting the assay only detected Fe^{2+}. To clarify this matter, ascorbate was omitted from the ferrozine Fe detection reagent and the results obtained indicated that Fe^{3+} could not be detected even up to 100 µM of $Fe_2(SO_4)_3$, with a colourless solution being formed. Unlike Fe^{3+}, Fe^{2+} could be detected, but only at concentration as high as 100 µM of $FeSO_4$, by forming a purple coloured solution. Thereby, it could be deduced that this assay was more reliable for determining the concentration of Fe^{2+} inside the cells, since Fe^{3+} was converted into Fe^{2+} by the ascorbate in the ferrozine Fe detection reagent.

2.8.2 Determination of intracellular Fe content

Following any particular treatment, Fe accumulation was terminated by washing MDA-MB-231 and A549 cells with 1 mL of PBS containing 1 mM of DFO. This was to remove Fe that unspecifically bound to the exterior of the cells, allowing for a measurement of intracellular Fe (Riemer *et al*., 2004). Then, the cells were rinsed with 1 mL of PBS to remove the DFO residue. After that, the cells were lysed with 150 µL of Tris-HCl lysis buffer (1% Triton X-100, 10 mM Tris, pH 8.5) as described in section 2.3. The cell lysates obtained (100 µL) were aliquoted into

microfuge tubes and mixed with 100 µL of 10 mM HCl (the solvent of the Fe standard) and 100 µL of 1.4 M HCl (Fe-releasing reagent). The mixture was incubated for 2 h at 60^{o}C followed by incubation with 30 µL of the ferrozine Fe detection reagent for 30 min. Then, the reaction mixture was transferred into a 96-well plate and the absorbance was read at 550 nm. The intracellular Fe content was normalised for protein content from the same sample determined using the Bradford assay.

2.9 Griess assay

A quantitative measurement of $^{\bullet}$NO is hard to perform as it is a very short-lived biological molecule (Leone *et al*., 1994; Beckman and Koppenol, 1996). Nevertheless, $^{\bullet}$NO is rapidly oxidised to nitrite (NO_2^-) and nitrate (NO_3^-), which provides a means to indirectly measure $^{\bullet}$NO production. Therefore, the efficacy of tDSNO to release $^{\bullet}$NO was confirmed using the Griess assay by measuring the production of NO_2^-. This assay involves a diazotisation of sulphanilamide and napthylethylenediamine that will form a chromogenic azo product at the end of the reactions (Verdon, *et al*., 1995).

A NO_2^- standard curve was first developed for this assay. 100 µM of stock sodium nitrite ($NaNO_2$) was prepared in distilled water and six serial twofold dilutions from 100 to 1 µM (100 µL per well) were performed in triplicates down the 96-well plate. Then, 25 µL of solution in each well was discarded and replaced with 25 µL of a mixture of an equal volume of 2% sulphanilamide in 5% phosphoric acid mixed with 0.2% napthylethylenediamine. The solution was mixed well by gently tapping the side of the plate. The plate was protected from light and incubated for 10 min at room temperature. Then, the absorbance of colour formed was measured at 540 nm. The measurement was made within 30 min as the colour faded after that.

2.10 Statistics

Statistical analyses of the present study were performed using OriginPro 8. Data that involved two or more factors (e.g. treatment and time) were analysed using two-way-ANOVA followed by a Bonferroni post-hoc test. This was applied to the analysis of data in time-course studies and comparisons of drug treatments in different assay conditions. For data that involved one factor, one-way-ANOVA was used followed by a Tukey post-hoc test. All the data were presented as mean ± SEM with n=8 unless otherwise stated. Means differences were considered significant at the 0.05 level, unless otherwise stated in figure legends.

CHAPTER 3: RESULTS

3.1 Characterisation of drug activity - Drug toxicity and the photoactivation effect

In this section, tDSNO was characterised by its capability to release $^{\bullet}$NO. The production of $^{\bullet}$NO was evaluated in both cell-free and cell-mediated systems. As tDSNO is a photoactive drug, the characterisation was performed based on the photoactivation mechanism, and this was applied throughout the study unless otherwise stated.

3.1.1 Evaluation 1: Quantification of $^{\bullet}$NO release in a cell-free system

A quantitative measurement of $^{\bullet}$NO is hard to perform as it has a very short half-life of ~6 s (Beckman and Koppenol, 1996). However, $^{\bullet}$NO is rapidly oxidised to NO_2^- and NO_3^-, which provides a means to indirectly measure $^{\bullet}$NO production. Therefore, $^{\bullet}$NO released by tDSNO was confirmed by measuring the production of NO_2^-.

3.1.1.1 NO_2^- standard curve

Firstly, a NO_2^- standard curve was obtained from a series of known concentrations of $NaNO_2$ (1 to 100 µM) (Figure 8). The regression coefficient was equal to 0.987 for NO_2^- formation. From this calibration curve, $^{\bullet}$NO release from a series of tDSNO concentrations (5 to 200 µM) was determined under conditions of photoactivation and non-photoactivation, in the presence and absence of FAC (Figures 9 and 10).

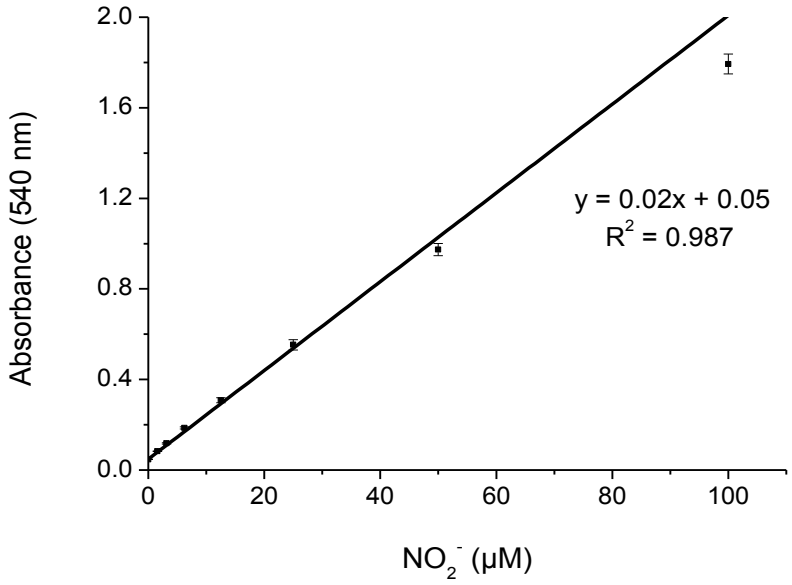

Figure 8 Standard curve for detecting NO_2^-. Assay was performed using $NaNO_2$ diluted in advanced DMEM containing 2% FBS, 1% antibiotic and 1% glutamine. Calibration curve was obtained for each assay to ensure the accuracy. Data are presented as mean ± SEM (n=3).

3.1.1.2 •NO released by tDSNO

The concentration of NO_2^- produced from tDSNO decomposition was measured with and without photoactivation. tDSNO as low as 25 μM was sufficient to produce a significant concentration of NO_2^- compared to vehicle control under both photoactivation and non-photoactivation conditions ($p<0.05$) (Figure 9). The production of NO_2^- was directly proportional to the increase of tDSNO concentrations, demonstrating that the release of •NO was concentration dependent. Significant differences in the production of NO_2^- between photoactivation and non-photoactivation conditions were observed from 50 to 200 μM ($p<0.05$).

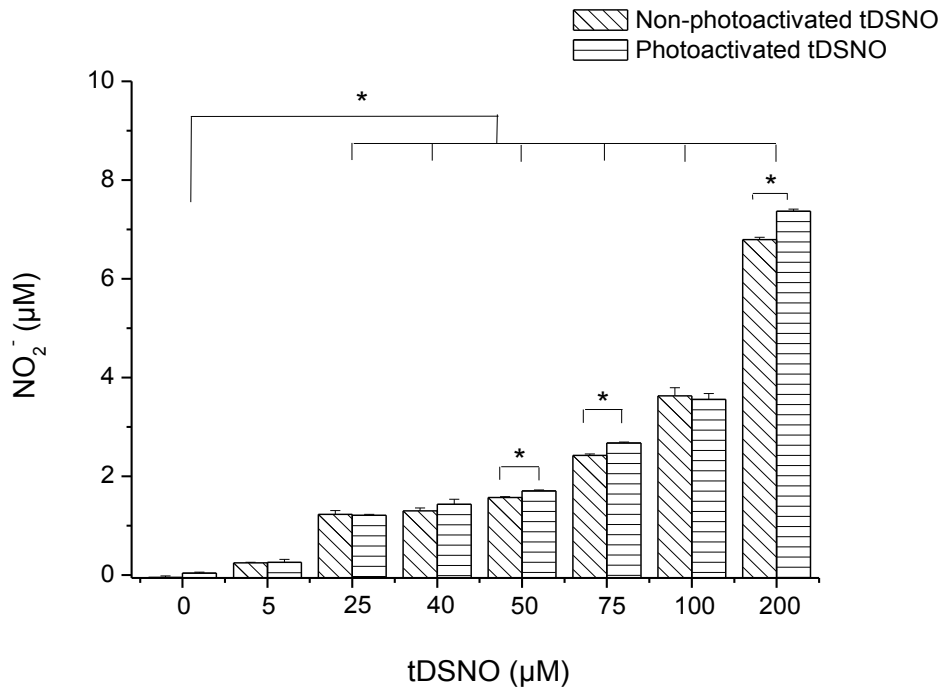

Figure 9 Concentration dependent release of •NO by tDSNO. Griess assay was performed on a series of tDSNO concentrations after 1 h of photoactivation and non-photoactivation. * indicates a significant difference compared to vehicle control ($p<0.05$). Significant differences between photoactivation and non-photoactivation conditions were observed from 50 to 200 μM of tDSNO ($p<0.05$). Data are presented as mean ± SEM (n=3).

3.1.1.3 The effect of Fe on •NO release from tDSNO

Fe has been implicated in the stability of *S*-nitrosothiol drugs (Vanin *et al*., 1997). Fe also has a high affinity to bind •NO and catalyse the formation of metal nitrosyl complexes (Stamler *et al*., 1992). As FAC was to be used as an additional Fe supplement in the cell culture studies for a determination of intracellular Fe content, the effect of Fe on the decomposition of tDSNO was investigated. This was examined by quantifying •NO released by tDSNO in a medium containing 10 μM FAC (See section 3.2.2.2 for further information about FAC).

Upon the addition of FAC, there was no dramatic change in the profile of •NO release from tDSNO (Figures 9 and 10). The first significant detection of NO_2^- production still occurred at 25 μM of tDSNO and a similar concentration dependent release of •NO was confirmed (Figure 10). However,

there were slight differences in that a significant difference in •NO release upon photoactivation was observed at 25 µM of tDSNO in the presence of FAC (Figure 10), while this was not apparent until 50 µM of tDSNO in the absence of FAC (Figure 9). The total amount of •NO release following photoactivation also appeared to increase slightly with the addition of FAC (Figure 10). Therefore, these results indicated that for tDSNO solution, Fe levels had little effect on the extent of •NO release as well as on the •NO released from tDSNO.

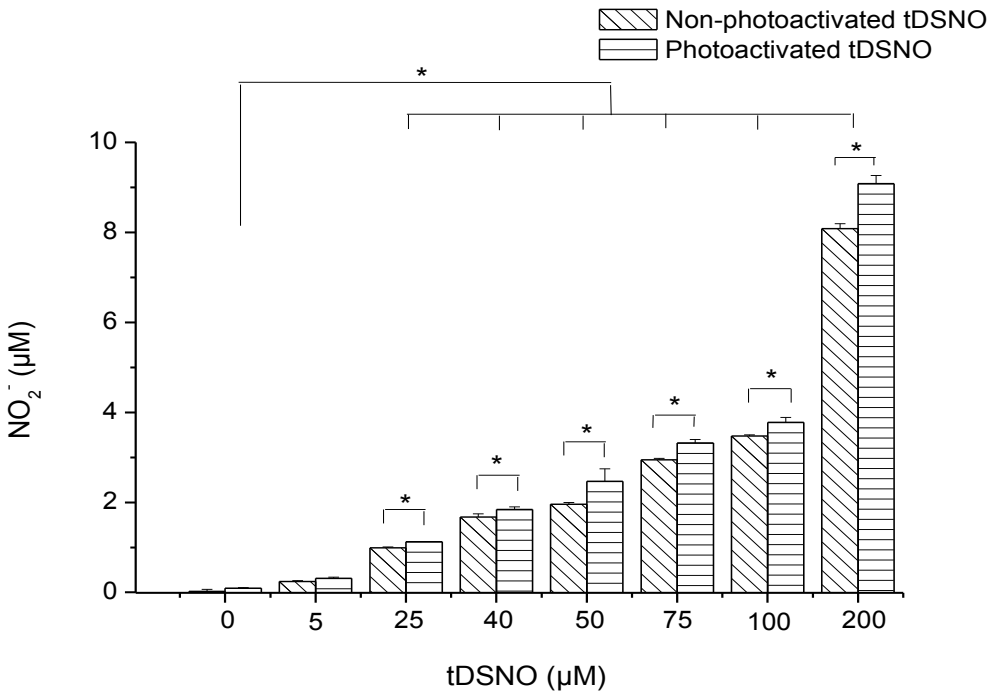

Figure 10 Effect of Fe on •NO release by tDSNO. Griess assay was performed on a series of tDSNO concentrations in the presence of 10 µM FAC, after 1 h of photoactivation and non-photoactivation. * indicates a significant difference compared to vehicle control ($p<0.05$). Significant differences between photoactivation and non-photoactivation conditions were observed from 25 to 200 µM of tDSNO ($p<0.05$). Data are presented as mean ± SEM (n=3).

3.1.2 Evaluation 2: Quantification of •NO release in a cell-mediated system

Following characterisation of tDSNO in a cell-free system, tDSNO was then characterised in the cellular system to study drug-cell interactions. For this purpose, a cell viability assay (MTT) was performed in MDA-MB-231 and A549 cells treated with a range of tDSNO concentrations (2 to 350 μM). From here, the non-cytotoxic threshold at which tDSNO would be used for subsequent experiments was established. Then, the cytotoxicity of tDSNO over a time-period was examined for further assessments of cellular Fe uptake and cell cytotoxicity.

3.1.2.1 Standard curve of MDA-MB-231 cells

Initially, to determine the range in which the MTT assay would give a linear result for cell viability, a calibration curve for cell number was constructed (Figure 11). The absorbance obtained at 550 nm was directly proportional to the cell number across the full cell range (5,000-25,000 cells), in which the linearity fits the early linear portion of a theoretical exponential growth curve.

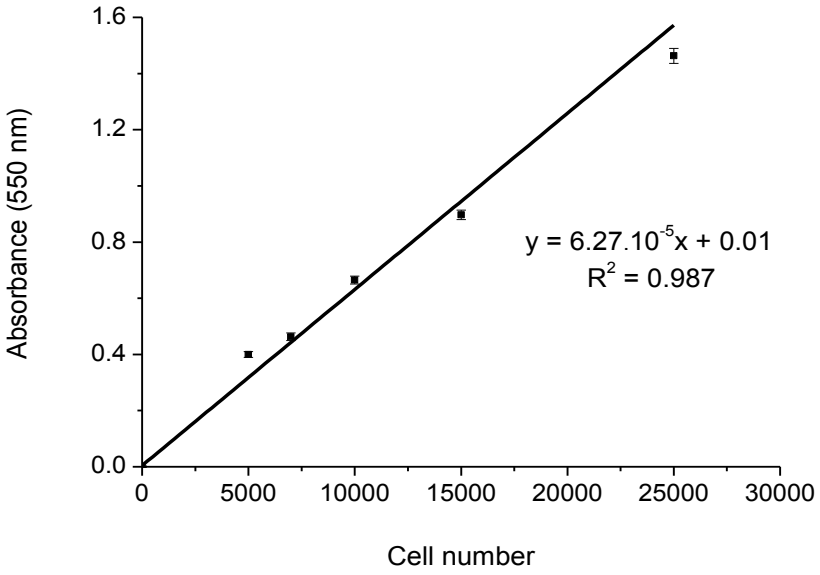

Figure 11 Standard curve of MDA-MB-231 cells. Cells were seeded in a 96-well plate in an increasing number from 5,000 to 25,000 cells per well. The MTT assay was performed after a period of 24 h when the cells were attached to the wells. Data are presented as mean ± SEM (n=8).

3.1.2.2 Cytotoxicity of tDSNO in MDA-MB-231 cells

In MDA-MB-231 cells, the IC_{50} of tDSNO without photoactivation was 183.3 ± 0.1 µM (Figure 12). Following photoactivation, this IC_{50} decreased significantly by 1.94-fold (94.5 ± 0.1 µM) ($p<0.05$). This was indicated by a shift to the left of the concentration response curve for cells exposed to photoactivated tDSNO relative to non-photoactivated tDSNO, thus confirming that photoactivation enhanced the activity of the drug. Without photoactivation, significant changes in cell viability were not observed until 100 µM tDSNO (15.1 ± 3.9% of cellular death) ($p<0.05$), while with photoactivation, the first significant differences were detected at a much lower drug concentration of 50 µM (16.2 ± 2.8% of cellular death) ($p<0.01$). Therefore, in order to examine Fe uptake in viable cells, 40 µM was chosen as a maximum non-cytotoxic limit to treat MDA-MB-231 cells throughout this study.

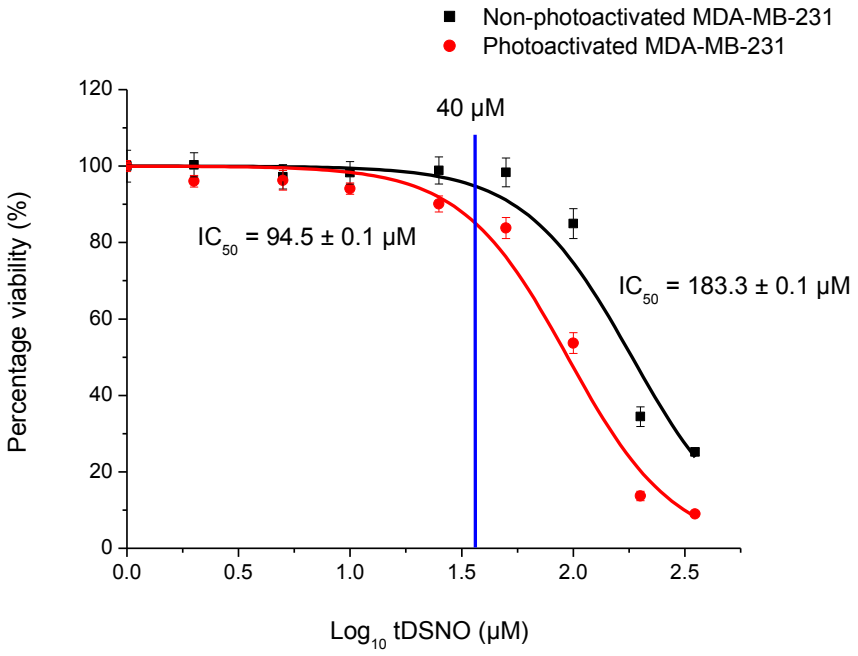

Figure 12 Cytotoxicity of tDSNO in MDA-MB-231 cells. Cells seeded in 96-well plates (10,000 cells per well) were treated with a range of tDSNO concentrations, with and without 1 h photoactivation followed by incubation at 37°C for 23 h. The MTT assay was performed after 24 h of treatment. Cell viability is expressed as a percentage of control. The blue line indicated the maximum non-cytotoxic drug concentration (40 µM), whereby beyond this point tDSNO began to display significant toxicity. Therefore, this concentration was used as a maximum limit for subsequent experiments unless otherwise stated. The IC_{50}'s between photoactivation and non-photoactivation conditions were significantly different to each other as analysed by Student's t-test ($p<0.05$). Data are presented as mean ± SEM (n=8). The concentration response curves were obtained from a non-linear curve fit.

3.1.2.3 Cytotoxicity of tDSNO in A549 cells

For A549 cells, the IC_{50} of tDSNO under the non-photoactivation condition was 114.5 ± 7.5 µM (Figure 13). Similar to MDA-MB-231 cells, the IC_{50} of tDSNO against A549 cells decreased significantly by 1.5-fold (76.9 ± 3.5 µM) following photoactivation ($p<0.05$). Without photoactivation, significant changes in cell viability were also first observed at 100 µM of tDSNO ($p<0.05$). However, for this cell line, the percentage of cellular death (45.0 ± 5.9%) was 3-fold higher than that found in MDA-MB-231 cells. Following photoactivation, the first significant decrease in cell viability was also observed at 50 µM of tDSNO, but with 1.6-fold higher of cellular death (26.4 ± 2.4%) compared to MDA-MB-231 cells ($p<0.05$). Therefore, in order to examine Fe uptake in viable cells, 40 µM was chosen as a maximum non-cytotoxic limit to treat A549 cells.

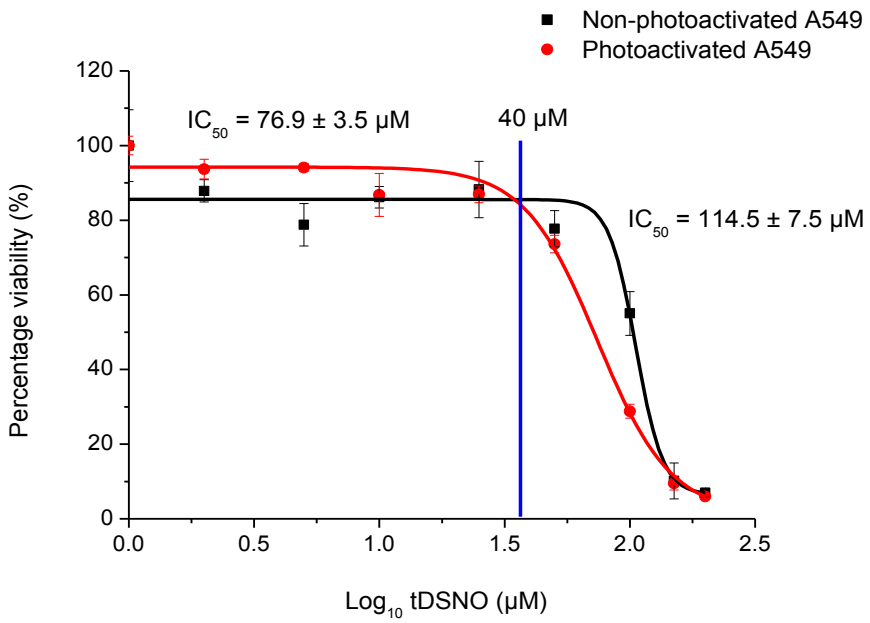

Figure 13 Cytotoxicity of tDSNO in A549 cells. Cells seeded in 96-well plates (8,000 cells per well) were treated with a range of tDSNO concentrations, with and without 1 h photoactivation followed by incubation at 37°C for 23 h. The MTT assay was performed after 24 h of treatment. Cell viability is expressed as a percentage of control. The blue line indicated the maximum non-cytotoxic drug concentration (40 µM), whereby beyond this point tDSNO began to display significant toxicity. Therefore, this concentration was used as a maximum limit for subsequent experiments unless otherwise stated. The IC_{50}'s between photoactivation and non-photoactivation conditions were significantly different to each other as analysed by Student's t-test ($p<0.05$). Data are presented as mean ± SEM (n=8). The concentration response curves were obtained from a non-linear curve fit.

3.1.2.4 Time-course cytotoxicity study of tDSNO

To examine the cytotoxicity of tDSNO over a time-course, MDA-MB-231 cells were treated with 40, 50 and 80 µM of tDSNO for 3 to 48 h and cell viability was determined by the MTT assay. The maximum non-cytotoxic (40 µM) and cytotoxic (50 and 80 µM) concentrations of tDSNO at 24 h were chosen as they would be used for further assessments of cellular Fe uptake and cell cytotoxicity. These experiments were performed without photoactivation in order to ensure the availability of tDSNO throughout 48 h of experimental duration with the half-life of 50 h. The results showed that MDA-MB-231 cells grew at a linear rate in the media containing vehicle of tDSNO (0.1% DMSO) (Figure 14). The cell number increased by 2-fold within 48 h. Upon the treatment with 40 µM of tDSNO, MDA-MB-231 cells remained static within the same cell number throughout the 48 h period ($p>0.05$). However, upon the treatments with 50 and 80 µM of tDSNO, a time and concentration dependent decrease in cell number was observed. The greatest decrease in cell number was apparent at 12 h, with the decreases were 38.7 ± 0.5 % and 66.4 ± 5.9% respectively at 50 and 80 µM of tDSNO ($p<0.05$). The post 12 h observations indicated that the cells, which were treated with 50 and 80 µM of tDSNO, remained static within the same cell number ($p>0.05$).

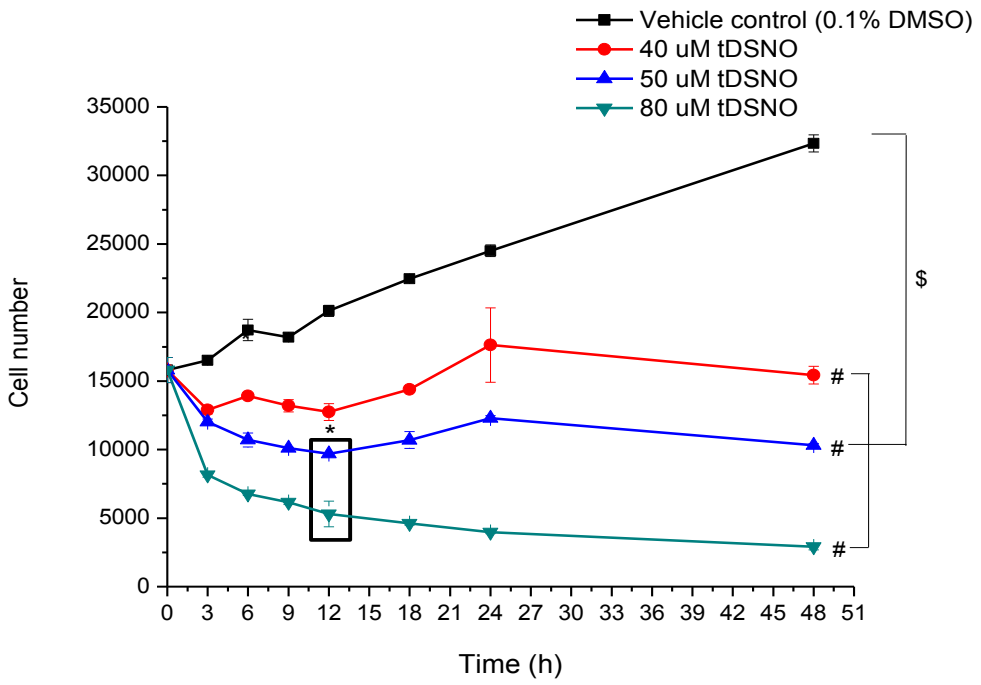

Figure 14 Growth rates of MDA-MB-231 cells treated with tDSNO. Cells seeded in 96-well plates (8,000 cells per well) were incubated at 37^{o}C for 48 h to allow the cells to attach to the wells. The treatment with tDSNO was started at 0 h and the MTT assay was performed after the corresponding time points. * ($p<0.05$) indicates a significant difference of treatment groups compared to control at 0 h, # ($p<0.05$) indicates a significant difference between different treatment groups and $ ($p<0.05$) indicates a significant difference of each treatment group compared to control. Data are presented as mean ± SEM (n=3).

3.1.3 Concluding remarks for section 3.1

The characterisation of tDSNO in a cell-free system revealed that •NO release from tDSNO was concentration dependent. Similarly, the activity of tDSNO was affected by Fe in a concentration dependent manner. Investigations of the drug-cell interactions revealed that the cytotoxicity of tDSNO in both MDA-MB-231 and A549 cells was accelerated by approximately 1.5- to 2.0-fold following photoactivation. The investigations of tDSNO cytotoxicity over 48 h without photoactivation revealed that tDSNO affected cell proliferation in a concentration and time dependent manner. Following 48 h of exposure to a range of tDSNO treatments (40, 50 and 80 μM), the greatest cellular death of 66.4 ± 5.9% was observable at 12 h, and this cytotoxic effect was followed by cytostatic effect which lasted until 48 h. Altogether, results from this section demonstrated that the efficacy of tDSNO was dependent on concentration, time, photoactivation, and cell type.

3.2 Hypothesis 1: Does a low level of •NO release cause cells to import Fe to cytotoxic levels?

Following characterisation of tDSNO in cell-free and cell-mediated systems, •NO release was evaluated for its capability to increase cellular Fe uptake. The •NO release was aimed to induce Fe overload in MDA-MB-231 and A549 cells as a means of cytotoxicity. To achieve this aim, cells were treated with non-cytotoxic concentrations of tDSNO (5, 25 and 40 µM) based on the established IC_{50}'s in the sections 3.1.2.2 and 3.1.2.3. Following these treatments, a series of ferrozine assays were performed and the evaluations are shown as follows.

3.2.1 Standard curve of $FeSO_4$

Initially, a calibration curve of known concentrations of $FeSO_4$ (0 to 200 µM) was obtained in order to determine the concentration of intracellular Fe content (Figure 15). The absorbance obtained at 550 nm was directly proportional to the formation of ferrous iron-ferrozine complex, with a correlation coefficient equal to 0.993.

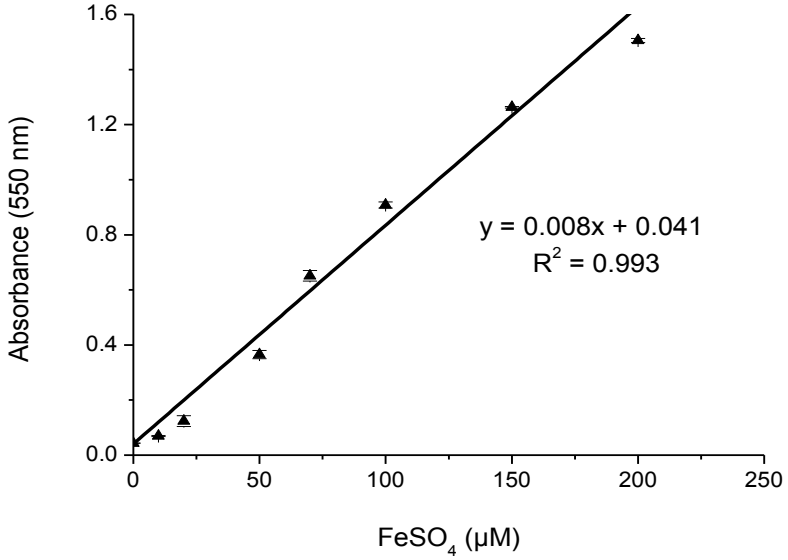

Figure 15 Standard curve of $FeSO_4$. The absorbance of ferrous iron-ferrozine complex was obtained from known concentrations of $FeSO_4$ at 550 nm. Data are presented as mean ± SEM of two separate experiments (n=4).

3.2.2 Quantification of intracellular Fe content in MDA-MB-231 cells

3.2.2.1 Treatment with tDSNO

To assess the first hypothesis that exposure to low concentrations of •NO would enhance Fe uptake, cellular Fe levels were measured after 24 h of exposure to non-cytotoxic concentrations of tDSNO (5, 25 and 40 µM) upon 1 h photoactivation. The results showed that following 24 h of these tDSNO treatments, the intracellular Fe content did not increase significantly compared to vehicle control ($p>0.05$) (Figure 16). Although 40 µM of tDSNO increased the intracellular Fe content by 1.13-fold, the increase was too small to give a significant difference with the vehicle control ($p>0.05$). Therefore, this indicated that •NO released from non-cytotoxic concentrations of tDSNO was unable to enhance the uptake of Fe in MDA-MB-231 cells after 1 h of photoactivation.

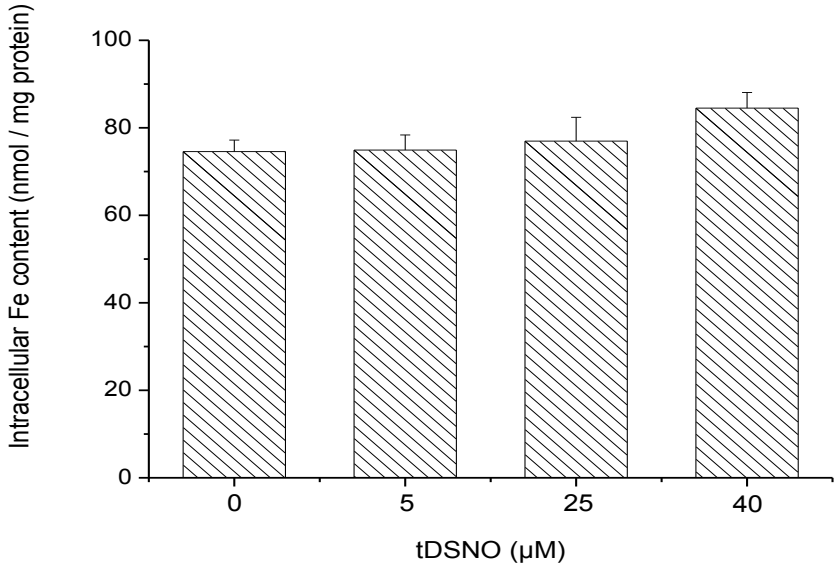

Figure 16 Intracellular Fe content in MDA-MB-231 cells treated with non-cytotoxic concentrations of tDSNO following photoactivation. Cells seeded in 6-well plates (200,000 cells per well) were treated with tDSNO for 1 h under photoactivation followed by incubation at 37°C for 23 h. The intracellular Fe content was measured after 24 h of treatment, with protein concentrations determined via the Bradford assay. No significant increase in intracellular Fe content was measured in all treatment groups compared to vehicle control ($p>0.05$). Data are presented as mean ± SEM from two separate experiments (n=4).

3.2.2.2 Treatment with FAC and tDSNO

One limitation of the cellular Fe uptake assay was that, even if •NO caused an up-regulation in the signalling pathways for Fe uptake, there might not be sufficient Fe in the extracellular medium for the changes in intracellular Fe content to be measurable. Therefore, in order to enhance Tf-bound Fe uptake, the experiments were also repeated using FAC as an additional Fe supply. In order to determine the maximum concentration of FAC that could be added to the media without inducing cytotoxicity, prior to these experiments, an MTT assay with FAC was performed. As can be seen in Figure 17, the IC_{50} of FAC was 474.3 ± 0.1 µM. Cell death became observable at 400 µM of FAC with a decrease in cell viability of 30.3 ± 2.9% ($p<0.05$).

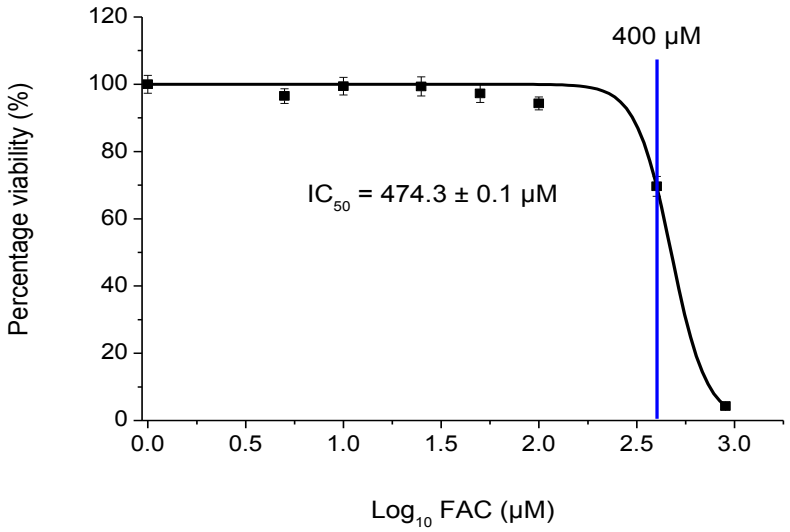

Figure 17 Cytotoxicity of FAC in MDA-MB-231 cells. Cells seeded in a 96-well plate (10,000 cells per well) were treated with a range of FAC concentrations at 37°C for 24 h. The MTT assay was performed after 24 h of treatment. The blue line indicated the threshold (400 µM) at which cell death became observable. Cell viability is expressed as a percentage of control with data presented as mean ± SEM (n=8). The concentration response curve was obtained from a non-linear curve fit.

As FAC was not cytotoxic until very high concentrations, a range of 10, 50 and 100 µM of FAC was used in the next experiment in order to determine which of these concentrations could increase the intracellular Fe content. The results showed that there was no significant increase in the intracellular Fe content relative to control, in all three concentrations used ($p>0.05$) (Figure 18). These results demonstrated that the addition of external, non-cytotoxic concentrations of Fe in the culture medium did not affect the intracellular Fe content.

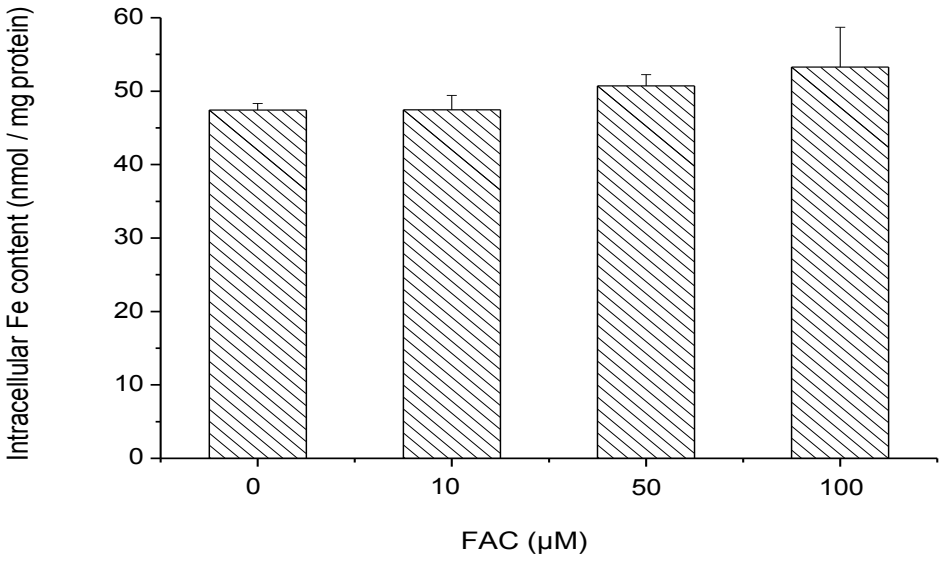

Figure 18 Intracellular Fe content in MDA-MB-231 cells treated with FAC. Cells seeded in 6-well plates (200,000 cells per well) were incubated with FAC at 37^{o}C. The ferrozine assay was performed after 24 h of treatment, with protein concentrations determined via the Bradford assay. No significant increase in intracellular Fe content was observed in all treatment groups compared to control ($p>0.05$). Data are presented as mean ± SEM from two separate experiments (n=3).

The results of the Griess assay indicated that FAC started to exhibit a slight effect on tDSNO decomposition by 25 µM (Figure 10). Therefore, to avoid interference with the drug, 10 µM was adopted as the upper limit for FAC in the Fe uptake experiments. Although these FAC levels were lower than commonly used in other studies, which typically used 100 to 150 µM of FAC (Richardson and Baker, 1992; Tulpule *et al.*, 2010), a prior literature search confirmed that Fe uptake had previously been quantified using 10 µM of FAC as the Fe supply (Hoepken *et al.*, 2004). Therefore, 10 µM of FAC was used in combination with non-cytotoxic concentrations of tDSNO (5, 25 and 40 µM) to investigate if this could increase the intracellular Fe uptake. Herein, the results indicated that these combination treatments did not significantly increase the intracellular Fe content compared to vehicle control ($p>0.05$) (Figure 19). Similar to 40 µM of tDSNO alone (Figure 16), a combination of 40 µM tDSNO with 10 µM FAC also caused a relatively small increase in intracellular Fe content (1.13-fold) that was not significant when compared to vehicle control ($p>0.05$) (Figure 19).

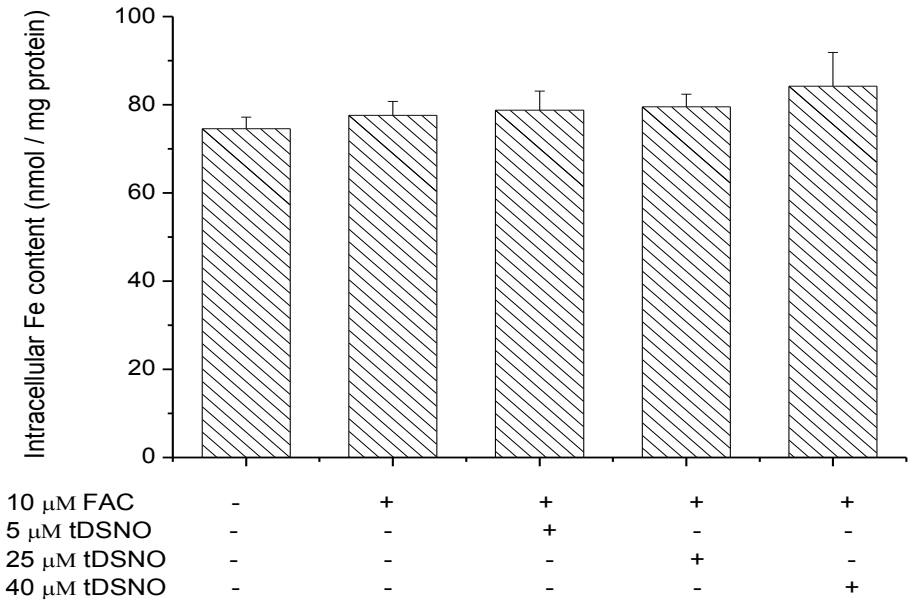

Figure 19 Intracellular Fe content in MDA-MB-231 cells treated with non-cytotoxic concentrations of tDSNO and FAC following photoactivation. Cells seeded in 6-well plates (200,000 cells per well) were treated with tDSNO prepared in media containing 10 µM of FAC. The treatment was performed for 1 h under photoactivation followed by incubation at 37^{o}C for 23 h. The intracellular Fe content was measured after 24 h of treatment, with protein concentrations determined via the Bradford assay. No significant increase in intracellular Fe content was observed in all treatment groups compared to vehicle control ($p>0.05$). Data are presented as mean ± SEM from two separate experiments (n=4).

3.2.2.3 Treatment with cytotoxic concentrations of tDSNO

From the first hypothesis, the non-cytotoxic concentrations of tDSNO (5 to 40 µM) were predicted to increase the intracellular Fe content and cause Fe overload as a means of cytotoxicity. However, as intracellular Fe content did not increase relative to control under this non-cytotoxic condition (Figure 16), the cellular Fe uptake was assessed under cytotoxic conditions, to examine if this could increase the intracellular Fe content in MDA-MB-231 cells to significant, higher levels than the control. The Griess assay indicated that at cytotoxic concentrations of tDSNO (50 to 200 µM), FAC significantly changed the extent of decomposition of tDSNO (Figure 10). Therefore, to avoid any effect of Fe on both tDSNO and the released $^{\bullet}$NO, FAC was omitted from this experiment. The results indicated that in contrast to the original hypothesis to increase the intracellular Fe content, cytotoxic concentrations of tDSNO caused a significant, gradual loss of intracellular Fe content in MDA-MB-231 cells ($p<0.05$) (Figure 20). tDSNO decreased the intracellular Fe content in a concentration dependent manner. The cytotoxicity assay (MTT) indicated that an increasing amount of cell death of 16.2 ± 2.8%, 44.2 ± 0.1%, 46.3 ± 2.7% and 86.3 ± 1.2% was observed at increasing concentrations of tDSNO from 50, 75, 100 to 200 µM respectively ($p<0.05$) (Figure 12). Therefore, these results indicated that the intracellular Fe loss was concomitant with the cytotoxicity of tDSNO.

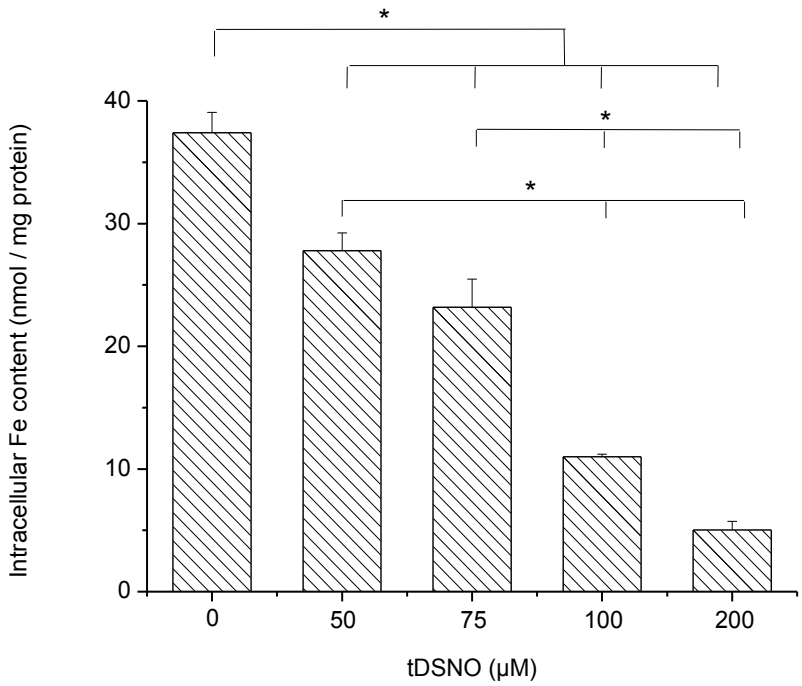

Figure 20 Intracellular Fe content in MDA-MB-231 cells treated with cytotoxic concentrations of tDSNO following photoactivation. Cells seeded in 6-well plates (200,000 cells per well) were treated with tDSNO for 1 h under photoactivation followed by incubation at 37^{o}C for 23 h. The intracellular Fe content was measured after 24 h of treatment, with protein concentrations determined via the Bradford assay. * indicates significant differences at $p<0.05$. Data are presented as mean ± SEM (n=3).

3.2.3 Time-course study of intracellular Fe uptake in MDA-MB-231 cells

As $^{\bullet}$NO release from tDSNO, neither from cytotoxic nor non-cytotoxic concentrations, met the current aim to increase the intracellular Fe content above the control level at 24 h of treatment (Figure 16 and 20), other time points from 2 to 48 h were examined to fully address the hypothesis. For this purpose, the highest non-cytotoxic concentration of tDSNO (40 µM) was selected. Higher concentrations were not the primary choice as they decreased the intracellular Fe content. Therefore, MDA-MB-231 cells were treated with 40 µM tDSNO and incubated for 2, 4, 8, 16, 24 and 48 h until the determination of intracellular Fe content. In the absence of tDSNO treatment, the results showed that there were fluctuations in the basal Fe levels of the control cells (~2-fold difference) compared with the earlier results (Figure 16, 18 and 19). In contrast to the original hypothesis of increasing the intracellular Fe content, the results also showed that within the early time points, prior to 24 h, a significant decrease in intracellular Fe content was observed (Figure 21). Without photoactivation, the intracellular Fe content decreased significantly at 4 h by 16.1 ± 0.4% and a similar result was obtained following photoactivation ($p<0.05$). Interestingly, a massive decrease in intracellular Fe content was observed at 16 h, with significant decreases of 54.5 ± 1.1% and 57.7 ± 0.9% respectively with and without photoactivation compared to vehicle control ($p<0.05$). This effect did not last long, as at 24 h of treatment, the intracellular Fe content was restored to control levels under both photoactivation and non-photoactivation conditions ($p>0.05$). At 48 h of tDSNO treatment however, the intracellular Fe content decreased by 20.12 ± 2.3% under the non-photoactivation condition ($p<0.05$), but this effect was not seen under the photoactivation condition ($p>0.05$). This effect was unlikely due to technical errors as all tDSNO treated MDA-MB-231 cells, at every time point investigated, had undergone the same protocols (e.g. following tDSNO treatment, the media were not replaced until end of the experiment). The cytotoxicity assay (MTT) indicated that MDA-MB-231 cell number remained static within 48 h of treatment with 40 µM tDSNO (Figure 14). This indicated that the fluctuation in the intracellular Fe content was not

related to the cytostatic mechanism of tDSNO drug action. This was contradicted to the decrease in intracellular Fe content observed at higher concentrations of tDSNO (50 to 200 µM), in which case the decrease in intracellular Fe content was in parallel to the decrease in cell viability (Figure 20). These results demonstrated that all the factors implemented including treatment and time did not increase the intracellular Fe content in MDA-MB-231 cells relative to control. Therefore, the series of Fe uptake assays in MDA-MB-231 cells finished at this point and the investigations were continued on A549 cells by repeating the Fe uptake assays.

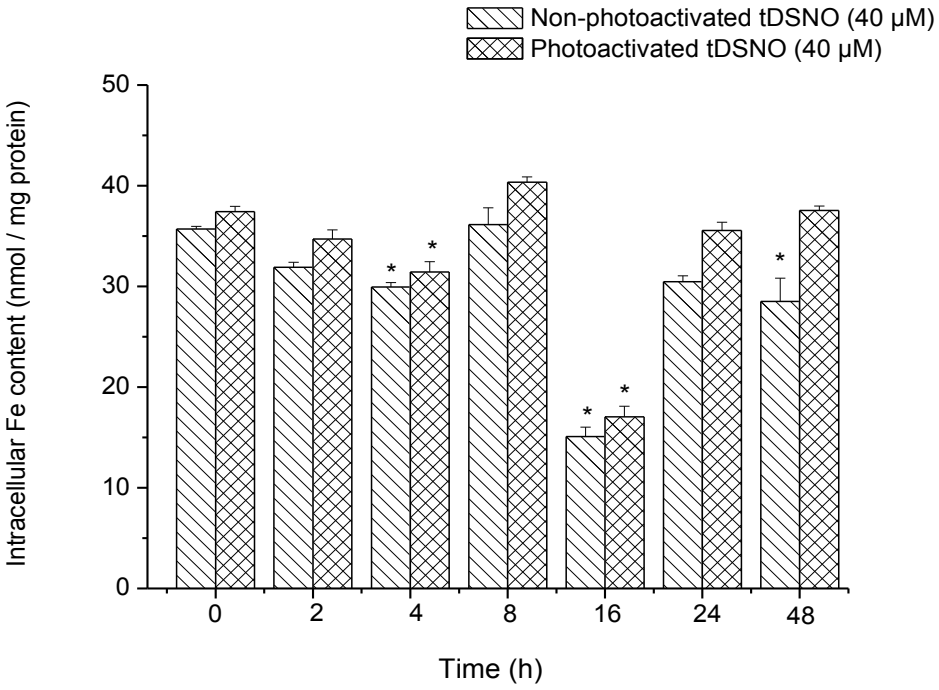

Figure 21 Time-course study of intracellular Fe uptake in MDA-MB-231 cells. Cells seeded in 6-well plates (200,000 cells per well) were exposed to tDSNO with and without 1 h photoactivation followed by incubation at 37^{o}C until the corresponding time points. The intracellular Fe content was measured after each time point, with protein concentrations determined via the Bradford assay. * indicates a significant difference compared to vehicle control ($p<0.05$). Data are presented as mean ± SEM (n=4).

3.2.4 Quantification of intracellular Fe content in A549 cells

The cellular Fe uptake in A549 cells was measured after 24 h of exposure to non-cytotoxic concentrations of tDSNO (5, 25 and 40 µM) and the results were compared with MDA-MB-231 cells. Interestingly, the basal intracellular Fe content in A549 cells was approximately 2 to 4 fold higher than that observed in MDA-MB-231 cells (Figures 22 and 23). Despite the additional Fe content, significant changes in intracellular Fe content were not observed in A549 cells compared to control following tDSNO treatment ($p>0.05$) (Figure 22). Nor were significant changes observed following tDSNO treatment in the presence of 10 µM FAC ($p>0.05$) (Figure 23). Therefore, no further experiments on A549 cells were conducted in this study.

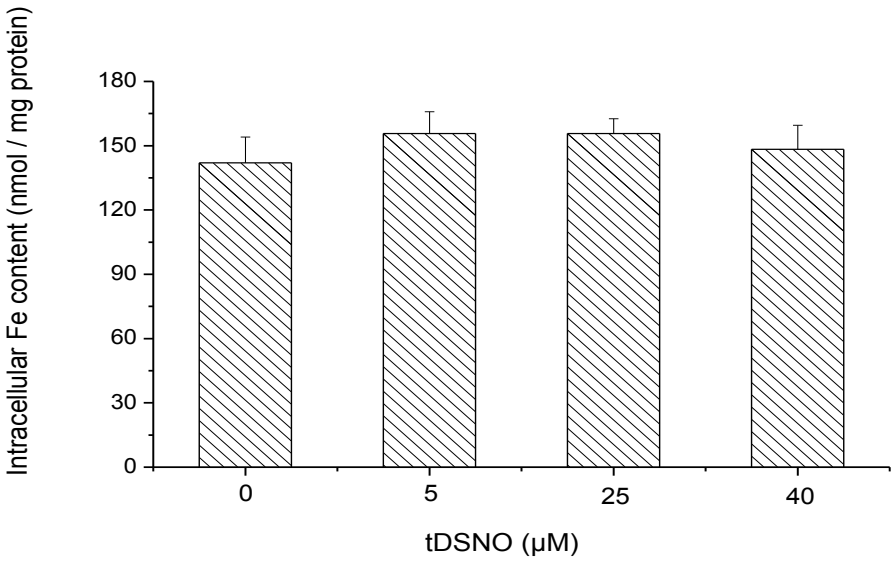

Figure 22 Intracellular Fe content in A549 cells treated with non-cytotoxic concentrations of tDSNO following photoactivation. Cells seeded in 6-well plates (160,000 cells per well) were treated with tDSNO for 1 h under photoactivation followed by incubation at 37^{o}C for 23 h. The intracellular Fe content was measured after 24 h of treatment, with protein concentrations determined via the Bradford assay. No significant increase in intracellular Fe content was observed in all treatment groups compared to vehicle control ($p>0.05$). The basal intracellular Fe content in A549 cells was approximately 2 to 4 fold higher than the basal intracellular Fe content in MDA-MB-231 cells. Data are presented as mean ± SEM from two separate experiments (n=3).

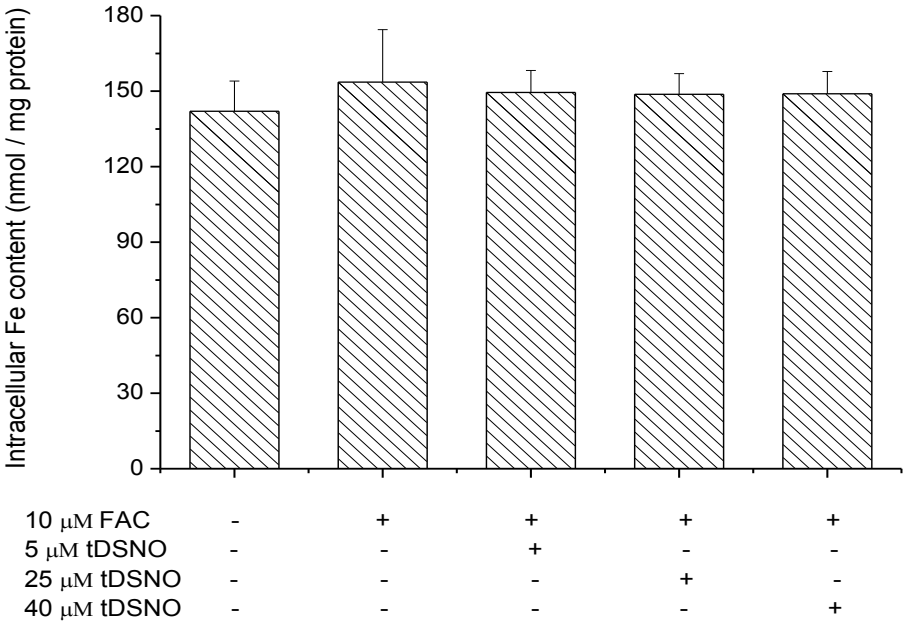

Figure 23 Intracellular Fe content in A549 cells treated with non-cytotoxic concentrations of tDSNO and FAC following photoactivation. Cells seeded in 6-well plates (160,000 cells per well) were treated with tDSNO prepared in media containing 10 μM of FAC. The treatment was performed for 1 h under photoactivation followed by incubation at 37^{o}C for 23 h. The intracellular Fe content was measured after 24 h of treatment, with protein concentrations determined via the Bradford assay. No significant increase in intracellular Fe content was measured in all treatment groups compared to vehicle control ($p>0.05$). The basal intracellular Fe content in A549 cells was approximately 2 to 4 fold higher than the basal intracellular Fe content in MDA-MB-231 cells. Data are presented as mean ± SEM from two separate experiments (n=3).

3.2.5 Concluding remarks for section 3.2

The investigations on MDA-MB-231 and A549 cells revealed that the effect of photoactivated tDSNO on cellular Fe levels was concentration and time dependent. Instead of increasing the intracellular Fe content higher than control levels as predicted, the intracellular Fe content decreased by 86.6 ± 0.7% following 24 h of treatment with cytotoxic concentrations of tDSNO (50 to 200 µM). The decrease in intracellular Fe content was associated with cellular death of up to 86.3 ± 1.2%. Similarly, following treatment with a non-cytotoxic concentration of tDSNO (40 µM), the intracellular Fe content decreased by 57.7 ± 0.9% and this was apparently at 16 h of tDSNO treatment, after which time Fe levels returned to their original levels. However, at 40 µM of tDSNO, this decrease in intracellular Fe content was unrelated to tDSNO cytotoxicity, as no cellular death was observed under these conditions.

3.3 Hypothesis 2: Does Fe deprivation increase the susceptibility of cells to •NO-induced cytotoxicity?

The efficacy of tDSNO was then evaluated based on its capability to cause cell death when MDA-MB-231 cells were depleted of Fe. This was accomplished by pre-treating the cells with the Fe chelator DFO, which is in a clinical use to treat thalassemia patients (Richardson *et al*., 1994). The evaluations are shown in the subsequent subsections.

3.3.1 The effect of DFO on cellular Fe uptake

Initially, the ferrozine assay was performed on MDA-MB-231 cells treated with 10 to 300 µM of DFO to determine the concentration that could significantly decrease the intracellular Fe content. Following 24 h of DFO treatment, the results demonstrated that 300 µM of DFO significantly decreased the intracellular Fe content by 19.2 ± 0.8% ($p<0.05$) (Figure 24). However, an earlier study using radioactive labelling demonstrated that the cellular Fe content decreased by 17 to 60% over 24 h of incubation with DFO at concentrations from 10 to 100 µM (Richardson *et al*., 1994). Therefore, 10, 100 and 300 µM of DFO were adopted for the next experiment.

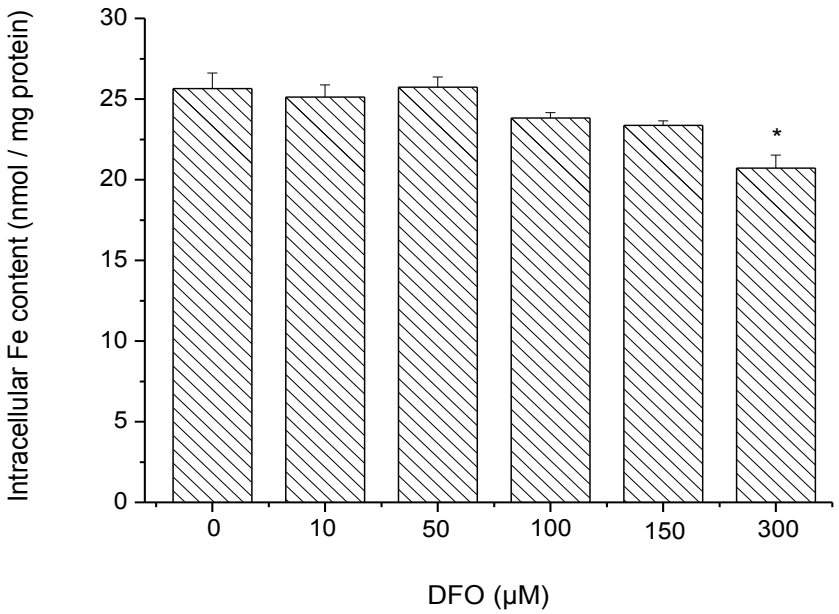

Figure 24 Intracellular Fe content in DFO-treated MDA-MB-231 cells. Cells seeded in 6-well plates (200,000 cells per well) were treated with DFO for 24 h at 37^{o}C. The Fe uptake assay was performed after 24 h of treatment, with protein concentrations determined via the Bradford assay. * indicates a significant difference compared to control ($p<0.05$). Data are presented as mean ± SEM (n=3).

3.3.2 The effect of tDSNO on the viability of DFO-treated MDA-MB-231 cells

It was demonstrated in earlier results (Figure 12) that 40 µM of tDSNO was non-toxic to MDA-MB-231 cells. Here, the efficacy of 40 µM tDSNO on DFO-treated MDA-MB-231 cells was investigated. Cells were pre-treated with 10, 100 and 300 µM of DFO for 24 h and the MTT assay was performed after 24 h of post-treatment with 40 µM tDSNO. The cytotoxic effects of DFO alone and in combination with tDSNO are shown below.

From the DFO treatment, the cytotoxicity assay indicated that DFO decreased cell viability in a concentration dependent manner (Figure 25). Upon the treatment with 10 µM of DFO, there was no significant cellular death observed compared to control irrespective of photoactivation or non-photoactivation ($p>0.05$). Parallel to this treatment, the Fe uptake assay indicated that 10 µM of DFO did not significantly decrease the intracellular Fe content relative to control ($p>0.05$) (Figure

24). Interestingly, when MDA-MB-231 cells were treated with 100 µM of DFO, significant cellular deaths of 27.5 ± 0.8% and 25.8 ± 1.5% were observed under non-photoactivation and photoactivation conditions respectively ($p<0.05$). In spite of this cytotoxicity, 100 µM of DFO did not significantly decrease the intracellular Fe content relative to control, similarly to 10 µM DFO ($p>0.05$) (Figure 24). Further, as the concentration of DFO increased to 300 µM, a significant cellular death of 44.8 ± 0.6% was observed under non-photoactivation conditions and following photoactivation, 41.2 ± 1.7% of cellular death was observed ($p<0.05$) (Figure 25). Parallel to these cellular deaths, 300 µM of DFO eventually decreased the intracellular Fe content by 19.2 ± 0.8% ($p<0.05$) (Figure 24).

Interestingly, upon a combination of 40 µM tDSNO with all three concentrations of DFO (10, 100 and 300 µM), cellular death increased in a concentration dependent manner (Figure 25). In contrast to 10 µM of DFO alone, its combination with 40 µM tDSNO caused a significant cellular death of 16.6 ± 1.3% without photoactivation ($p<0.05$). Following photoactivation, a significant 13.4 ± 1.6% cellular death was observed ($p<0.05$), although this was slightly lower than that observed under the non-photoactivation condition ($p>0.05$). Upon the treatment with 40 µM tDSNO in combination with 100 µM DFO, a significant, higher increase in cellular death was observed ($p<0.05$). Specifically, 44.0 ± 1.6% and 47.0 ± 1.9% cellular death were observed under non-photoactivation and photoactivation conditions respectively ($p<0.05$). Indeed, these percentages of cellular death were higher by 1.6- and 1.8-fold relative to the treatment with 100 µM of DFO alone under photoactivation and non-photoactivation conditions respectively ($p<0.05$). Similarly, when MDA-MB-231 cells were treated with 40 µM tDSNO in combination with 300 µM DFO, a significant cellular death of 59.1 ± 1.2% was observed under non-photoactivation conditions, while following photoactivation, a significant 54.5 ± 1.6% of cellular death was observed ($p<0.05$). These percentages of cellular death were higher by 1.3-fold relative to the treatment with 300 µM of DFO alone under both photoactivation and non-photoactivation conditions ($p<0.05$). Altogether, results

from this experiment demonstrated that, unlike the case of Fe-replete cells, 40 μM of tDSNO was cytotoxic to DFO-treated MDA-MB-231 cells. However, photoactivation did not cause significant changes in tDSNO cytotoxicity relative to non-photoactivation conditions ($p>0.05$).

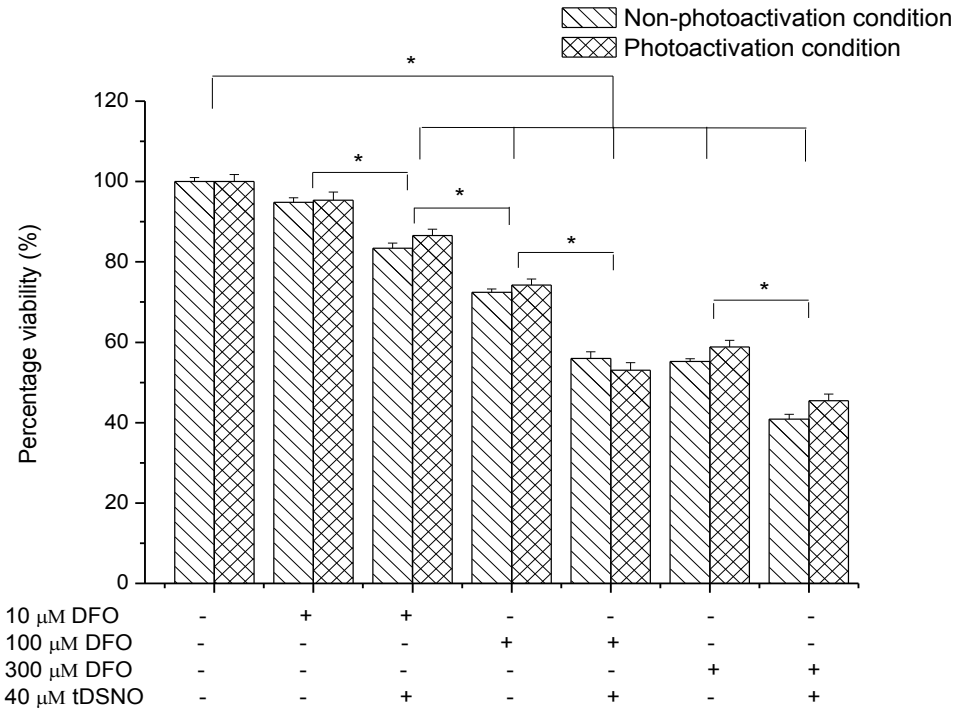

Figure 25 Effect of tDSNO on the viability of DFO-treated MDA-MB-231 cells. Cells seeded in 96-well plates (10,000 cells per well) were treated with DFO for 24 h at 37^{o}C followed by 24 h of treatment with tDSNO, with and without 1 h photoactivation. The MTT assay was performed after 48 h of both treatments. Cell viability is expressed as a percentage of control. * indicates significant differences at $p<0.05$. Data are presented as mean ± SEM (n=8).

3.3.3 The effect of a combination therapy of tDSNO with a non-cytotoxic level of DFO on the growth rate of MDA-MB-231 cells

As a combination of tDSNO (40 µM) with a non-cytotoxic concentration of DFO (10 µM) caused a significant cellular death at 24 h of treatment (Figure 25), it was attempted to investigate the cytotoxic effect of a range of tDSNO concentrations elicited by this DFO concentration over a time-course. For this purpose, DFO-pre-treated MDA-MB-231 cells were treated with non-cytotoxic (40 µM) and cytotoxic (50 and 80 µM) concentrations of tDSNO. Instead of 24 h as investigated earlier (Figure 25), the experimental duration was extended to 48 h, and the cell viability assay (MTT) was performed after each corresponding time point. The experiments were performed under non-photoactivation conditions as there was no significant difference of cytotoxicity between photoactivation and non-photoactivation conditions ($p>0.05$) (Figure 25).

The results indicated that upon the treatment with 10 µM of DFO, MDA-MB-231 cells grew in a linear manner, similar to the vehicle control, with the exception of the 3 h time point, where the cell number dropped slightly, insignificantly by 1.1-fold ($p>0.05$) (Figure 26). The cell number increased by approximately 2-fold within 48 h. However, the number of DFO-treated MDA-MB-231 cells was lower by 1.0- to 1.3-fold throughout the 48 h period relative to vehicle control ($p<0.05$). Interestingly, following this combination treatment of tDSNO with DFO, a time and concentration dependent decrease in cell number was observed. Following 48 h of treatment with 40, 50 and 80 µM of tDSNO on DFO-treated MDA-MB-231 cells, a gradual decrease in cell number was observed within the early time points, prior to 9 h, with the decrease dependent on tDSNO concentrations. Maximum decreases were 46.6 ± 1.1%, 64.0 ±2.5% and 72.5 ± 0.4% respectively at 40, 50 and 80 µM of tDSNO ($p<0.05$). Unlike 40 and 50 µM of tDSNO, cells that were treated with 80 µM of tDSNO showed a significant 83.3 ± 1.1% decrease in cell number at 12 h ($p<0.05$). The post 9 h period indicated that all DFO-treated cells that were exposed to tDSNO

were maintained and remained steady within the same range of cell number ($p>0.05$), and this was independent of concentration of tDSNO given (40, 50 and 80 µM). Altogether, the results demonstrated that DFO treatment increased the toxicity of tDSNO in MDA-MB-231 cells and the efficacy was time and concentration dependent.

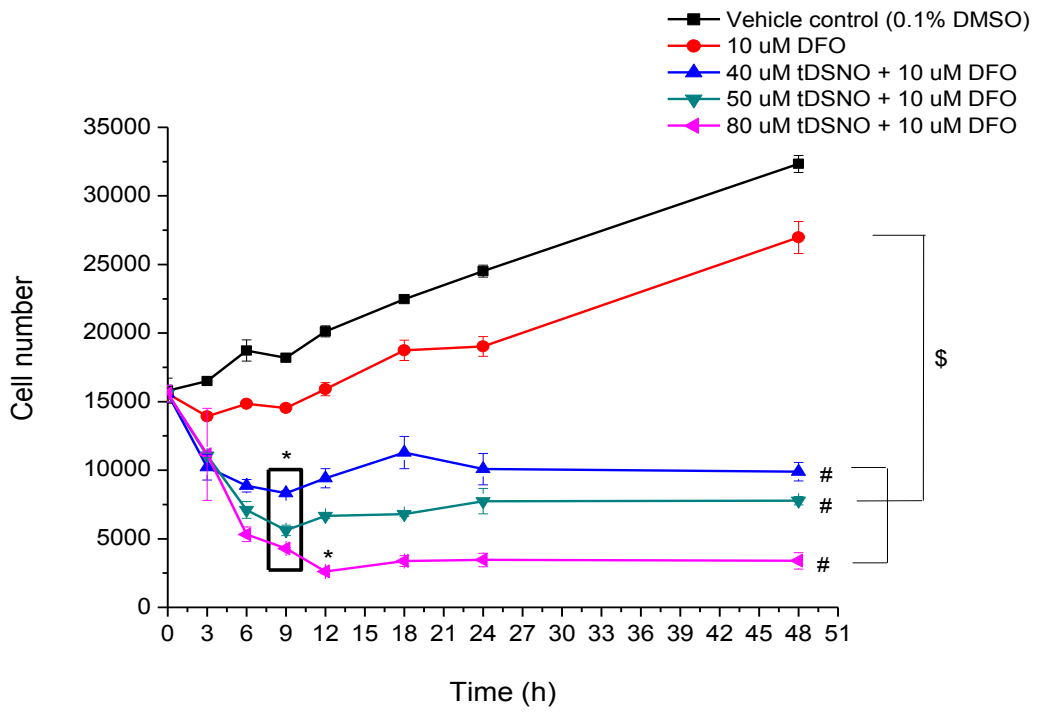

Figure 26 Growth rates of DFO-pre-treated MDA-MB-231 cells post-treated with tDSNO. Cells seeded in 96-well plates (8,000 cells per well) were incubated at 37^{o}C for 24 h to allow the cells to attach to the wells. The cells were then treated with DFO for 24 h followed by a treatment with tDSNO at 0 h. The MTT assay was performed after the corresponding time points. * ($p<0.05$) indicates a significant difference of treatment groups compared to control at 0 h, # ($p<0.05$) indicates a significant difference between different treatment groups and $ ($p<0.05$) indicates a significant difference of each treatment group compared to control (10 µM of DFO). Data are presented as mean ± SEM (n=3).

3.3.4 Concluding remarks for section 3.3

Parallel to the proposed hypothesis, the susceptibility of MDA-MB-231 cells to tDSNO (40 µM) increased following 24 h of DFO treatment (10, 100, 300 µM). tDSNO was cytotoxic to DFO-treated cells, even at concentrations that were previously non-cytotoxic (40 µM). The investigations also revealed that tDSNO in combination with DFO elicited a time and concentration dependent cytotoxicity. The earlier cytotoxicity assay (Figure 14) indicated that the greatest cellular death (66.4 ± 5.9%) upon a range of tDSNO treatment (40, 50 and 80 µM) was observable at 12 h and this cytotoxic effect was followed by a cytostatic effect which lasted until 48 h. Surprisingly, similar cytotoxic and cytostatic effects were observed following 10 µM of DFO treatment, but the greatest cellular death (72.5 ± 0.4%) upon a range of tDSNO treatment (40, 50 and 80 µM) was seen at a much earlier time point of 9 h and the extent of cellular death also increased.

CHAPTER 4: DISCUSSIONS & CONCLUSIONS

4.1 •NO-induced cytotoxicity. The photoactivation effect

- Characterisation of •NO release from tDSNO

The anti-cancer activity of •NO has been examined in a variety of cancer cells including ovarian, prostate and liver cancers (Garban and Bonavida, 1999; Chaiswing *et al*., 2008; Chen *et al*., 2008). However, therapeutic applications of •NO are limited due to its short biological half-life of ~6 s (Beckman and Koppenol, 1996). In order to overcome this problem, various studies have designed targeted drug carriers to stabilise •NO in the biological system and to deliver it to the desired site (Butler *et al*., 1998; Miller and Megson, 2007). Recently, tDSNO was designed based on *S*-nitrosothiol functionality to meet the characteristics and criteria of a •NO donating drug to be used therapeutically, especially for cancer therapy. Therefore, tDSNO drug action was initially characterised in cell culture cancer models using human triple negative breast cancer cells (MDA-MB-231) and human epithelial-like lung carcinoma cells (A549). For this purpose, it was necessary to evaluate a range of tDSNO concentrations to establish optimum conditions for cellular treatment throughout the study. Choosing the right concentration of tDSNO is important as •NO in micromolar concentrations is detrimental to the cells (Colasanti and Suzuki, 2000; Hofseth *et al*., 2003). Therefore, tDSNO in a range of 5 to 40 µM was used so that the production of •NO from tDSNO would not reach a cytotoxic level. Griess assay results confirmed that 40 µM of tDSNO produced approximately 2 µM of NO_2^- over 60 min, which is in proportion to the estimated rate of •NO release. In the cytotoxicity assay (MTT), a minimal, non-significant cytotoxicity was observed at this concentration, thus confirming that this concentration of tDSNO is non-detrimental to the cells (although producing micromolar concentrations of •NO).

tDSNO is a photoactivated drug. Therefore, its cytotoxicity is determined based on modulation of photoactivation and non-photoactivation conditions. Under photoactivation conditions, the IC_{50} of tDSNO against MDA-MB-231 cells was approximately 2-fold lower than the IC_{50} without photoactivation. Likewise, the IC_{50} of tDSNO against A549 cells was lower by 1.5-fold following photoactivation. These results suggest that a photolytic release of $^{\bullet}NO$ from tDSNO resulted in an enhanced cytotoxic effect. However, there was a cytotoxicity associated with tDSNO under non-photoactivation conditions, thus indicating that either some $^{\bullet}NO$ release did occur or that the drug tDSNO exhibited cytotoxicity independent of $^{\bullet}NO$ release. Comparative to MDA-MB-231 cells, the IC_{50}'s of tDSNO against A549 cells were lower by 1.2- and 1.6-fold under photoactivation and non-photoactivation conditions respectively. This suggests a higher sensitivity of A549 cells to $^{\bullet}NO$ exposure compared to MDA-MB-231 cells. Different IC_{50}'s of tDSNO in different cell lines suggest that tDSNO-mediated cytotoxicity is likely to depend upon the cell type, although the reason for this discrepancy is unknown. Despite the differences, both of these cell lines have IC_{50}'s for tDSNO that changed substantially following photoactivation. This suggests that tDSNO could be used as a suitable vehicle for $^{\bullet}NO$ delivery using phototherapeutic control for $^{\bullet}NO$ release. This is relevant for cancer treatment as the availability of the drug at the desired site could be controlled using photoactivation. The exposure of light at the required site will prevent unwanted, excessive release of $^{\bullet}NO$ at undesired sites and therefore will protect against damaging effects on healthy cells.

Similar to tDSNO, GSNO is also a photoactivated *S*-nitrosothiol, making it comparable to tDSNO. A previous study reported that the IC_{50} of GSNO changed from 0.44 to 0.41 mM following photoactivation (Sexton *et al*., 1994). This is a comparatively small change in IC_{50}'s, thus suggesting that GSNO was not an optimum drug candidate for phototherapy. Moreover, regardless of photoactivation or non-photoactivation, the IC_{50}'s of GSNO were higher by 2- to 6-fold than the IC_{50}'s of tDSNO against MDA-MB-231 and A549 cells, thus suggesting that tDSNO was superior drug candidate for phototherapy. This also suggests that tDSNO exerted a more potent cytotoxic

effect compared to GSNO. This is important as tDSNO could be used at low concentrations to avoid side effects of high concentrations. Moreover, using a low concentration of tDSNO would allow the drug to be metabolised faster and avoid an accumulation of unwanted drug metabolites in the cellular system. Therefore, this suggests that tDSNO is a better •NO releasing drug, which has therapeutic and experimental value, especially because of its •NO release in a controlled manner.

4.2 Targeting Fe overload for Fe-induced cytotoxicity. The intervention of •NO

- Hypothesis 1: Does a low level of •NO release cause cells to import Fe to cytotoxic levels?

A close link exists between •NO and Fe homeostasis. •NO has been reported to disrupt Fe regulation in normal and cancer cells including fibroblast, macrophages, lung and leukaemia cells (Oria *et al*., 1995; Gehring *et al*., 1999; Mulero and Brock, 1999; Wang *et al*., 2006). In the present study, the role of tDSNO in modulating Fe regulation in cancer cells was evaluated. MDA-MB-231 and A549 cells were used as test systems. These cell lines were chosen as they possess high Fe transport protein TfR relative to their normal counterparts (Walker and Day, 1986; Kondo *et al*., 1990). Therefore, following characterisation of •NO released by tDSNO upon photoactivation, the effectiveness of tDSNO to promote Fe overload in these cell lines was evaluated. As mentioned in section 1.4, FAC was used to increase Tf-bound Fe uptake by increasing extracellular Fe. FAC was chosen as it has no effect on the Tf binding site (Richardson and Baker, 1992). Any modification of this binding site might affect the mechanism of Fe uptake. Moreover, most Fe uptake studies used FAC instead of other sources of Fe (Hoepken *et al*., 2004; Riemer *et al*., 2004; Tulpule *et al*., 2010).

A 10 µM concentration of FAC was used for cellular treatments as a previous study conducted by Hoepken *et al.*, (2004) indicated that cellular Fe content increased by 5-fold at this concentration. Moreover, at this concentration, FAC proved to be non-toxic to the cells as it exhibited an IC_{50} of 474 µM. The Griess assay confirmed that Fe supplied from this 10 µM of FAC had no effect on

tDSNO activity, as the extent of •NO release did not change. However, the Fe uptake assay indicated that MDA-MB-231 cells treated with 10 to 100 µM of FAC did not change their intracellular Fe content compared with the control. This was surprising, as previous studies had shown that these levels of FAC resulted in 10- to 50-fold increases in the intracellular Fe content (Richardson and Baker, 1992; Hoepken *et al.*, 2004). This discrepancy could be due to a lack of assay sensitivity that restricted the detection of changes in the intracellular Fe content. In the earlier studies, changes in Fe levels from 10 to 150 µM of FAC treatment were detected using radioactive labelling and atomic absorption spectroscopy (Richardson and Baker, 1992; Hoepken *et al.*, 2004). In addition to this, these conflicting results could also be explained by the different cell lines used, as the 10- to 50-fold increases in the intracellular Fe content were detected in human melanoma cells and primary rat astrocyte cultures.

However, regardless of the presence or absence of FAC, tDSNO was unable to promote Fe overload in MDA-MB-231 cells. Similarly, Fe overload was also not developed in A549 cells, despite a higher expression of Fe transport proteins responsible for the uptake of Fe into this cell line, as suggested by 2- to 4-fold increase in the basal intracellular Fe content in A549 cells compared to MDA-MB-231 cells. The non-significant change in intracellular Fe content can be explained by taking into account four considerations. First, the concentrations of tDSNO used (5 to 40 µM), regardless of the presence or absence of FAC, may have been insufficient to disrupt cellular Fe regulation. An appreciable fraction of •NO released by tDSNO may have been disappeared in the air space. Therefore, irrespective of a high lipophilicity of •NO (Patel *et al*., 1999), the anticipated modulation of Fe regulation may have not occurred. Second, •NO released by tDSNO may have caused a minor effect on proteins involved in Fe regulation, but these modifications may have been repaired prior to Fe uptake. Third, it may also be due to insufficient time within which the tDSNO was photoactivated. Therefore, the 1 h photoactivation may not fully decompose tDSNO to release •NO. The fourth consideration is the sensitivity of the assay used as mentioned earlier. It could be

that the ferrozine assay was not sensitive enough to detect small changes in the intracellular Fe content caused by •NO.

Given that non-cytotoxic concentrations of tDSNO (5 to 40 µM) did not increase intracellular Fe content relative to control, cytotoxic concentrations of tDSNO (50 to 200 µM) were evaluated to investigate if, under these conditions, Fe levels had increased and this was why cell death occurred. Interestingly, in contrast to the original hypothesis that •NO would increase cellular Fe uptake, under cytotoxic conditions, the intracellular Fe content gradually decreased. From our point of view, the mechanisms of cytotoxicity may or may not be related to the decrease in Fe levels. However, if cell death was caused by an Fe decrease, three possible mechanisms may have been involved. First, •NO released by tDSNO may favour Fe chelation (Watts *et al*., 2006). In view of this, •NO may be capable of chelating Fe from cells, causing them to die because of Fe deprivation. A potential mechanism could be that •NO intercepts Fe immediately after it has been released from Tf in the endosome, allowing the resulting Fe-nitrosyl complex to diffuse out of the cells. Otherwise, •NO may intercept Fe before it is incorporated into ferritin. For this mechanism, •NO could directly chelate ferritin-bound Fe or indirectly chelate Fe in the LIP, leading to ferritin releasing its Fe. This is supported by a previous *in vitro* study by Watts and Richardson, (2002), who had shown that •NO not only releases Fe from ferritin but also intercepts Fe en route to this ferritin. Second, •NO release may have inhibited Fe uptake into the cells (Richardson *et al*., 1995). •NO is known to prevent Fe from binding to Tf at the cell membrane before it can be internalised into the cells via the Tf-TfR complex. This decreases the efficiency of Fe uptake without affecting the expression of TfR protein (Mulero and Brock, 1999). Third, instead of interacting with aconitase, •NO may have been scavenged by reacting with other Fe-containing molecules, such as enzymes containing a catalytically active Fe (Cleeter *et al*., 1994). •NO may have bound to haem Fe of cytochrome c oxidase, inhibiting oxygen utilisation and cellular respiration. This would result in

the inhibition of the mitochondrial respiratory chain and other major cellular processes. Indeed, this effect may have been exaggerated in our experimental system (aerobic environment) as $^{\bullet}NO$ release may have reacted with O_2^- to produce a more potent oxidant, $ONOO^-$, and cause a more profound inhibition (Castro *et al*., 1994; Cassina and Radi, 1996). Therefore, while it is possible that the decreases in Fe were related to $^{\bullet}NO$-induced cell death, the mechanism has yet to be ascertained.

As an increase in Fe levels was not observed at 24 h, further experiments were carried out to investigate if intracellular Fe content varied at other time points between 2 to 50 h, as by which time point, half of the drug should have decomposed. Changes in Fe levels were indeed observed, with a major decrease of 58% occurring at 16 h of post tDSNO treatment, which returned to control levels after 24 h. This suggested that 16 h was the maximum time for tDSNO to give its optimum effect in modulating cellular Fe homeostasis. Additionally, this also suggested that the effect of tDSNO on cellular Fe homeostasis was time dependent. However, regardless of the 58% decrease in intracellular Fe content, which was caused by the highest non-cytotoxic concentration of tDSNO (40 µM), the time-course proliferation assay indicated that at this concentration, MDA-MB-231 cell number remained static throughout the 48 h period. Therefore, in addition to the fact that 40 µM of tDSNO was non-cytotoxic, this finding revealed that at this level, tDSNO caused a cytostatic effect. However, as a fluctuation in intracellular Fe content still occurred over 48 h irrespective of the cytostatic effect of tDSNO on MDA-MB-231 cells, this suggested that the efficacy of tDSNO on cellular Fe homeostasis could be unrelated to the cytostatic mechanism of tDSNO action. An alternative possibility was that Fe loss might have caused the cells to change their survival mechanism and remain static. Regardless of these possibilities, one striking feature from this finding was that both cellular Fe modulation and cytostasis were observed within 48 h of tDSNO administration, even though tDSNO was present at non-cytotoxic concentrations. The two events may coincide if, by chance, $^{\bullet}NO$ affected both processes independently but over the same time

course. Therefore, the exact mechanism through which the efficacy of tDSNO is mediated is yet to be elucidated.

4.3 Fe deprivation: A potential mechanism for tDSNO-induced cytotoxicity

- Hypothesis 2: Does Fe deprivation increase the susceptibility of cells to $^{\bullet}$NO-induced cytotoxicity?

Fe is essential for cellular proliferation (Le and Richardson, 2004). Removing Fe from cells will prevent the cells from proliferating, which will lead to apoptosis and cause eventual cellular death. Therefore, Fe deprivation was predicted to exaggerate the effects of $^{\bullet}$NO exposure. This led to the investigation of the efficacy of tDSNO in combination with the Fe chelator DFO. Initially, it was necessary to evaluate a range of DFO concentrations to establish optimum conditions for Fe chelation. Previous literature indicated that 10 µM of DFO would be sufficient to deplete cellular Fe levels (Richardson *et al*., 1994; Darnell and Richardson, 1999). These studies reported that after 24 h of incubation with 10 µM DFO, cellular Fe levels decreased by 17% in human neuroblastoma and melanoma cells. Similarly, 25 µM of DFO decreased 40% of astrocyte Fe levels within 3 h of incubation (Tulpule *et al*., 2010). Therefore, it was anticipated that Fe deprivation should be seen after 24 h of incubation with 10 µM DFO. However, in MDA-MB-231 cells, 10 µM of DFO did not display any significant Fe chelation activity. As discussed earlier in section 4.2, this could be due to the insensitivity of the ferrozine assay used. Therefore, as there was no observable change in the intracellular Fe content following the treatment with 10 µM DFO, a range of higher concentrations from 10 to 300 µM of DFO were examined. There was no change in the intracellular Fe content detected until the upper limit of 300 µM was reached. At this concentration, the intracellular Fe content was decreased by 20%. This was again less than expected, as previous studies indicated that 100 µM of DFO decreased 60 to 80% of cellular Fe content (Richardson *et al*., 1994; Tulpule *et al*., 2010). Therefore, to allow for potential inaccuracies with the Fe detection assay, the efficacy of

tDSNO was examined in combination with 10 and 100 µM (to be comparable to earlier studies) and 300 µM (as this was the point at which a decrease in intracellular Fe content was observed in MDA-MB-231 cells).

Initial cytotoxicity assays revealed that 10 µM DFO induced 5% cell death in MDA-MB-231 cells. This was parallel to the previous study by Becton and Bryles, (1988), who had reported that 10 µM of DFO was necessary for Fe deprivation with a minimal cell killing. Interestingly, when the maximum non-cytotoxic concentration of tDSNO (40 µM) was given to these cells for a combination treatment, 17% cellular death was observed. This suggested a synergistic cytotoxic effect of tDSNO and DFO, despite a non-observable change in the intracellular Fe content at this 10 µM of DFO. Promisingly, upon a combination of tDSNO (40 µM) with higher concentrations of DFO (100 and 300 µM), the cytotoxicity assay indicated that 45 to 60% of MDA-MB-231 cells were dead. These combination treatments were undeniably more cytotoxic than that observed upon a combination of 40 µM tDSNO with a lower concentration of 10 µM DFO, thus strongly supporting our hypothesis that cancer cells, particularly MDA-MB-231 cells, were vulnerable to tDSNO in combination with Fe deprivation. Indeed, these suggested that a minimal concentration of DFO could be used in combination with tDSNO to give a profound cytotoxic effect. The combination may therefore be effective at preventing known side effects of DFO monotherapy (e.g. hypersensitivity reactions, neurological and hematologic adverse reactions), which are due to DFO rapidly penetrating the blood-brain barrier and accumulating at a significant level after systemic administration (Shadid *et al*., 1998; Okauchi *et al*., 2009).

The cytotoxic effect of tDSNO on DFO-treated MDA-MB-231 cells was also investigated based on cellular growth rate. For this purpose, the non-cytotoxic concentration of DFO (10 µM) was chosen to treat the cells as a synergistic cytotoxic effect in combination with tDSNO was observed at this concentration. Moreover, a low concentration of DFO was required in order to avoid any

confounding cytotoxic effects with tDSNO. Over a period of 48 h, MDA-MB-231 cells with normal Fe homeostasis grew at a linear rate, with cell number doubling within 48 h (Figure 26). This was in line with the anticipated, exponential behaviour of cellular growth. A similar pattern of cellular growth was observed in MDA-MB-231 cells treated with 10 μM DFO, with the exception at 3 h time point, where the cell number dropped slightly, presumably due to seeding variability. Despite the similarity in the pattern of cellular growth, the number of DFO-treated MDA-MB-231 cells was lower by 1.0- to 1.3-fold throughout the 48 h period compared to MDA-MB-231 cells with normal Fe homeostasis. As the cytotoxicity assay indicated that 10 μM of DFO was non-cytotoxic, with only 5% of cellular death, it could be that this DFO level might have altered the morphology of the cells and decreased the ability to adhere to plastic surfaces (Becton and Bryles, 1988), giving an apparent reduction in cell number in the assay.

Interestingly, upon a combination of a range of tDSNO concentrations (40, 50 and 80 μM) with DFO (10 μM), two different phases of cellular response was observed. In the first cytotoxic phase, from 0 to 9 h, cell number decreased down to approximately 30% in a concentration dependent manner. In the second cytostatic phase, from 9 to 48 h, cell number was maintained and remained steady, and this was independent of all tDSNO concentrations given (Figure 26). This suggested that the efficacy of tDSNO was dependent on both time and concentration. tDSNO was cytotoxic when first exposed to MDA-MB-231 cells, but caused a cytostatic effect at later time points. The time dependence of cytotoxicity of tDSNO could be due to differential sensitivity within a heterogeneous cell population. However, as the cytotoxic effect was short-lived, it could be that the concentrations of $^{\bullet}NO$ release might not be high enough to give a greater, long-lasting cytotoxic effect. In view of this, sustained exposure to a moderate concentration of $^{\bullet}NO$ might have a more lasting effect than a brief exposure to a large concentration of $^{\bullet}NO$ (Stuehr and Nathan, 1989). It could also be that the $^{\bullet}NO$ produced might have been oxidised into NO_2^- and NO_3^- as it diffused away from its source. Besides, it could also be due to the instability of tDSNO in the cellular

system. Several physiological factors might have affected the stability of tDSNO. As mentioned in the Introduction (section 1.2.4.2.2), this could include enzymatic activities of γ-glutamyl transpeptidase and the presence of metal ions such as Cu^{2+} that might have enhanced the decomposition of tDSNO. To explain the cytostatic effect observed at the second phase of cellular response, it is tempting to speculate that the presence of a nitrosative stress might have triggered a defence mechanism to protect the MDA-MB-231 cells, so that they underwent cell cycle arrest to repair oxidative damage before proceeding with replication (Beltran *et al.*, 2000). However, whether the cells have undergone this mechanism remains to be investigated.

4.4 Conclusions

This study was performed to explore the interaction of •NO and Fe in MDA-MB-231 and A549 cells. The characteristics of •NO released by tDSNO modulated by photoactivation have been demonstrated. Upon photoactivation, the efficacy of tDSNO was enhanced, as indicated by 1.5- to 2-fold decrease in IC_{50}'s values compared with non-photoactivation conditions. The cytotoxic effect of •NO release from tDSNO was cell line dependent. Regardless of photoactivation, the lung carcinoma cell line, A549 cells, exhibited a higher sensitivity towards tDSNO as indicated by 1.6-fold decrease in IC_{50}'s values compared with the triple negative breast cancer cell line, MDA-MB-231 cells. Using this cytotoxic profile, the interactions of tDSNO with cellular Fe levels were examined as a potential photochemotherapeutic treatment for breast and lung cancers.

Based on two hypotheses, the crosstalk between •NO and Fe in breast and lung cancer cells was explored.

Does a low level of •NO release cause cells to import Fe to cytotoxic levels?

For the first time, this study reported an attempt to induce Fe overload in MDA-MB-231 and A549 cells as a means of cytotoxicity. Although not conclusive, data presented suggest that the first attempt to promote Fe overload to cause cytotoxicity was unsuccessful, and hence, disapproved the first hypothesis. tDSNO was unable to increase intracellular Fe content above the control level by all means investigated, even when FAC was used to enhance the Tf-bound Fe uptake. It is certainly possible that the study failed to demonstrate a significant increase in intracellular Fe content simply because the ferrozine assay used was insensitive, the sample size chosen was too small and the time within which the measurement was made was beyond the actual time where the drug action occurred. Therefore, these factors put a strict limit on tDSNO drug actions to be evaluated,

especially if the increases in intracellular Fe content were below the detection threshold of the assay.

However, in contrast to the hypothesis that •NO exposure would increase the intracellular Fe content, •NO release from photoactivated tDSNO was observed to decrease Fe levels in MDA-MB-231 cells by 87% following 24 h of treatment with cytotoxic concentrations of tDSNO (50 to 200 µM). This decrease in intracellular Fe content was associated with cellular death of up to 86%. Likewise, following 24 h of treatment with a non-cytotoxic concentration of tDSNO (40 µM), a similar decrease in intracellular Fe content of 58% was observed in MDA-MB-231 cells. However, this decrease in intracellular Fe content was seen at a much earlier time point of 16 h and Fe returned to control levels by 24 h, with the cell number remaining static throughout the 48 h of the experimental period. Altogether, these findings demonstrated that the efficacy of photoactivated tDSNO on cellular Fe homeostasis, particularly in MDA-MB-231 cells, was dependent on time and concentration. Indeed, these findings were in agreement with a previous report that showed •NO decreased Fe levels in melanoma cells in a time and concentration dependent manner, with the maximum decrease to 57% of the control observed at 4 h following 24 h of exposure to •NO donor SNP (Richardson *et al*., 1995). Therefore, data from this study would corroborate the current available data to define the efficacy of •NO in modulating cellular Fe homeostasis.

Does Fe deprivation increase the susceptibility of cells to •NO-induced cytotoxicity?

In contrast to the first hypothesis, the second target to enhance the cytotoxicity of tDSNO was promising. MDA-MB-231 cells were more vulnerable to tDSNO when pre-treated with 10, 100 and 300 µM of DFO for 24 h. The percentage of viable cells dropped down to 45% when they were exposed to a maximum non-cytotoxic concentration of tDSNO (40 µM) for 24 h. Promisingly, a combination of 40, 50 and 80 µM of tDSNO with 10 µM DFO elicited a time and concentration

dependent cytotoxicity. Two different phases of cellular response were observed following 48 h of these combination treatments. The first phase was a cytotoxic phase, which occurred at the early time point, prior to 9 h. The second phase was a cytostatic phase, which occurred post 9 h of tDSNO treatment and lasted until 48 h. In addition, the percentage of cell death in MDA-MB-231 cells following these combination treatments also appeared to increase by 1.6-fold relative to MDA-MB-231 cells with normal Fe homeostasis. Therefore, the pathway elicited by the Fe deprivation agent DFO proved to be promising for tDSNO-induced cytotoxicity. The efficacy of tDSNO through the principle mechanism of Fe deprivation corroborates the current available data from other sources of $^{\bullet}$NO donors (e.g. SNP and SNAP) indicating a decrease in intracellular Fe levels induces cell death after the exposure to $^{\bullet}$NO (Feger *et al*., 2001). Therefore, the present study would help to define new therapeutic approaches to combine $^{\bullet}$NO and Fe chelation therapy.

4.5 Future directions

This *in vitro* study suggests that •NO released by tDSNO has a role in regulating Fe metabolism in cancer cells, particularly MDA-MB-231 cells. One indication that cellular Fe uptake may have occurred was that an increase in mean intracellular Fe content of 1.13-fold was observed at 40 µM tDSNO (Figure 16). However, this increase in intracellular Fe content was relatively small to give a significant statistical difference with the control. One potential issue was that the ferrozine assay may not be sensitive enough to detect small variations in intracellular Fe content. Therefore, future studies are likely to address the issue with Fe overload, in which a more sensitive method would be necessary. For example, a quantification of intracellular Fe content could be done using atomic absorption spectroscopy. This method is proven to be sensitive as it can detect Fe as low as 10 nmol per mg protein (Hoepken *et al*., 2004). If increased intracellular Fe content is observed, this could be followed by investigating the mechanism through which Fe influx occurs in cells. As the membrane-bound Tf-TfR complex is one important pathway for cellular Fe transportation, a radiolabelling study of Tf with iodine-125 would allow a measurement of cellular Fe influx. This measurement would allow further insight into the capability of tDSNO in modulating Fe utilisation by cancer cells.

In addition to the small increase (1.13-fold) in mean intracellular Fe content following 24 h of treatment with 40 µM tDSNO, in order to increase the likelihood of detecting Fe uptake if changes in Fe levels are small, it might appear reasonable to increase the sample size (e.g. from 4 to 8). This would be worthwhile to confirm that these small changes can occur upon post tDSNO treatment.

No increase in intracellular Fe content was observed within a 50 h period. Therefore, it would be worthwhile to extend the selected time period to measure if tDSNO increases the intracellular Fe uptake after 50 h (because tDSNO might require a longer time to take action with its half-life of 50

h). It would also be worth it to extend the time period of measuring the growth rate of DFO-treated MDA-MB-231 cells. This would allow further observation of the effects of tDSNO on cell proliferation. Moreover, this would also allow further characterisation of tDSNO, by determining the onset and offset of drug effects which would correlate with the stability and metabolism of tDSNO in the cellular system. Furthermore, this extended time course study would provide additional information regarding the mechanism of tDSNO drug action.

High concentrations (50 to 200 µM) of tDSNO decreased intracellular Fe content and caused 16 to 86 % cell death. The cytotoxicity may be mediated by the mitochondrial respiratory chain as this is one important system that contains Fe-dependent protein complexes responsible for cellular energy metabolism (Beltran *et al*., 2000). Therefore, measuring the integrity of the mitochondrial membrane (e.g. by mitochondrial cytochrome c release) would confirm this mechanism of cytotoxicity. Besides, the cytotoxicity may be mediated by Fe loss (Watts *et al*., 2006). This may affect some of the major components of Fe regulatory proteins, including ferritin and TfR proteins (Oria *et al*., 1995). A modulation of Fe regulatory proteins might have occurred in the case of decreased intracellular Fe content at 16 h of tDSNO treatment which recovered at 24 h. Therefore, it would be worth investigating the expression of these proteins (e.g. Western blot analysis of TfR) to confirm the mechanism involved and to examine the implications of tDSNO on Fe regulation.

DFO (10 µM) in combination with tDSNO (40 µM) caused a synergistic cytotoxic effect. DFO is known to cause cell cycle arrest and stop cell division (Kulp *et al*., 1996), and this could lead to apoptosis (Yu and Richardson, 2011). However, this has only been shown with much higher levels of DFO, between 100 to 150 µM (Kulp *et al*., 1996). In order to confirm whether the synergistic cytotoxic effect was mediated by cell cycle arrest, it is suggested to perform cell cycle analysis by single labelling the treated cells with Propidium Iodide (PI) and perform analysis using flow cytometry. Additionally, Fe deprivation has been shown to affect multiple components of the

MAPK pathway, including JNK and p38 (Yu and Richardson, 2011). Activation of these stress-activated protein kinases increased phosphorylation of the downstream protein p53, leading to apoptosis. Therefore, it would be worthwhile to elucidate this mechanism, as the cytotoxicity of tDSNO may be mediated through apoptotic pathways. This could be determined by double labelling the treated cells with Annexin V and PI, which would discriminate between whether the cells are undergoing apoptotic or necrotic cell death (Lecoeur *et al*., 2001).

Last but not least, it is highly recommended that the efficacy of tDSNO could also be evaluated in non-malignant breast and lung cells. This would allow a comparison of its effects with cancer cells, apart from confirming the specification of tDSNO in affecting normal and cancer cells, in which both the vulnerability to anti-cancer drugs are different dependent on the sensitivity and selectivity of the cells to the drug. Additionally, it is also highly recommended to perform the evaluation of tDSNO *in vivo* as this would provide a useful insight into the pharmacokinetics of tDSNO, including rates of absorption, biotransformation, bio-distribution and excretion. Moreover, the efficacy of tDSNO *in vivo* could later be correlated with clinical responses.

CHAPTER 5: REFERENCES

Abel, EL, Angel, JM, Kiguchi, K, DiGiovanni, J (2009) Multi-stage chemical carcinogenesis in mouse skin: Fundamentals and applications. *Nat. Protoc* **4**(9)**:** 1350-1362.

Al-Hajj, M, Wicha, MS, Benito-Hernandez, A, Morrison, SJ, Clarke, MF (2003) Prospective identification of tumorigenic breast cancer cells. *PNAS* **100**(7)**:** 3983-3988.

Aken, PAV, Liebscher, B, Styrsa, VJ (1998) Quantitative determination of iron oxidation states in minerals using Fe L2,3-edge electron energy-loss near-edge structure spectroscopy. *Phys Chem Miner* **25**(5)**:** 323-327.

Almazan, G, Liu, H-N, Khorchid, A, Sundararajan, S, Martinez-Bermudez, AK, Chemtob, S (2000) Exposure of developing oligodendrocytes to cadmium causes HSP72 induction, free radical generation, reduction in glutathione levels, and cell death. *Free Radical Bio Med* **29**(9)**:** 858-869.

Al-Sa'doni, H, Ferro, A (2000) S-nitrosothiols: A class of nitric oxide-donor drugs. *Clin Sci* **98**(5)**:** 507-520.

Aisen, P, Wessling-Resnick, M, Leibold, EA (1999) Iron metabolism. *Curr Opin Chem Biol* **3**(2)**:** 200-206.

Askew, SC, Butler, AR, Flitney, FW, Kemp, GD, Megson, IL (1995) Chemical mechanisms underlying the vasodilator and platelet anti-aggregating properties of *S*-nitroso-*N*-acetyl--penicillamine and S-nitrosoglutathione. *Bioorg Med Chem* **3**(1)**:** 1-9.

Bali, PK, Zak, O, Aisen, P (1991) A new role for the transferrin receptor in the release of iron from transferrin. *Biochem* **30**(2)**:** 324-328.

Batchelor, AM, Bartus, K, Reynell, C, Constantinou, S, Halvey, EJ, Held, KF, *et al.* (2010) Exquisite sensitivity to sub-second, picomolar nitric oxide transients conferred on cells by guanylyl cyclase-coupled receptors. *PNAS* **107**(51)**:** 22060-22065.

Bates, JN, Baker, MT, Guerra Jr, R, Harrison, DG (1991) Nitric oxide generation from nitroprusside by vascular tissue: Evidence that reduction of the nitroprusside anion and cyanide loss are required. *Biochem Pharm* **42:** S157-S165.

Bauer, KR, Brown, M, Cress, RD, Parise, CA, Caggiano, V (2007) Descriptive analysis of oestrogen receptor (ER)-negative, progesterone receptor (PR)-negative, and HER2-negative invasive breast cancer, the so-called triple-negative phenotype. *Cancer* **109**(9)**:** 1721-1728.

Beckman, JS, Koppenol, WH (1996) Nitric oxide, superoxide, and peroxynitrite: the good, the bad, and ugly. *Am J Physiol-Cell Ph* **271**(5)**:** C1424-C1437.

Becton, DL, Bryles, P (1988) Deferoxamine inhibition of human neuroblastoma viability and proliferation. *Cancer Res* **48:** 7189-7192.

Beinert, H, Kennedy, M (1993) Aconitase, a two-faced protein: enzyme and iron regulatory factor. *FASEB J* **7**(15)**:** 1442-1449.

Beinert, H, Kennedy, MC, Stout, CD (1996) Aconitase as iron sulfur protein, enzyme, and iron-regulatory protein. *Chem Rev* **96**(7)**:** 2335-2374.

Beinert, H, Holm, RH, Munck, E (1997) Iron-sulfur clusters: nature's modular, multipurpose structures. *Sci* **277**(5326)**:** 653-659.

Beinert, H, Kiley, PJ (1999) Fe-S proteins in sensing and regulatory functions. *Curr Opin Chem Biol* **3**(2)**:** 152-157.

Beinert, H (2000) Iron-sulfur proteins: ancient structures, still full of surprises. *J Biol Inorg Chem* **5**(1)**:** 2-15.

Beltran, B, Mathur, A, Duchen, MR, Erusalimsky, JD, Moncada, S (2000) The effect of nitric oxide on cell respiration: A key to understanding its role in cell survival or death. *PNAS* **97**(26)**:** 14602-14607.

Bennett, BM, Leitman, DC, Schroder, H, Kawamoto, JH, Nakatsu, K, Murad, F (1989) Relationship between biotransformation of glyceryl trinitrate and cyclic GMP accumulation in various cultured cell lines. *J Pharm Exp Ther* **250**(1)**:** 316-323.

Bhattacharjee, A, Richards, WG, Staunton, J, Li, C, Monti, S, Vasa, P, *et al.* (2001) Classification of human lung carcinomas by mRNA expression profiling reveals distinct adenocarcinoma subclasses. *PNAS* **98**(24)**:** 13790-13795.

Bomford, A, Isaac, J, Roberts, S, Edwards, A, Young, S, Williams, R (1986) The effect of desferrioxamine on transferrin receptors, the cell cycle and growth rates of human leukaemic cells. *Biochem J* **236**(1)**:** 243-249.

Bothwell, TH (1995) Overview and mechanisms of iron regulation. *Nutr Rev* **53**(9)**:** 237-245.

Bouton, C, Raveau, M, Drapier, J-C (1996) Modulation of iron regulatory protein functions. *J Biol Chem* **271**(4)**:** 2300-2306.

Butler, AR, Al-Sa'doni, HH, Megson, IL, Flitney, FW (1998) Synthesis, decomposition, and vasodilator action of some new *S*-nitrosated dipeptides. *Nitric Oxide* **2**(3)**:** 193-202.

Butler, AR, Glidewell, C (1987) Recent chemical studies of sodium nitroprusside relevant to its hypotensive action. *Chem Soc Rev* **16:** 361-380.

Cairo, G, Recalcati, S, Pietrangelo, A, Minotti, G (2002) The iron regulatory proteins: targets and modulators of free radical reactions and oxidative damage. *Free Radical Biol Med* **32**(12)**:** 1237-1243.

Cassina, A, Radi, R (1996) Differential inhibitory action of nitric oxide and peroxynitrite on mitochondrial electron transport. *Arch Biochem Biophys* **328**(2)**:** 309-316.

Castro, L, Rodriguez, M, Radi, R (1994) Aconitase is readily inactivated by peroxynitrite, but not by its precursor, nitric oxide. *J Biol Chem* **269**(47)**:** 29409-29415.

Cavanaugh, PG, Jia, LB, Zou, YY, Nicolson, GL (1999) Transferrin receptor overexpression enhances transferrin responsiveness and the metastatic growth of a rat mammary adenocarcinoma cell line. *Breast Cancer Res Treat* **56**(3)**:** 201-215.

Chaiswing, L, Zhong, W, Cullen, JJ, Oberley, LW, Oberley, TD (2008) Extracellular redox state regulates features associated with prostate cancer cell invasion. *Cancer Res* **68**(14)**:** 5820-5826.

Chen, Z, Zhang, J, Stamler, JS (2002) Identification of the enzymatic mechanism of nitroglycerin bioactivation. *PNAS* **99**(12)**:** 8306-8311.

Chen, L, Zhang, Y, Kong, X, Lan, E, Huang, Z, Peng, S, *et al.* (2008) Design, synthesis, and anti-hepatocellular carcinoma activity of nitric oxide releasing derivatives of oleanolic acid. *J Med Chem* **51**(15)**:** 4834-4838.

Chen, C, Samuel, TK, Sinclair, J, Dailey, HA, Hamza, I (2011) An intercellular haem-trafficking protein delivers maternal haem to the embryo during development in C. elegans. *Cell* **145**(5)**:** 720-731.

Cho, Y, Gorina, S, Jeffrey, P, Pavletich, N (1994) Crystal structure of a p53 tumour suppressor-DNA complex: Understanding tumorigenic mutations. *Sci* **265**(5170)**:** 346-355.

Chua, ACG, Klopcic, B, Lawrence, IC, Olynyk, JK, Trinder, D (2010) Iron: An emerging factor in colorectal carcinogenesis. *World J Gastroenterol* **16**(6)**:** 663.

Cleeter, MWJ, Cooper, J, Darley-Usmar, V, Moncada, S, Schapira, A (1994) Reversible inhibition of cytochrome c oxidase, the terminal enzyme of the mitochondrial respiratory chain, by nitric oxide: Implications for neurodegenerative diseases. *FEBS Letters* **345**(1)**:** 50.

Cohen, SM, Ellwein, LB (1991) Genetic errors, cell proliferation, and carcinogenesis. *Cancer Res* **51**(24)**:** 6493-6505.

Colasanti, M, Suzuki, H (2000) The dual personality of NO. *Trends Pharmacol Sci* **21**(7)**:** 249-252.

Connor, JR, Menzies, SL, Martin, SMS, Mufson, EJ (1990) Cellular distribution of transferrin, ferritin, and iron in normal and aged human brains. *J Neurosci Res* **27**(4)**:** 595-611.

Cook, JA, Krishna, MC, Pacelli, R, DeGraff, W, Liebmann, J, Mitchell, JB, *et al.* (1997) Nitric oxide enhancement of melphalan-induced cytotoxicity. *Br J Cancer* **76**(3)**:** 325-334.

Cooper, CE, Lynagh, GR, Hoyes, KP, Hider, RC, Cammack, R, Porter, JB (1996) The relationship of intracellular iron chelation to the inhibition and regeneration of human ribonucleotide reductase. *J Biol Chem* **271**(34)**:** 20291-20299.

Curtis, E, Wright, C, Wall, M (2005) The epidemiology of breast cancer in Maori women in Aotearoa New Zealand: Implications for ethnicity data analysis. *NZ Med J* **118**(1209)**:** 1-10.

Dabbagh, AJM, T. Lynch, S. M. Frei, B. (1994) The effect of iron overload on rat plasma liver oxidant status *in vivo*. *Biochem J* **300**(3)**:** 799-803.

Daniels, TR, Delgado, T, Rodriguez, JA, Helguera, G, Penichet, ML (2006) The transferrin receptor part I: Biology and targeting with cytotoxic antibodies for the treatment of cancer. *Clin Immunol* **121**(2)**:** 144-158.

Darnell, G, Richardson, DR (1999) The potential of iron chelators of the pyridoxal isonicotinoyl hydrazone class as effective antiproliferative agents III: The effect of the ligands on molecular targets involved in proliferation. *Blood* **94**(2)**:** 781-792.

DeBerardinis, RJ, Lum, JJ, Hatzivassiliou, G, Thompson, CB (2008) The biology of cancer: Metabolic reprogramming fuels cell growth and proliferation. *Cell Metab* **7**(1)**:** 11-20.

Denizot, Fo, Lang, R (1986) Rapid colorimetric assay for cell growth and survival: Modifications to the tetrazolium dye procedure giving improved sensitivity and reliability. *J Immunol Meth* **89**(2)**:** 271-277.

deRojas-Walker, T, Tamir, S, Ji, H, Wishnok, JS, Tannenbaum, SR (1995) Nitric oxide induces oxidative damage in addition to deamination in macrophage DNA. *Chem Res Toxicol* **8**(3)**:** 473-477.

Eisenstein, RS (2000) Iron regulatory proteins and the molecular control of mammalian iron metabolism. *Annu Rev Nutr* **20**(1)**:** 627-662.

Esposito, BP, Epsztejn, S, Breuer, W, Cabantchik, ZI (2002) A review of fluorescence methods for assessing labile iron in cells and biological fluids. *Anal Biochem* **304**(1)**:** 1-18.

Faulk, WP, Stevens, PJ, Hsi, B-L (1980) Transferrin and transferrin receptors in carcinoma of the breast. *Lancet* **316:** 390-392.

Feger, F, Ferry-Dumazet, H, Matsuda, MM, Bordenave, J, Dupouy, M, Nussler, AK, *et al.* (2001) Role of iron in tumour cell protection from the pro-apoptotic effect of nitric oxide. *Cancer Res* **61**(13)**:** 5289-5294.

Fenton, C, Wellington, K, Easthope, SE (2006) 0.4% nitroglycerin ointment: In the treatment of chronic anal fissure pain. *Drugs* **66**(3)**:** 343-349.

Ford, PC, Bourassa, J, Miranda, K, Lee, B, Lorkovic, I, Boggs, S, *et al.* (1998). Photochemistry of metal nitrosyl complexes. Delivery of nitric oxide to biological targets. *Coordin Chem Rev* **171**(0)**:** 185-202.

Forrester, K, Ambs, S, Lupold, SE, Kapust, RB, Spillare, EA, Weinberg, WC, *et al.* (1996) Nitric oxide-induced p53 accumulation and regulation of inducible nitric oxide synthase expression by wild-type p53. *PNAS* **93**(6)**:** 2442-2447.

Fotakis, G, Timbrell, JA (2006) In vitro cytotoxicity assays: Comparison of LDH, neutral red, MTT and protein assay in hepatoma cell lines following exposure to cadmium chloride. *Toxicol Lett* **160**(2)**:** 171-177.

Fukumura, D, Kashiwagi, S, Jain, RK (2006) The role of nitric oxide in tumour progression. *Nat Rev Cancer* **6**(7)**:** 521-534.

Furchgott, RF, Zawadzki, JV (1980) The obligatory role of endothelial cells in the relaxation of arterial smooth muscle by acetylcholine. *Nature (London)* **288**(5789)**:** 373-376.

Ganz, T, Nemeth, E (2006) Regulation of iron acquisition and iron distribution in mammals. *BBA-Mol Cell Res* **1763**(7)**:** 690-699.

Gao, J, Richardson, DR (2001) The potential of iron chelators of the pyridoxal isonicotinoyl hydrazone class as effective anti-proliferative agents, IV: The mechanisms involved in inhibiting cell-cycle progression. *Blood* **98**(3): 842-850.

Garban, HJ, Bonavida, B (1999) Nitric oxide sensitizes ovarian tumour cells to Fas-induced apoptosis. *Gynecol Oncol* **73**(2)**:** 257-264.

Gardner, PR, Nguyen, D-DH, White, CW (1994) Aconitase is a sensitive and critical target of oxygen poisoning in cultured mammalian cells and in rat lungs. *PNAS* **91**(25)**:** 12248-12252.

Gardner, PR, Costantino, G, Szabo, C, Salzman, AL (1997) Nitric oxide sensitivity of the aconitases. *J Biol Chem* **272**(40)**:** 25071-25076.

Gehring, NH, Hentze, MW, Pantopoulos, K (1999) Inactivation of both RNA binding and aconitase activities of iron regulatory protein-1 by quinone-induced oxidative stress. *J Biol Chem* **274**(10)**:** 6219-6225.

Geissler, C, Singh, M (2011) Iron, meat and health. *Nutr* **3**(3)**:** 283-316.

Gerlier, D, Thomasset, N (1986) Use of MTT colorimetric assay to measure cell activation. *J Immunol Meth* **94**(1-2)**:** 57-63.

Giles, GI, Emilie, B, Giles, NM (2008) Synthetic *S*-nitrosothiols as anti-cancer agents. *Free Radical Biol Med* **45**(1): 82-83.

Giustarini, D, Milzani, A, Colombo, R, Dalle-Donne, I, Rossi, R (2003) Nitric oxide and S-nitrosothiols in human blood. *Clin Chim Acta* **330:** 85-98.

Goldhaber, SB (2003) Trace element risk assessment: essentiality vs. toxicity. *Regul Toxicol Pharmacol* **38**(2)**:** 232-242.

Golub, TR (2001) Genome-wide views of cancer. *N Engl J Med* **344**(8)**:** 601-602.

Grossi, L, Montevecchi, PC (2002) A kinetic study of *S*-nitrosothiol decomposition. *Chem Eur J* **8**(2)**:** 380-387.

Grossi, L, D'Angelo, S (2005) Sodium nitroprusside: Mechanism of NO release mediated by sulfhydryl-containing molecules. *J Med Chem* **48**(7)**:** 2622-2626.

Guo, B, Phillips, JD, Yu, Y, Leibold, EA (1995) Iron regulates the intracellular degradation of iron regulatory protein 2 by the proteasome. *J Biol Chem* **270**(37)**:** 21645-21651.

Habashy, H, Powe, D, Staka, C, Rakha, E, Ball, G, Green, A, *et al.* (2010) Transferrin receptor (CD71) is a marker of poor prognosis in breast cancer and can predict response to tamoxifen. In: *Breast Cancer Res Treat* **119**: 283-293.

Hallberg, L, Hulten, L, Gramatkovski, E (1997) Iron absorption from the whole diet in men: How effective is the regulation of iron absorption? *Am J Clin Nutr* **66**(2)**:** 347-356.

Hann, H-WL, Evans, AE, Siegel, SE, Wong, KY, Sather, H, Dalton, A, *et al.* (1985) Prognostic importance of serum ferritin in patients with stages III and IV neuroblastoma: the children's cancer study group experience. *Cancer Res* **45**(6)**:** 2843-2848.

Harrison, PM, Arosio, P (1996) The ferritins: molecular properties, iron storage function and cellular regulation. *BBA-Bioenerg* **1275**(3)**:** 161-203.

Hentze, MW, Kuhn, LC (1996) Molecular control of vertebrate iron metabolism: mRNA-based regulatory circuits operated by iron, nitric oxide, and oxidative stress. *PNAS* **93**(16)**:** 8175-8182.

Hirst, D, Robson, T (2007) Targeting nitric oxide for cancer therapy. *J Pharm Pharmacol* **59**(1)**:** 3-13.

Hoepken, HH, Korten, T, Robinson, SR, Dringen, R (2004) Iron accumulation, iron-mediated toxicity and altered levels of ferritin and transferrin receptor in cultured astrocytes during incubation with ferric ammonium citrate. *J Neurochem* **88**(5)**:** 1194-1202.

Hofseth, LJ, Hussain, SP, Wogan, GN, Harris, CC (2003) Nitric oxide in cancer and chemoprevention. *Free Radical Biol Med* **34**(8)**:** 955-968.

Hogg, N (2000) Biological chemistry and clinical potential of *S*-nitrosothiols. *Free Radical Biol Med* **28**(10)**:** 1478-1486.

Hogg, N (2002) The biochemistry and physiology of *S*-nitrosothiols. *Annu Rev Pharmacol Toxicol* **42**(1)**:** 585-600.

Hoyes, KP, Hider, RC, Porter, JB (1992) Cell cycle synchronization and growth inhibition by 3-hydroxypyridin-4-one iron chelators in leukaemia cell lines. *Cancer Res* **52**(17)**:** 4591-4599.

Huang, X (2003) Iron overload and its association with cancer risk in humans: evidence for iron as a carcinogenic metal. *Mutat Res-Fund Mol M* **533**(1-2)**:** 153-171.

Iacopetta, BJ, Morgan, EH (1983) The kinetics of transferrin endocytosis and iron uptake from transferrin in rabbit reticulocytes. *J Biol Chem* **258**(15)**:** 9108-9115.

Janssen-Heijnen, MLG, Coebergh, J-WW (2001) Trends in incidence and prognosis of the histological subtypes of lung cancer in North America, Australia, New Zealand and Europe. *Lung cancer (Amsterdam, Netherlands)* **31**(2-3)**:** 123.

Kakhlon, O, Cabantchik, ZI (2002) The labile iron pool: Characterization, measurement, and participation in cellular processes. *Free Radical Biol Med* **33**(8)**:** 1037-1046.

Kharitonov, VG, Sundquist, AR, Sharma, VS (1995) Kinetics of nitrosation of thiols by nitric oxide in the presence of oxygen. *J Biol Chem* **270**(47)**:** 28158-28164.

Kennedy, MC, Antholine, WE, Beinert, H (1997) An EPR investigation of the products of the reaction of cytosolic and mitochondrial aconitases with nitric oxide. *J Biol Chem* **272**(33)**:** 20340-20347.

Kondo, K, Noguchi, M, Mukai, K, Matsuno, Y, Sato, Y, Shimosato, Y, *et al.* (1990) Transferrin receptor expression in adenocarcinoma of the lung as a histopathologic indicator of prognosis. *Chest* **97**(6)**:** 1367-1371.

Konijn, AM, Glickstein, H, Vaisman, B, Meyron-Holtz, EG, Slotki, IN, Cabantchik, ZI (1999) The cellular labile iron pool and intracellular ferritin in K562 cells. *Blood* **94**(6)**:** 2128-2134.

Kulp, KS, Green, SL, Vulliet, PR (1996) Iron deprivation inhibits cyclin-dependent kinase activity and decreases cyclin D/CDK4 protein levels in asynchronous MDA-MB-453 human breast cancer cells. *Exp Cell Res* **229**(1)**:** 60-68.

Kumar, S, Bandyopadhyay, U (2005) Free haem toxicity and its detoxification systems in human. *Toxicol Lett* **157**(3): 175-188.

Lala, PK, Chakraborty, C (2001) Role of nitric oxide in carcinogenesis and tumour progression. *Lancet Oncol* **2**(3)**:** 149-156.

Le, NTV, Richardson, DR (2002) The role of iron in cell cycle progression and the proliferation of neoplastic cells. *BBA-Rev Cancer* **1603**(1)**:** 31-46.

Le, NTV, Richardson, DR (2004) Iron chelators with high anti-proliferative activity up-regulate the expression of a growth inhibitory and metastasis suppressor gene: a link between iron metabolism and proliferation. *Blood* **104**(9)**:** 2967-2975.

Lecoeur, H, Prevost, M-C, Gougeon, M-L (2001) Oncosis is associated with exposure of phosphatidylserine residues on the outside layer of the plasma membrane: A reconsideration of the specificity of the Annexin V/Propidium Iodide assay. *Cytometry* **44**(1)**:** 65-72.

Lederman, H, Cohen, A, Lee, J, Freedman, M, Gelfand, E (1984) Deferoxamine: A reversible S-phase inhibitor of human lymphocyte proliferation. *Blood* **64**(3)**:** 748-753.

Leone, AM, Francis, PL, Rhodes, P, Moncada, S (1994) A rapid and simple method for the measurement of nitrite and nitrate in plasma by high performance capillary electrophoresis. *Biochem Biophys Res Commun* **200**(2)**:** 951-957.

Levy, RM, Prince, JM, Billiar, TR (2005) Nitric oxide: A clinical primer. *Crit Care Med* **33:** 492-495.

Liang, Z, Wu, H, Xia, J, Li, Y, Zhang, Y, Huang, K, *et al.* (2009) Involvement of miR-326 in chemotherapy resistance of breast cancer through modulating expression of multidrug resistance-associated protein 1. *Biochem Pharm* **79**(6)**:** 817-824.

Lill, R (2009). Function and biogenesis of iron sulphur proteins. *Nature* **460**(7257)**:** 831-838.

Lynch, SR (2011) Why nutritional iron deficiency persists as a worldwide problem. *J Nutr* **141**(4)**:** 763S-768S.

Masini, A, Ceccarelli, D, Giovannini, F, Montosi, G, Garuti, C, Pietrangelo, A (2000) Iron-induced oxidant stress leads to irreversible mitochondrial dysfunctions and fibrosis in the liver of chronic iron-dosed gerbils. The effect of Silybin. *J Bioenerg Biomembr* **32**(2)**:** 175-182.

Mayfield, JA, Dehner, CA, DuBois, JL (2011) Recent advances in bacterial haem protein biochemistry. *Curr Opin Chem Biol* **15:** 260-266.

Meneghini, R (1997) Iron homeostasis, oxidative stress, and DNA damage. *Free Radical Bio Med* **23**(5)**:** 783-792.

Miller, MR, Megson, IL (2007) Recent developments in nitric oxide donor drugs. *Brit J Pharm* **151**(3)**:** 305-321.

Minn, AJ, Gupta, GP, Siegel, PM, Bos, PD, Shu, W, Giri, DD, *et al.* (2005) Genes that mediate breast cancer metastasis to lung. *Nature* **436**(7050)**:** 518-524.

Mooradian, DL, Hutsell, TC, Keefer, LK (1995) Nitric oxide (NO) donor molecules: Effect of NO release rate on vascular smooth muscle cell proliferation *in vitro*. *J Cardiovasc Pharm* **25**(4)**:** 674-678.

Mordechai, C (1988) A site-specific mechanism for free radical induced biological damage: The essential role of redox-active transition metals. *Free Radical Biol Med* **5**(1)**:** 27-37.

Mulero, V, Brock, JH (1999) Regulation of iron metabolism in murine J774 macrophages: Role of nitric oxide -dependent and -independent pathways following activation with gamma interferon and lipopolysaccharide. *Blood* **94**(7)**:** 2383-2389.

Murata, J-I, Tada, M, Iggo, RD, Sawamura, Y, Shinohe, Y, Abe, H (1997) Nitric oxide as a carcinogen: analysis by yeast functional assay of inactivating p53 mutations induced by nitric oxide. *Mutat Res-Fund Mol M* **379**(2)**:** 211-218.

Myers, BM, Prendergast, FG, Holman, R, Kuntz, SM, LaRusso, NF (1991) Alterations in the structure, physicochemical properties, and pH of hepatocyte lysosomes in experimental iron overload. *J Clin Invest* **88**(4)**:** 1207-1215.

Napier, I, Ponka, P, Richardson, DR (2005) Iron trafficking in the mitochondrion: Novel pathways revealed by disease. *Blood* **105**(5)**:** 1867-1874.

Ohshima, H, Bartsch, H (1994) Chronic infections and inflammatory processes as cancer risk factors: possible role of nitric oxide in carcinogenesis. *Mutat Res-Fund Mol M* **305**(2)**:** 253-264.

Okauchi, M, Hua, Y, Keep, RF, Morgenstern, LB, Xi, G (2009) Effects of deferoxamine on intracerebral hemorrhage-induced brain injury in aged rats. *Stroke* **40**(5)**:** 1858-1863.

Oliveira, L, Drapier, J-C (2000) Down-regulation of iron regulatory protein 1 gene expression by nitric oxide. *PNAS* **97**(12)**:** 6550-6555.

Oria, R, Sanchez, L, Houston, T, Hentze, M, Liew, F, Brock, J (1995) Effect of nitric oxide on expression of transferrin receptor and ferritin and on cellular iron metabolism in K562 human erythroleukemia cells. *Blood* **85**(10)**:** 2962-2966.

Panter, SS (1993) Release of iron from haemoglobin. *Letterman Army Inst of Res Presidio of San Francisco Ca Div of Blood Res*. pp: 1-25.

Paoli, M, Anderson, BF, Baker, HM, Morgan, WT, Smith, A, Baker, EN (1999) Crystal structure of hemopexin reveals a novel high-affinity haem site formed between two β-propeller domains. *Nat Struct Biol* **6**(10)**:** 926-931.

Paoli, M, Marles-Wright, J, Smith, A (2002) Structure function relationships in haem-proteins. *DNA Cell Biol* **21**(4)**:** 271-280.

Patel, RP, McAndrew, J, Sellak, H, White, CR, Jo, H, Freeman, BA, *et al.* (1999) Biological aspects of reactive nitrogen species. *Biochim Biophys Acta Bioenerg* **1411**(2-3)**:** 385-400.

Pantopoulos, K, Weiss, Gn, Hentze, MW (1994) Nitric oxide and the post-transcriptional control of cellular iron traffic. *Trends Cell Biol* **4**(3)**:** 82-86.

Pantopoulos, K, Hentze, MW (1995) Nitric oxide signalling to iron-regulatory protein: Direct control of ferritin mRNA translation and transferrin receptor mRNA stability in transfected fibroblasts. *PNAS* **92**(5)**:** 1267-1271.

Pike, MC, Spicer, DV, Dahmoush, L, Press, MF (1993) Oestrogens, progestogens, normal breast cell proliferation, and breast cancer risk. *Epidemiol Rev* **15**(1)**:** 17-30.

Pluta, RM, Oldfield, EH, Boock, RJ (1997) Reversal and prevention of cerebral vasospasm by intracarotid infusions of nitric oxide donors in a primate model of subarachnoid haemorrhage. *J Neurosurg* **87**(5)**:** 746-751.

Poderoso, JJ, Lisdero, C, Schopfer, F, Riobo, N, Carreras, MC, Cadenas, E, *et al.* (1999) The regulation of mitochondrial oxygen uptake by redox reactions involving nitric oxide and ubiquinol. *J Biol Chem* **274**(53)**:** 37709-37716.

Ponka, P (1999). Cellular iron metabolism. *Kidney Int* **55**(69)**:** 2-11.

Preston-Martin, S, Pike, MC, Ross, RK, Jones, PA, Henderson, BE (1990) Increased cell division as a cause of human cancer. *Cancer Res* **50**(23)**:** 7415-7421.

Punnonen, K, Irjala, K, Rajamaki, A (1997) Serum transferrin receptor and its ratio to serum ferritin in the diagnosis of iron deficiency. *Blood* **89**(3)**:** 1052-1057.

Radi, R, Beckman, JS, Bush, KM, Freeman, BA (1991) Peroxynitrite-induced membrane lipid peroxidation: The cytotoxic potential of superoxide and nitric oxide. *Arch Biochem Biophys* **288**(2)**:** 481-487.

Rao, VA, Klein, SR, Agama, KK, Toyoda, E, Adachi, N, Pommier, Y, *et al.* (2009) The iron chelator Dp44mT causes DNA damage and selective inhibition of topoisomerase IIα in breast cancer cells. *Cancer Res* **69**(3)**:** 948-957.

Reedy, CJ, Gibney, BR (2004) Haem protein assemblies. *Chem Rev* **104**(2)**:** 617-650.

Reis-Filho, JS, Tutt, ANJ (2008) Triple negative tumours: a critical review. *Histopathology* **52**(1)**:** 108-118.

Richardson, DR, Baker, E (1990) The uptake of iron and transferrin by the human malignant melanoma cell. *BBA-Mol Cell Res* **1053**(1)**:** 1-12.

Richardson, DR, Baker, E (1992) The effect of desferrioxamine and ferric ammonium citrate on the uptake of iron by the membrane iron-binding component of human melanoma cells. *Biochim Biophys Acta Biomembr* **1103**(2)**:** 275-280.

Richardson, DR, Baker, E (1994) Two saturable mechanisms of iron uptake from transferrin in human melanoma cells: The effect of transferrin concentration, chelators, and metabolic probes on transferrin and iron uptake. *J Cell Physiol* **161**(1)**:** 160-168.

Richardson, D, Ponka, P, Baker, E (1994) The effect of the iron(III) chelator, desferrioxamine, on iron and transferrin uptake by the human malignant melanoma cell. *Cancer Res* **54**(3)**:** 685-689.

Richardson, DR, Neumannova, V, Nagy, E, Ponka, P (1995) The effect of redox-related species of nitrogen monoxide on transferrin and iron uptake and cellular proliferation of erythroleukemia (K562) cells. *Blood* **86**(8)**:** 3211-3219.

Richardson, DR, Ponka, P (1997) The molecular mechanisms of the metabolism and transport of iron in normal and neoplastic cells. *Biochim Biophys Acta Biomembr* **1331**(1)**:** 1-40.

Richardson, DR (2002) Iron chelators as therapeutic agents for the treatment of cancer. *Crit Rev Oncol Hematol* **42**(3)**:** 267-281.

Richardson, DR, Lane, DJR, Becker, EM, Huang, ML-H, Whitnall, M, Rahmanto, YS, *et al.* (2010) Mitochondrial iron trafficking and the integration of iron metabolism between the mitochondrion and cytosol. *PNAS* **107**(24)**:** 10775-10782.

Riemer, J, Hoepken, HH, Czerwinska, H, Robinson, SR, Dringen, R (2004) Colorimetric ferrozine-based assay for the quantitation of iron in cultured cells. *Anal Biochem* **331**(2)**:** 370-375.

Robbins, AH, Stout, CD (1989) The structure of aconitase. *Proteins: Structure, Function, and Bioinformatics* **5**(4)**:** 289-312.

Saletta, F, Kovacevic, Z, Richardson, DR (2011) Research Spotlight: Iron chelation: deciphering novel molecular targets for cancer therapy. The tip of the iceberg of a web of iron-regulated molecules. *Future Med Chem* **3**(16)**:** 1983-1986.

Samaniego, F, Chin, J, Iwai, K, Rouault, TA, Klausner, RD (1994) Molecular characterization of a second iron-responsive element binding protein, iron regulatory protein 2. Structure, function, and post-translational regulation. *J Biol Chem* **269**(49)**:** 30904-30910.

Sarfati, D, Blakely, T, Shaw, C, Cormack, D, Atkinson, J (2006) Patterns of disparity: Ethnic and socio-economic trends in breast cancer mortality in New Zealand. *Cancer Causes Control* **17**(5)**:** 671-678.

Sexton, DJ, Muruganandam, A, McKenney, DJ, Mutus, B (1994) Visible light photochemical release of nitric oxide from *S*-nitrosoglutathione: Potential photochemotherapeutic applications. *Photochem Photobiol* **59**(4)**:** 463-467.

Shadid, M, Buonocore, G, Groenendaal, F, Moison, R, Ferrali, M, Berger, HM, *et al.* (1998) Effect of deferoxamine and allopurinol on non-protein-bound iron concentrations in plasma and cortical brain tissue of newborn lambs following hypoxia-ischemia. *Neurosci Lett* **248**(1)**:** 5-8.

Simpson, PT, Reis-Filho, JS, Gale, T, Lakhani, SR (2005) Molecular evolution of breast cancer. *J Pathol* **205**(2)**:** 248-254.

Soto, AM, Sonnenschein, C (2011) The tissue organization field theory of cancer: A testable replacement for the somatic mutation theory. *BioEssays* **33**(5)**:** 332-340.

Soyer, HP, Smolle, J, Torne, R, Kerl, H (1987) Transferrin receptor expression in normal skin and in various cutaneous tumors. *J Cutan Pathol* **14**(1)**:** 1-5.

Stamler, J, Singel, D, Loscalzo, J (1992) Biochemistry of nitric oxide and its redox-activated forms. *Sci* **258**(5090)**:** 1898-1902.

Stevens, RG, Graubard, BI, Micozzi, MS, Neriishi, K, Blumberg, BS (1994) Moderate elevation of body iron level and increased risk of cancer occurrence and death. *Int J Cancer* **56**(3)**:** 364-369.

Stevens, W, Stevens, G, Kolbe, J, Cox, B (2007) Lung cancer in New Zealand: Patterns of secondary care and implications for survival. *J Thorac Oncol* **2**(6)**:** 481-493.

Stevens, W, Stevens, G, Kolbe, J, Cox, B (2008) Ethnic differences in the management of lung cancer in New Zealand. *J Thorac Oncol* **3**(3)**:** 237-244.

Stuehr, DJ, Nathan, CF (1989) Nitric oxide: A macrophage product responsible for cytostasis and respiratory inhibition in tumor target cells. *J Exp Med* **169**(5)**:** 1543-1555.

Tamir, S, Tannenbaum, SR (1996) The role of nitric oxide (NO·) in the carcinogenic process. *BBA-Rev Cancer* **1288**(2)**:** 31-36.

Tamir, S, Burney, S, Tannenbaum, SR (1996) DNA damage by nitric oxide. *Chem Res Toxicol* **9**(5)**:** 821-827.

Thomsen, LL, Miles, DW, Happerfield, L, Bobrow, LG, Knowles, RG, Moncada, S (1995) Nitric oxide synthase activity in human breast cancer. *Br J Cancer* **72**(1)**:** 41-44.

Tian, J, Peehl, DM, Knox, SJ (2010) Metalloporphyrin synergizes with ascorbic acid to inhibit cancer cell growth through Fenton chemistry. *Cancer Biother Radiopharm* **25**(4)**:** 439-448.

To, KKW, Robey, RW, Knutsen, T, Zhan, Z, Ried, T, Bates, SE (2009) Escape from hsa-miR-519c enables drug-resistant cells to maintain high expression of ABCG2. *Mol Cancer Ther* **8**(10)**:** 2959-2968.

Toyokuni, S (1996) Iron-induced carcinogenesis: The role of redox regulation. *Free Radical Biol Med* **20**(4)**:** 553-566.

Tulpule, K, Robinson, SR, Bishop, GM, Dringen, R (2010) Uptake of ferrous iron by cultured rat astrocytes. *J Neurosci Res* **88**(3)**:** 563-571.

Uchiyama, A, Kim, J-S, Kon, K, Jaeschke, H, Ikejima, K, Watanabe, S, *et al.* (2008) Translocation of iron from lysosomes into mitochondria is a key event during oxidative stress-induced hepatocellular injury. *Hepatol* **48**(5)**:** 1644-1654.

Umemura, T, Sai, K, Takagi, A, Hasegawa, R, Kurokawa, Y (1990) Formation of 8-hydroxydeoxyguanosine (8-OH-dG) in rat kidney DNA after intraperitoneal administration of ferric nitrilotriacetate (Fe-NTA). *Carcinogenesis* **11**(2)**:** 345-347.

Vanderford, PA, Wong, J, Chang, R, Keefer, LK, Soifer, SJ, Fineman, JR (1994) Diethylamine/nitric oxide (NO) adduct, an NO donor, produces potent pulmonary and systemic vasodilation in intact newborn lambs. *J Cardiovasc Pharm* **23**(1)**:** 113.

Vanin, AF, Malenkova, IV, Serezhenkov, VA (1997) Iron catalyses both decomposition and synthesis of *S*-nitrosothiols: Optical and electron paramagnetic resonance studies. *Nitric Oxide* **1**(3)**:** 191-203.

Verdon, CP, Burton, BA, Prior, RL (1995) Sample pre-treatment with nitrate reductase and glucose-6-phosphate dehydrogenase quantitatively reduces nitrate while avoiding interference by $NADP^+$ when the Griess reaction is used to assay for nitrite. *Anal Biochem* **224**(2)**:** 502-508.

Wang, J, Fillebeen, C, Chen, G, Andriopoulos, B, Pantopoulos, K (2006) Sodium nitroprusside promotes IRP2 degradation via an increase in intracellular iron and in the absence of *S*-nitrosylation at C178. *Mol Cell Biol* **26**(5)**:** 1948-1954.

Wang, J, Pantopoulos, K (2011) Regulation of cellular iron metabolism. *Biochem J* **434**(3)**:** 365-381.

Walker, RA, Day, SJ (1986) Transferrin receptor expression in non-malignant and malignant human breast tissue. *J Pathol* **148**(3)**:** 217-224.

Watts, RN, Richardson, DR (2002) The mechanism of nitrogen monoxide (NO)-mediated iron mobilization from cells. NO intercepts iron before incorporation into ferritin and indirectly mobilizes iron from ferritin in a glutathione-dependent manner. *Eur J Biochem* **269**(14): 3383-3392.

Watts, RN, Hawkins, C, Ponka, P, Richardson, DR (2006) Nitrogen monoxide (NO)-mediated iron release from cells is linked to NO-induced glutathione efflux via multidrug resistance-associated protein 1. *PNAS* **103**(20)**:** 7670-7675.

Weiss, G, Werner-Felmayer, G, Werner, ER, Grunewald, K, Wachter, H, Hentze, MW (1994) Iron regulates nitric oxide synthase activity by controlling nuclear transcription. *J Exp Med* **180**(3)**:** 969-976.

Whitnall, M, Howard, J, Ponka, P, Richardson, DR (2006) A class of iron chelators with a wide spectrum of potent antitumor activity that overcomes resistance to chemotherapeutics. *PNAS* **103**(40)**:** 14901-14906.

Wyatt, MD, Pittman, DL (2006) Methylating agents and DNA repair responses: Methylated bases and sources of strand breaks. *Chem Res Toxicol* **19**(12)**:** 1580-1594.

Xu, W, Liu, LZ, Loizidou, M, Ahmed, M, Charles, IG (2002) The role of nitric oxide in cancer. *Cell Res* **12**(5-6)**:** 311-320.

Yuan, J, Lovejoy, DB, Richardson, DR (2004) Novel di-2-pyridyl–derived iron chelators with marked and selective antitumor activity: *In vitro* and *in vivo* assessment. *Blood* **104**(5)**:** 1450-1458.

Yu, Y, Richardson, DR (2011) Cellular iron depletion stimulates the JNK and p38 MAPK signalling transduction pathways, dissociation of ASK1-thioredoxin, and activation of ASK1. *J Biol Chem* **286**(17)**:** 15413-15427.

Yurtseven, N, Karaca, P, Kaplan, M, Ozkul, V, Tuygun, AK, Aksoy, T, *et al.* (2003) Effect of nitroglycerin inhalation on patients with pulmonary hypertension undergoing mitral valve replacement surgery. *Anesthesiol* **99**(4)**:** 855-858.

Zepp, RG, Faust, BC, Hoigne, J (1992) Hydroxyl radical formation in aqueous reactions (pH3-8) of iron(II) with hydrogen peroxide: The photo-Fenton reaction. *Environ Sci Technol* **26**(2)**:** 313-319.

Zhelyaskov, VR, Gee, KR, Godwin, DW (1998) Control of NO concentration in solutions of nitrosothiol compounds by light. *Photochem Photobiol* **67**(3)**:** 282-288.